

# Reversible Gelation, Thermoresponsiveness and Formation of Double Networks by *N*-alkylated Poly(*N*-vinylamide)s

Von der Fakultät für Mathematik, Informatik und Naturwissenschaften der RWTH Aachen University zur Erlangung des akademischen Grades einer Doktorin der Naturwissenschaften genehmigte Dissertation

vorgelegt von

Chunchen Zhang, Dr.-Ing.

aus

Henan, Volksrepublik China

Berichter: Universitätsprofessor Dr. rer. nat. Martin Möller
Universitätsprofessor Dr. rer. nat. Andrij Pich

Tag der mündlichen Prüfung: 13.03.2025

Diese Dissertation ist auf den Internetseiten der Universitätsbibliothek verfügbar.

The scientific work presented in this dissertation was performed at DWI-Leibniz-Institute for Interactive Materials e.V. at the RWTH Aachen University from August 2019 to July 2022 under the supervision of Prof. Dr. rer. nat. Martin Möller.

Die in dieser Dissertation vorgestellten wissenschaftlichen Arbeiten wurde am DWI-Leibniz-Institut für Interaktive Materialien e.V. an der RWTH Aachen von August 2019 bis Juli 2022 unter der Leitung von Prof. Dr. rer. nat. Martin Möller durchgeführt.

# **Declaration of authorship**

#### I, Chunchen Zhang

declare that this thesis and the work presented in it are my own and has been generated by me as the result of my own original research.

Hiermit erkläre ich an Eides statt / I do solemnely swear that:

- 1. This work was done wholly or mainly while in candidature for the doctoral degree at this faculty and university;
- 2. Where any part of this thesis has previously been submitted for a degree or any other qualification at this university or any other institution, this has been clearly stated;
- 3. Where I have consulted the published work of others or myself, this is always clearly attributed;
- 4. Where I have quoted from the work of others or myself, the source is always given. This thesis is entirely my own work, with the exception of such quotations;
- 5. I have acknowledged all major sources of assistance;
- 6. Where the thesis is based on work done by myself jointly with others, I have made clear exactly what was done by others and what I have contributed myself;
- 7. Parts of this work have been published before as:
  - Zhang, C.; Demco, D. E.; Rimal, R.; Köhler, J.; Vinokur, R.; Singh, S.; Tenbusch, J.; Möller, M. Hydrophobic Interaction within Sparsely *N*-Alkylated Poly(*N*-vinylacetamide)s Enables Versatile Formation of Reversible Hydrogels. *Macromolecules* 2023, 56 (23), 9616-9625.

Π	21	H	Δ	
u	$\boldsymbol{a}$	L.	C	

Signature:

# **Acknowledgements**

Time flies and it comes soon to the end of my PhD study in DWI-Leibniz Institute for Interactive Materials at the RWTH Aachen University under the program provided by Max Planck School Matter to Life. Here I would like to show my appreciation to all people who provided help in the past years.

My most profound appreciation goes to my supervisor, Prof. Dr. Martin Möller, for proposing an interesting and challenging topic and guiding me throughout the program. I'm very grateful for the time and energy he spent on the discussions concerning my projects, which improved my understanding of the topic, enhanced my abilities to solve experimental problems, and paved the way for the success in my thesis. I also would like to thank Prof. Dr. Andrij Pich for the evaluation of my dissertation as the second reviewer.

Next, I would like to express my gratitude to Max Planck School Matter to Life for the great opportunity to be part of a multidisciplinary network and work on my PhD projects. The academic lectures and activities with all the students and fellows broadened my horizons and brought much inspiration for my research as well.

Many thanks go to all colleagues in DWI for the technical assistance in my research. In particular, I would like to thank Dr. Jens Köhler, Pascal Max Jeschenko, Janko Stoffels, Aisa Hosseinnejad, and Oliver Fiukowski for polymer synthesis and analysis, Rahul Rimal and Dr. Smriti Singh for the help in cell culture, Prof. Dr. Dan Eugen Demco, Dr. Meike Emondts and Ms. Ines Bachmann-Remy for NMR measurements,

Dr. Rostislav Vinokur for DSC measurements, Miriam Al Enezy-Ulbrich and Thorsten Fischer for rheological measurements, Claudia Formen and Thomke Belthle for cloud point measurements, Dr. Michael Pohl and Rainer Haas for SEC tests, Dr. Tamás Haraszti for optical microscopy, Markus Reichelt and Markus Nobis for the material issues.

I would also like to give my thanks to my friends, in particular, Jingnan Wu, Dr. Helin Li, Dr. Chaolei Hu, Elizaveta Selezneva, Yuanyuan Cao, Prachi Desai, Manuela Rosario Garay Sarmiento, Dr. Yue Zhao (Patureau Group), Zhitao Yang, Yi Chen, Peidan Li, Xun Lu, Kang Qin, Feng Xiong, Wenjun Wang, for their accompany and help during my stay in Germany.

I also wish to show my appreciation to Dr. med. Yejun Hu (Zhejiang University), Qingping Ding (Zhejiang University), Dr. Zheng Xing (Beihang University), Chen Zhao (Tsinghua University), Dr. Deyou Yu (Zhejiang sci-tech university) for their support during my master's studies. I am extremely grateful to the education sponsorship offered by SHKP-Kwoks' Foundation (by Sun Hung Kai Properties Limited, Hong Kong) for my bachelor study.

I would also express my gratitude to my biology teacher, Mrs. Hongmei Wang and my physics teacher, Mrs. Xinmei Chen in my high school. They played the most important role in triggering my curiosity in science and encouraging me to pursue a career in science.

Last but most sincerely, I would like to give my thanks to my families for their support.

# **Table of Contents**

De	eclara	tion of	authorship	3				
Ac	know	ledgen	nents	4				
Lis	st of a	bbrevi	ations	9				
1	Intr	Introduction						
	1.1	Moti	vation of the thesis	12				
	1.2	Scop	e of the thesis	13				
	1.3	Refe	rences	15				
2	Lite	rature	review	18				
	2.1	Singl	le network hydrogels	18				
	2.2	Doul	ole network hydrogels	19				
	2.3	Ther	moresponsive double network hydrogels	22				
	2.4	Ther	moresponsive N-alkylated poly(N-vinylamide)s	32				
	2.5	Refe	rences	33				
3	-	_	oic interaction within sparsely N-alkylated					
vi	nylace	etamid	e)s enables versatile formation of reversible hydrogels.	44				
	3.1	Intro	oduction	44				
	3.2	3.2 Experimental section		47				
		3.2.1	Materials	47				
		3.2.2	Sample denotation	47				
		3.2.3	Synthesis of poly(N-vinylacetamide)	47				
		3.2.4	N-alkylation of poly(N-vinylacetamide)	48				
		3.2.5	Nuclear magnetic resonance	49				
		3.2.6	Size exclusion chromatography	50				

	3.2.7	Differential scanning calorimetry	
	3.2.8	Hydrogel preparation	50
	3.2.9	Swelling	52
	3.2.10	Rheology	51
	3.2.11	Cytotoxicity and cell adherence studies	52
3.3	Resu	lts and discussion	53
	3.3.1	Synthesis of polymers	53
	3.3.2	Gel formation	54
	3.3.3	Biocompatibility	57
	3.3.4	Structural characterization of the hydrogels	58
	3.3.5	Mechanical characterization of hydrogels	61
3.4	Conc	lusion	69
3.5	Refer	ences	70
3.6	Sunn	orting information	7/
Synt	thesis	and thermoresponsive properties of <i>N</i> -alkylated	poly(N
Synt Iylam	thesis iide)s a	and thermoresponsive properties of <i>N</i> -alkylated nd their hydrogels	poly( <i>N</i> 8
Synt nylam 4.1	thesis nide)s a Intro	and thermoresponsive properties of N-alkylated nd their hydrogelsd	<b>poly(</b> <i>N</i> 88
Synt Iylam	thesis nide)s a Intro Expe	and thermoresponsive properties of N-alkylated nd their hydrogelsd duction	<b>poly(</b> <i>N</i> 88 89
Synt nylam 4.1	thesis aide)s a Intro Expe 4.2.1	and thermoresponsive properties of N-alkylated nd their hydrogels  duction rimental section  Materials	<b>poly(</b> <i>N</i> 88 89
Synt nylam 4.1	Intro Expe 4.2.1 4.2.2	and thermoresponsive properties of N-alkylated nd their hydrogels  duction rimental section  Materials  Sample nomenclature	<b>poly(</b> <i>N</i> 889192
Synt nylam 4.1	Intro Expe 4.2.1 4.2.2 4.2.3	and thermoresponsive properties of N-alkylated nd their hydrogels  duction rimental section  Materials  Sample nomenclature  Synthesis of poly(N-vinylamide)s	<b>poly(</b> <i>N</i> 889192
Synt nylam 4.1	Intro Expe 4.2.1 4.2.2 4.2.3 4.2.4	and thermoresponsive properties of N-alkylated nd their hydrogels	poly(N 88 91 92 92
Synt nylam 4.1	Intro Expe 4.2.1 4.2.2 4.2.3 4.2.4 4.2.5	and thermoresponsive properties of N-alkylated nd their hydrogels	poly(N
Synt nylam 4.1	Intro Expe 4.2.1 4.2.2 4.2.3 4.2.4 4.2.5 vinylad	and thermoresponsive properties of N-alkylated nd their hydrogels	poly(N
Synt nylam 4.1	Intro Expe 4.2.1 4.2.2 4.2.3 4.2.4 4.2.5 vinylac 4.2.6	and thermoresponsive properties of N-alkylated nd their hydrogels	poly(N
Synt nylam 4.1	Intro Expe 4.2.1 4.2.2 4.2.3 4.2.4 4.2.5 vinylac 4.2.6 4.2.7	and thermoresponsive properties of N-alkylated nd their hydrogels	poly(N
Synt nylam 4.1	Intro Expe 4.2.1 4.2.2 4.2.3 4.2.4 4.2.5 vinylac 4.2.6 4.2.7 4.2.8	and thermoresponsive properties of N-alkylated nd their hydrogels	poly(N
Synt nylam 4.1	Intro Expe 4.2.1 4.2.2 4.2.3 4.2.4 4.2.5 vinylac 4.2.6 4.2.7 4.2.8 4.2.9	and thermoresponsive properties of N-alkylated nd their hydrogels	poly(A

	4.4	Conc	clusion	111		
	4.5	Refe	rences	112		
	4.6	Supp	oorting information	116		
5			sponsive double network hydrogels from <i>N-a</i>			
vir	ıylace	etamid	e)s	122		
	5.1	Intro	oduction	122		
	5.2	Expe	125			
		5.2.1	Materials	125		
		5.2.2	Sample denotation	125		
		5.2.3	Polymer synthesis	125		
		5.2.4	Characterization of polymers	127		
		5.2.5	Hydrogel preparation	127		
		5.2.6	Characterization of hydrogels	129		
	5.3	Resu	lts and discussion	131		
	5.4	Conc	Conclusion15			
	55	Pofo	rancas	150		

# List of abbreviations

AIBN 2,2'-azobis(2-methylpropionitrile)

AMPS 2-acrylamido-2-methyl-1-propanesulfonic acid

ASR Apparent swelling ratio

ATCC American type culture collection

CP-MAS Cross-polarization magic angle spinning

DEGMA Diethylene glycol dimethacrylate

DI water Deionized water

DMA Dynamic mechanical analysis

DMEM Dulbecco's modified eagle medium

DMF Dimethylformamide

DMPA 2,2-Dimethoxy-2-phenylacetophenone

DMSO Dimethyl sulfoxide

DN Double network

*DP* Degree of polymerization

DP-MAS Direct-polarization magic angle spinning

DS Degree of substitution

DSC Differential scanning calorimetry

full-IPNs Full-interpenetrating double network hydrogels

GG Guar gum

LCST Lower critical solution temperature

MC Methylcellulose

MEDSAH [2-(methacryloyloxy)ethyl]dimethyl-(3-sulfopropyl)ammonium

hydroxide

NHDF Normal human dermal fibroblasts

NMR Nuclear magnetic resonance

NMVA *N*-methyl-*N*-vinylacetamide

NVA *N*-vinylacetamide

NVCL *N*-vinylcaprolactam

NVF *N*-vinylformamide

NVP *N*-vinylpyrrolidone

OEGMA Oligo (ethylene glycol) methyl ether methacrylate

PAAm Polyacrylamide

PAMPS Poly(2-acrylamido-2-methyl-1-propanesulfonic acid)

PDEAAm Poly(N,N'-diethylacrylamide)

*PDI* Polydispersity index

PDMA Poly(*N*,*N*-dimethylacrylamide)

PMEO<sub>2</sub>MA Poly(2-(2-methoxyethoxy) ethyl methacrylate)

PMMA Poly(methyl methacrylate)

PNaAMPS Poly(2-acrylamido-2-methylpropanesulfonic acid sodium salt)

PNAGA Poly(*N*-acryloyl glycinamide)

PNIPAM Poly(*N*-isopropylacrylamide)

PNVA Poly(*N*-vinylacetamide)

PNVCL Poly(*N*-vinylcaprolactam)

PNVF Poly(*N*-vinylformamide)

PVA Polyvinyl alcohol

PVP Polyvinylpyrrolidone

SEC Size exclusion chromatography

semi-IPNs Semi-interpenetrating double network hydrogels

SN Single network

SR Swelling ratio

 $T_{\rm cp}$  Cloud point temperature

T-DN Thermoresponsive double network

Temp. Temperature

THF Tetrahydrofuran

UV Ultraviolet

VA-044 2,2'-azobis[2-(2-imidazolin-2-yl)propane]dihydrochloride

VPTT Volume phase transition temperature

XG Xanthan gum

# 1 Introduction

#### 1.1 Motivation of the thesis

Hydrogels have been playing an important role in biomedical fields over 100 years for their widely tunable chemical, physical and bio-relevant properties. However, still, we face important challenges for conventional single network hydrogels in order to meet specific scientific study requirements for the understanding and advancing structure-property relations and application needs. An important example addresses the poor mechanical performance of synthetic hydrogels compared to many natural hydrogels. Other examples address tailoring their responsiveness to variations of state variables (p, V, T, n).

Inspired by the structure of load-bearing soft tissues, the double network approach was proposed. Thermoresponsive double network hydrogels, which combines (boasts) the superior mechanical properties of double network hydrogels with the easy-to-control feature of thermoresponsive hydrogels, have received much attention for various applications, including biosensors, soft robotics, and drug delivery. So far, only limited pairs of combinations of polymers have been studied, and the thermoresponsive networks were mainly poly(N-isopropylacrylamide)(PNIPAM) or its copolymers. However, PNIPAM is potentially cytotoxic because the low molecular weight amino compounds can be generated by hydrolysis. Therefore, new thermoresponsive polymers with better biocompatibility are strongly desired for thermoresponsive double network hydrogels designed for biomedical applications.

Poly(*N*-vinylamide)s, a class of water-soluble carbon chain polymers with the amide group tied directly to the polymer backbone, present an isomeric alternative to polyacrylamides offering versatile chemical modification via the backbone-linked amine functionality after hydrolysis.<sup>14, 15</sup> Poly(*N*-vinylacetamide)(PNVA) and poly(*N*-vinylformamide)(PNVF) are of good biocompatibility, and they are able to be readily modified by *N*-substitution at the amide position.<sup>16, 17</sup> Alkylated PNVAs and PNVFs have been proved as LCST-type polymers,<sup>18-21</sup> which can work as alternatives to PNIPAM for the development of biocompatible thermoresponsive double network hydrogels.

#### 1.2 Scope of the thesis

In this thesis, we developed a series of *N*-alkylated poly(*N*-vinylamide)s with different side chain length by *N*-substitution of the constituent monomer units of PNVAs or PNVFs. The amphiphilic nature of these poly(*N*-alkyl-*N*-vinylamide)s was adjusted by the molecular weight and structure of backbone polymer, alkyl side chain length, as well as degree of alkyl chain substitution. Based on the hydrophobicity, we firstly developed a series of physically crosslinked hydrogels and thermoresponsive hydrogels, and then we investigated various thermoresponsive double network hydrogels prepared from the combinations of the aforementioned two types of poly(*N*-alkyl-*N*-vinylacetamide)s. It was demonstrated that poly(*N*-vinylacetamide)s derivatives are promising components for thermoresponsive tough double network hydrogels.

**Chapter 2** gives a detailed analysis of the literature on double network hydrogels.

**Chapter 3** describes reversible hydrogel formation by hydrophobic interaction for poly(*N*-alkyl-*N*-vinylacetamide)s with 3 mol% of alkyl chains (side chain length = 10, 12,

14, 16 and 18). The polymers dissolve in ethanol and can be cast to thin films in a mould. When immersed in water, they swell and form biocompatible hydrogels. Polymers with alkyl substituents of different length demonstrate strong differences in strength of the hydrophobic association. Relatively short alkyl substituents yield hydrogels which flow upon shearing but still segregate from excess water, i.e., exhibit syneresis. Longer alkyl substituents yield hydrogels with mechanical properties approaching those of permanently crosslinked hydrogels. Hydrogels were characterized by strain- and stress-controlled rheological experiments. Their rheological properties follow a time-temperature-stickiness superposition principle indicating that the side chains serve as sticky substituents which extend the terminal relaxation time according to their hydrophobicity.

Chapter 4 reports on the thermoresponsive properties of poly(*N*-alkyl-*N*-vinylacetamide)s and poly(*N*-alkyl-*N*-vinylformamide)s modified by *N*-substitution of poly(*N*-vinylamide)s with short hydrocarbon substituents. Demixing in aqueous solution was tailored over a wide temperature range by substituting the poly(*N*-vinylamide)s by relatively short alkyl side chains (e.g., *n*-propyl, *n*-butyl or allyl groups). Introduction of a small fraction of allyl groups allowed preparation of hydrogels by photo-initiated thiolene addition. Hydrogels were characterized for their temperature-dependent swelling and swelling kinetics. We observed inverse molecular weight dependence of the cloud points of polymers meaning that the lower molecular weight samples have lower cloud points. Covalently crosslinked hydrogels of these polymers showed the corresponding volume phase transition. Once the hydrogels collapsed at elevated temperature, swelling would recover below the volume phase transition temperature in short time but only to reduced

degree of swelling. Further swelling to the original degree of swelling appeared to be extremely slow and was difficult to be observed because of the long times needed. As an explanation, we discuss the formation of ordered clusters from stereoregular segments in the polymer chain: These clusters appear to result in extra quasi-permanent crosslinks which reduce reswelling.

Chapter 5 describes double network hydrogels consisting of a covalently crosslinked alkylated PNVA network and a reversibly crosslinked alkylated PNVA network. For each network, polymers with different alkyl chain lengths and molecular weights were used to study the effects on the temperature-dependent swelling behavior and mechanical properties of the double network hydrogels. A key challenge in this study was caused by the solubility and viscosity limitations for the choice of the fractions of the components and their concentrations during the chemical crosslinking step. Enhanced mechanical strength and tissue-like stress-strain mechanical response were achieved for selected double network hydrogels.

#### 1.3 References

- [1] Cascone, S.; Lamberti, G. Hydrogel-based commercial products for biomedical applications: A review. *International Journal of Pharmaceutics* **2020**, *573*, 118803. DOI: 10.1016/j.ijpharm.2019.118803.
- [2] Liu, X.; Liu, J.; Lin, S.; Zhao, X. Hydrogel machines. *Materials Today* **2020**, *36*, 102-124. DOI: 10.1016/j.mattod.2019.12.026.
- [3] Lee, Y.; Song, W. J.; Sun, J. Y. Hydrogel soft robotics. *Materials Today Physics* **2020**, *15*, 100258. DOI: 10.1016/j.mtphys.2020.100258.
- [4] Du, J.; Zhang, Y.; Huang, Y.; Zhang, Q.; Wang, W.; Yu, M.; Xu, L.; Xu, J. Dual-Cross-Linked Chitosan-Based Antibacterial Hydrogels with Tough and Adhesive

- Properties for Wound Dressing. *Macromolecular Rapid Communications* **2023**, *44* (23), 2300325. DOI: 10.1002/marc.202300325.
- [5] Chen, G.; Huang, J.; Gu, J.; Peng, S.; Xiang, X.; Chen, K.; Yang, X.; Guan, L.; Jiang, X.; Hou, L. Highly tough supramolecular double network hydrogel electrolytes for an artificial flexible and low-temperature tolerant sensor. *Journal of Materials Chemistry A* **2020**, *8* (14), 6776-6784. DOI: 10.1039/D0TA00002G.
- [6] Gong, J. P. Why are double network hydrogels so tough? *Soft Matter* **2010**, *6* (12), 2583-2590. DOI: 10.1039/B924290B.
- [7] Na, Y. H. Double network hydrogels with extremely high toughness and their applications. *Korea-Australia Rheology Journal* **2013**, *25* (4), 185-196. DOI: 10.1007/s13367-013-0020-y.
- [8] Li, Z.; Zhou, Y.; Li, T.; Zhang, J.; Tian, H. Stimuli-responsive hydrogels: Fabrication and biomedical applications. *VIEW* **2022**, *3* (2), 20200112. DOI: 10.1002/VIW.20200112.
- [9] Gong, J. P.; Katsuyama, Y.; Kurokawa, T.; Osada, Y. Double-Network Hydrogels with Extremely High Mechanical Strength. *Advanced Materials* **2003**, *15* (14), 1155-1158. DOI: 10.1002/adma.200304907.
- [10] Zhang, X.-Z.; Wu, D.-Q.; Chu, C.-C. Synthesis, characterization and controlled drug release of thermosensitive IPN–PNIPAAm hydrogels. *Biomaterials* **2004**, *25* (17), 3793-3805. DOI: 10.1016/j.biomaterials.2003.10.065.
- [11] Fei, R.; Means, A. K.; Abraham, A. A.; Locke, A. K.; Coté, G. L.; Grunlan, M. A. Self-Cleaning, Thermoresponsive P(NIPAAm-co-AMPS) Double Network Membranes for Implanted Glucose Biosensors. *Macromolecular Materials and Engineering* **2016**, *301* (8), 935-943. DOI: 10.1002/mame.201600044.
- [12] Zheng, W. J.; An, N.; Yang, J. H.; Zhou, J.; Chen, Y. M. Tough Al-alginate/Poly(*N*-isopropylacrylamide) Hydrogel with Tunable LCST for Soft Robotics. *ACS Applied Materials & Interfaces* **2015**, *7* (3), 1758-1764. DOI: 10.1021/am507339r.
- [13] Kan, K.; Ajiro, H. Switchable Thermal Responsive Interpenetrated Polymer Network Gels of Poly(*N*-vinylacetamide) and Poly(*N*-vinylisobutyramide). *Chemistry Letters* **2018**, *47* (4), 591-593. DOI: 10.1246/cl.171191.
- [14] Kirsh, Y. E. Water Soluble Poly-*N*-Vinylamides: Synthesis and Physicochemical Properties. 1998; John Wiley & Sons, Inc.: 1998.

- [15] Pelton, R. Polyvinylamine: A Tool for Engineering Interfaces. *Langmuir* 2014, 30 (51), 15373-15382. DOI: 10.1021/la5017214.
- [16] Ajiro, H.; Watanabe, J.; Akashi, M. Cell Adhesion and Proliferation on Poly(*N*-vinylacetamide) Hydrogels and Double Network Approaches for Changing Cellular Affinities. *Biomacromolecules* **2008**, *9* (2), 426-430. DOI: 10.1021/bm701221c.
- [17] Marhefka, J. N.; Marascalco, P. J.; Chapman, T. M.; Russell, A. J.; Kameneva, M. V. Poly(*N*-vinylformamide)A Drag-Reducing Polymer for Biomedical Applications. *Biomacromolecules* **2006**, *7* (5), 1597-1603. DOI: 10.1021/bm060014i.
- [18] Ajiro, H.; Takemoto, Y.; Akashi, M.; Chua, P. C.; Kelland, M. A. Study of the Kinetic Hydrate Inhibitor Performance of a Series of Poly(*N*-alkyl-*N*-vinylacetamide)s. *Energy & Fuels* **2010**, *24* (12), 6400-6410. DOI: 10.1021/ef101107r.
- [19] Kelland, M. A.; Abrahamsen, E.; Ajiro, H.; Akashi, M. Kinetic Hydrate Inhibition with *N*-Alkyl-*N*-vinylformamide Polymers: Comparison of Polymers to n-Propyl and Isopropyl Groups. *Energy & Fuels* **2015**, *29* (8), 4941-4946. DOI: 10.1021/acs.energyfuels.5b01251.
- [20] Kawatani, R.; Kan, K.; Kelland, M. A.; Akashi, M.; Ajiro, H. Remarkable Effect on Thermosensitive Behavior Regarding Alkylation at the Amide Position of Poly(*N*-vinylamide)s. *Chemistry Letters* **2016**, *45* (6), 589-591. DOI: 10.1246/cl.160145.
- [21] Zhang, Q.; Kawatani, R.; Ajiro, H.; Kelland, M. A. Optimizing the Kinetic Hydrate Inhibition Performance of *N*-Alkyl-*N*-vinylamide Copolymers. *Energy & Fuels* **2018**, *32* (4), 4925-4931. DOI: 10.1021/acs.energyfuels.8b00251.

# 2 Literature review

#### 2.1 Single network hydrogels

Hydrogels, three-dimensional physically or chemically crosslinked hydrophilic polymer networks which swell but do not dissolve in water,<sup>1</sup> have received extensive attention in diverse biomedical fields including but not limited to drug delivery,<sup>2</sup> wound dressing,<sup>3</sup> tissue engineering,<sup>4</sup> contact lens,<sup>5</sup> hygiene products,<sup>6</sup> biosensors,<sup>7</sup> hydrogel machines,<sup>8</sup> and soft robots<sup>9</sup>. Furthermore, they have also played an important role in the corresponding commercial markets<sup>10, 11</sup> since the term "hydrogel" was first proposed in 1894<sup>12</sup>.

In particular, for countless biomedical applications, hydrogels are of further increasing interest owing to their widely tunable chemical, physical and bio-relevant properties. However, there still remain some major problems for conventional single network hydrogels (SN gels) to be solved in order to meet all the requirements of various scientific and industrial needs, 9, 13, 14 most noteworthy, their mechanical weakness (strength < 50 kPa, stiffness < 10 kPa, toughness < 10 J/m<sup>2</sup>). 15

For their good biocompatibility, hydrogels have been extensively used as structural substitute or template of human tissue in tissue engineering.<sup>4</sup> However, conventional chemically crosslinked SN gels are usually weak and brittle, which limits their use as substitute materials for load-bearing soft tissues, such as articular cartilage, tendon, ligament and muscle.<sup>16, 17</sup>

Hydrogels have been considered as ideal wound dressing materials to promote wound healing process for their comprehensive properties, such as the ability to cool the wound area, absorb tissue exudates, as well as protect the wound from bacteria. 18, 19 However, when frequent bending or complex motions are involved in the neighbourhood of the wound, the chance for bacterial infection could be largely increased, 18 because the hydrogel dressing can break before the wound gets fully recovered.

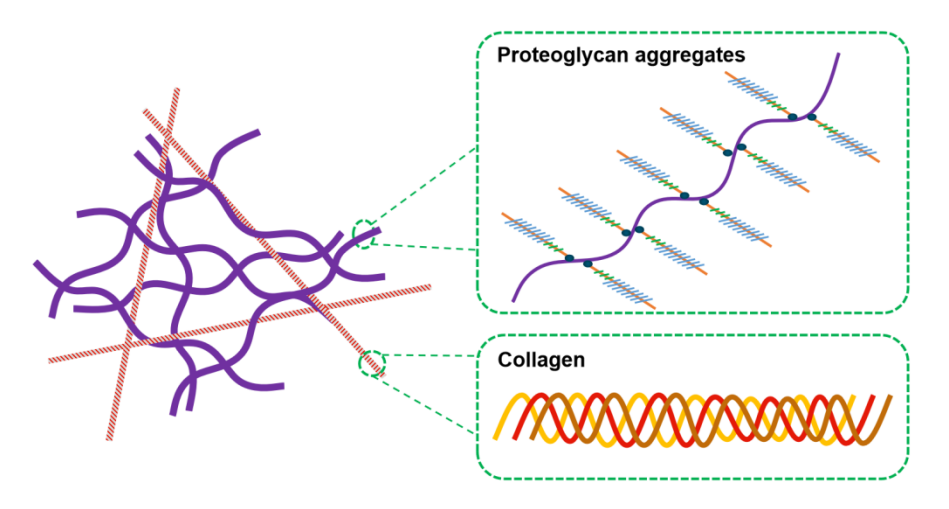
Hydrogels are also promising materials for implantable bio-sensors with integrated flexible electronic devices, and health-monitoring systems to monitor health-related parameters to assist diagnosis and treatment.<sup>20</sup> Yet, the poor mechanical properties also limited their application, for instance, strain and pressure sensors need to tolerate cyclic compression or stretching, therefore, the devices must have excellent mechanical properties to ensure the accuracy of the data acquired and the durability of the sensor.<sup>21</sup>

Furthermore, hydrogels have attracted considerable attention in emerging fields like soft robotics based on their excellent features including flexibility, stretchability, transparency and biocompatibility. For these purposes, mechanically strong hydrogels which can tolerate cyclic large deformations are also required. For these purposes, mechanically strong hydrogels which can tolerate cyclic large deformations are also required.

For all these requirements, many hydrogel systems have been investigated to develop mechanically strong hydrogels. Examples are nanocomposite hydrogels,<sup>23</sup> topological hydrogels,<sup>24</sup> hydrophobic association hydrogels<sup>25</sup>, and double network hydrogels (DN gels)<sup>26</sup>.

## 2.2 Double network hydrogels

It is noteworthy that natural hydrogels of bio-tissues consist of multi-components with multi-scale hierarchical structures. 15 By this, they are soft and strong at the same time. They have low modulus at small strain while they exhibit high modulus at large strain; in contrast, synthetic SN gels are usually weak.<sup>15</sup> The articular cartilage, which is mainly composed of water (around 70 wt.%), collagen (around 20 wt.%) and proteoglycan (around 10 wt.%) with a fracture modulus over 10 MPa under compression,<sup>27</sup> can maintain its structure and function after subjected to daily compressive force up to 20 MPa for lifetime. <sup>28</sup> The excellent mechanical performance of articular cartilage is attributed to the interpenetrating network structure formed by collagen and proteoglycan aggregates.<sup>29</sup> As shown in **Scheme 1**, collagen consists of three polypeptide chains which twist tightly into a rope-like triple helix structure stabilised by hydrogen bonds;<sup>27, 28</sup> while each proteoglycan has a bottle-brush-like structure formed by as many as 100 chondroitin sulfate and 30 keratan sulfate side chains which are linked laterally to a core protein, and proteoglycan aggregate is formed by many proteoglycans bonded with a hyaluronic acid backbone by link protein.<sup>28</sup> The flexible proteoglycan aggregates network tends to spread out due to the mutual repulsion between negatively charged proteoglycan molecules, and they are immobilised in the rigid collagen framework without a chance to move out of tissue.<sup>29</sup>



**Scheme 1.** Simplified illustration for network structure of articular cartilage (modified according to literature<sup>30</sup>). Other components including chondrocytes, non-collagenous proteins, and glycoproteins, etc., are omitted.

Inspired by the excellent mechanical performance of load-bearing bio-tissues, the theory of DN gels was first proposed by Gong group in 2003.<sup>26</sup> For such high performance, the double networks, typically, the first network is made of a strongly crosslinked polyelectrolyte, while the second network is made of a loosely crosslinked neutral polymer with a molar concentration of 20 to 30 times of the first network. <sup>16</sup> This type of DN gels were prepared by a two-step polymerization process: firstly the first network is formed by the reaction of monomer, initiator and crosslinker, and secondly the first gel is immersed into the precursor solution of the second network which is crosslinked successively within the first network. After the two-step crosslinking, the first network interpenetrates the second network and remains under strain. Upon deformation, the first network is broken into small clusters and dissipates large amount of energy, and then these clusters present as elastic filler of the flexible second network. The first network work as sacrificial bonds to make the double network tough.<sup>31</sup> Since the DN theory was proposed, various material combinations, crosslinking strategies, and potential biomedical applications had been extensively investigated.<sup>32</sup>

Neutral polymers often do not swell strongly in monomer solutions, therefore, it can be difficult to use them as the first network polymer to make strong hydrogels directly from the combination of two neutral polymers. To further extend the range of polymers which can be used to build tough DN gels, a molecular stent technique<sup>33</sup> was proposed: introduce a linear polyelectrolyte to entangle with the neutral polymer network as the first network to highly expand and swell this composite network in the second monomer solution by the increased osmotic pressure.

According to the types of crosslinking of the two constituent networks, DN gels can be classified into full-interpenetrating DN gels (full-IPNs), semi-interpenetrating DN gels (semi-IPNs), and mechanical blends.<sup>34, 35</sup> Full-IPNs consist of two or more chemically crosslinked networks which interpenetrate into but do not chemically bonded with each other, therefore, any one of the constituent networks cannot be removed without breaking chemical bonds; in contrast, semi-IPNs are made of two networks but only one of the network is chemically crosslinked, therefore, the separation of the two networks do not need to break the chemical bonds. The mechanical blends refer to the mixture of two or more polymers without any chemical crosslinking.

## 2.3 Thermoresponsive double network hydrogels

Thermoresponsive hydrogels are probably the most extensively studied stimulus-responsive hydrogels, because their properties can be easily controlled by small variation of local temperature, which can be manipulated by numerous methods.<sup>36, 37</sup> If such hydrogels are filled with magnetic nanoparticles or photo-thermal agents, the local temperature can be controlled remotely by applying external magnetic field<sup>38</sup> or near

infrared laser irradiation<sup>39</sup>, so that the swelling ratio and other properties of hydrogels can be manipulated.

Thermoresponsive double network hydrogels (T-DN gels), which combine the superior mechanical properties of DN gels with the easy-to-control feature of thermoresponsive hydrogels, have drawn much attention in diverse fields including biosensor, <sup>40</sup> soft robotics, <sup>41</sup> drug delivery, <sup>42</sup> and 4D printing, <sup>43</sup> etc.

To make mechanically strong T-DN gels, the combination of a thermoresponsive polymer and a non-thermoresponsive polymer were usually used. 41, 44-51

As early as the year of 1994, Gutowska et al. had already proposed the concept of T-DN gels. They prepared semi-IPNs consisting of crosslinked poly(*N*-isopropylacrylamide) (PNIPAM) and physically entangled linear poly(ether urethaneurea) (Biomer). With higher content of hydrophobic Biomer, the compression modulus of semi-IPNs could be increased to around ten times that of PNIPAM SN gels due to the higher apparent crosslinking density and lower degree of swelling. The thermosensitivity was reduced compared with the PNIPAM SN gels whereas the VPTT was unchanged.

Krakovský et al. prepared a series of T-DN gels consisting of thermoresponsive PNIPAM first network with varying crosslinking densities and hydrophilic polyacrylamide (PAAm) second network with constant crosslinking density. It was observed that incorporation of the hydrophilic second network could reinforce the shear modulus but lower the thermosensitivity regardless of the crosslinking density of the thermoresponsive first network; and the shear modulus of these T-DN gels was positively correlated with the crosslinking density of the first network.

Muniz et al. prepared thermoresponsive semi-IPNs consisting of chemically crosslinked PAAm and physically entangled PNIPAM.<sup>46, 47</sup> Temperature-dependent permeability<sup>46</sup> and compressive elastic modulus<sup>47</sup> of these semi-IPNs were comprehensively investigated. Compared with the crosslinked PAAm SN gel, the semi-IPNs had lower equilibrium degree of swelling, higher polymer volume fraction as well as higher apparent crosslinking density due to the incorporation of relatively more hydrophobic PNIPAM; at higher temperatures above the LCST (32°C), although no large shrinking was observed due to the supporting effect of the crosslinked PAAm network for the collapsed PNIPAM chains,<sup>47</sup> the permeability of the semi-IPNs to model drug was largely increased because of the increased pore volume and amount of water expelled resulted by the collapse of PNIPAM chains, which could enhance the diffusion of the model drug,<sup>46</sup> and the semi-IPNs exhibited higher compressive elastic modulus owing to the entangled PNIPAM chains collapsing around the PAAm network as a solid filler.<sup>47</sup>

Boon-in et al. fabricated T-DN gels composed of poly(2-acrylamido-2-methyl-1-propanesulfonic acid) (PAMPS) as the first network and PNIPAM as the second network to serve as flexible and strong dressings which could provide prolonged cooling at above 32°C for inflamed skins to relieve pain and dissipate the heat caused by inflammation.<sup>48</sup> Incorporation of the PAMPS led to stronger DN gels with a storage modulus of 3850 Pa, which was around three times that of PNIPAM SN gel (1315 Pa), and also led to more prolonged cooling.

Zheng et al. designed T-DN gels composed of physically crosslinked alginate and chemically crosslinked PNIPAM for all-hydrogel soft robotics. <sup>41</sup> Tunable LCST (22.5°C to 32°C) and enhanced mechanical properties (compressive stress of 6.3 MPa and

uniaxial stretch of 9.95) were accomplished by optimizing the concentration of the AlCl<sub>3</sub> used for preparation. The (Na-alginate/PNIPAM)/(Al-alginate/PNIPAM) bilayer hydrogel actuator could be actuated above 22.5°C and grip an object when made into a four-arm shape.

Means et al. developed a T-DN gel exhibiting ultra-high compressive strength around 23 MPa and compressive modulus around 1.5 MPa by using tightly crosslinked and highly negatively charged PAMPS as the first network, and loosely crosslinked thermoresponsive and zwitterionic P(NIPAM-co-MEDSAH), a copolymer of NIPAM [2-(methacryloyloxy)ethyl]dimethyl-(3-sulfopropyl)ammonium and hydroxide (MEDSAH) as the second network.<sup>49</sup> Apart from the excellent mechanical properties, which were ascribed to the intra-network ionic interactions of the highly negatively charged first network and zwitterionic second network as well as the inter-network ionic this DN gel interactions between the two networks, also retained the thermoresponsiveness of PNIPAM hydrogel and had a VPTT of around 35°C, which make it a promising candidate for thermoresponsive smart materials.

Li et al. fabricated T-DN gels composed of poly(2-acrylamido-2-methylpropanesulfonic acid sodium salt) (PNaAMPS) as the rigid and brittle first network and poly(*N*-isopropyl acrylamide-*co*-acrylamide) (P(NIPAM-*co*-AAm)) as the soft and ductile second network.<sup>50</sup> It was proved that these T-DN gels exhibited desirable thermally controlled swelling properties, good biocompatibility, and antibacterial functions for biomedical applications like wound dressing and skin replacement. The optimized DN gel exhibited excellent mechanical properties with a tensile strength of 1.37 MPa, elongation fracture strain of 673.3%, and elastic modulus of 0.76 MPa.

Guo et al. fabricated two topologically opposite semi-IPNs by the combination of hydrophilic poly(*N*,*N*-dimethylacrylamide) (PDMA) and thermoresponsive PNIPAM with the same polymer compositions and investigated the differences in their thermoresponsive properties.<sup>51</sup> It was demonstrated that in swollen isochoric condition, the thermo-toughening effect of the semi-IPN with crosslinked PNIPAM was much more notable than that of the semi-IPN with crosslinked PDMA. When the temperature was increased from 20°C to 60°C, semi-IPN with crosslinked PNIPAM had a 10 times increase in the elastic modulus and much higher fracture energy; while the semi-IPN with crosslinked PDMA only had 3 times increase in the elastic modulus and little higher fracture energy.

The combination of two thermoresponsive polymers could also lead to mechanically strong T-DN gels. 40, 42, 52-56

X. Zhang et al. reported T-DN gels consisting of two chemically crosslinked PNIPAM networks to make an easy-to-remove drug-carrier with better thermosensitivity and more sustained drug release profile. The polymer content of the first network was kept constant while that of the second network was varied. Compared with the PNIPAM SN gels, these full-IPNs exhibited almost unchanged LCSTs, higher glass transition temperatures, higher thermosensitivity, enhanced mechanical performance, and more sustained drug release profile. The compression and tensile modulus of the PNIPAM based T-DN gels were positively correlated with the content of the second network component, and could reach 13.34 kPa and 33 kPa, which were times higher than that of the single network PNIPAM hydrogel, 3.8 kPa and 1.96 kPa, respectively. The contribution of the second network to the excellent mechanical properties of the T-DN

gels were attributed to the increase in polymer mass per volume, the enhancement in the intermolecular and intramolecular interactions as well as the interlocking between the two networks.

Fei et al. designed PNIPAM T-DN gels consisting of two PNIPAM networks with different crosslinking densities, then they prepared micropillar arrays using these T-DN gels by UV-assisted micropatterning technique to improve the thermoresponsitivity for more efficient thermally modulated cell release.<sup>52</sup> To achieve high equilibrium degree of swelling, Fei et al. prepared PNIPAM T-DN gels incorporated with polysiloxane nanoparticles which were added during the formation of the first network or the second network,<sup>53</sup> by varying the composition, it was found that the DN gel which was loaded with polysiloxane nanoparticles (around 200 nm in diameter) during the formation of the first network, exhibited optimal performance including higher equilibrium degree of swelling, higher thermosensitivity than the SN and DN PNIPAM gels, as well as higher modulus, strength and fracture strain compared with PNIPAM SN gel.

Furthermore, Fei et al. developed ultra-strong T-DN gels by the combination of tightly crosslinked ionized P(NIPAM-co-AMPS) comprised of different amounts of AMPS (100:0 to 25:75 wt.% ratio of NIPAM:AMPS) as the first network and loosely crosslinked PNIPAM as the second network.<sup>54</sup> It was observed that these T-DN gels had higher thermosensitivity with an around 1°C lower VPTT compared with the PNIPAM-based SN gel and T-DN gel; higher AMPS content resulted in improved water uptake capacity, lower extent and rate of deswelling, as well as enhanced reswelling behavior. An ultra-strong hydrogel, which had an ultimate compressive strength (17.5 MPa), high compressive modulus (0.085 MPa) as well as high fracture strain (95%) at 25°C, was

accomplished by using NIPAM:AMPS at a mass ratio of 25:75 wt.% for the first network. The aforementioned T-DN gels were further investigated to assess their potential to be used as self-cleaning membranes for implanted glucose biosensors, <sup>40</sup> for this application, small amount (1-2 wt.%) of *N*-vinylpyrrolidone (NVP) comonomer was incorporated into the PNIPAM network to raise the VPTT over 38°C in order to keep the T-DN gels in the maximum swollen state when implanted into the tissue to guarantee that the glucose diffusion was maximized. It was proved that this type of T-DN gels had enhanced mechanical properties, good cytocompatibility, and high thermosensitivity, and owing to these features, they could achieve thermally driven cell detachment from the gel surface to maintain glucose diffusion and thus elongate the lifetime of implanted glucose biosensors.

C. Liu et al. prepared nanocomposite T-DN gels composed of starch-based microspheres crosslinked oligo (ethylene glycol) methyl ether methacrylate (POEGMA) and diethylene glycol dimethacrylate (DEGMA) crosslinked poly(2-(2-methoxyethoxy) ethyl methacrylate) (PMEO<sub>2</sub>MA) by two-step free radical polymerization.<sup>55</sup> Interestingly, the DN gels only went through a volume phase transition at 20.2°C (the LCST of PMEO<sub>2</sub>MA) without further collapse at 68.0°C (the LCST of POEGMA) due to the homogeneity of both networks. Incorporation of these starch-based microspheres could enhance the physical adherence and entanglements between the microspheres and the polymer network and thus make the networks more perfect; meanwhile, it could also bring in larger internal friction to avoid fracture caused by stretching. The T-DN gel with optimized composition exhibited high toughness (91.1 ± 1.2 kJ/m³), fracture stress (49.2

 $\pm$  0.7 kPa), elastic modulus (8.1  $\pm$  0.3 kPa) as well as large fracture strain (5.7  $\pm$  0.1) under stretching.

Hanyková et al. prepared T-DN gels consisting of highly crosslinked thermoresponsive poly(*N*,*N*'-diethylacrylamide) (PDEAAm) as the first network and loosely crosslinked PDEAAm or PAAm or PAMPS as the second network. <sup>56</sup> It was observed that the thermosensitivity of these T-DN gels could be lowered by non-thermoresponsive polymers (PAAm or PAMPS), but enhanced by the PDEAAm in the second network. For the high swelling ratio of PAMPS, the temperature-dependent deswelling of the T-DN gels was severely hindered; therefore, the thermosensitivity decreased dramatically with increasing amount of PAMPS until disappeared. For the PDEAAm/PDEAAm or PDEAAm/PAAm T-DN gels, the Young's modulus could reach 2-3 times that of the PDEAAm SN gels and decrease with the increasing swelling ratio for each type of DN gels.

Apart from enhancing the mechanical properties, T-DN gels were also designed to tailor other properties of SN gels to improve their utility or efficacy for various applications. <sup>57-63</sup>

Z. Liu et al. reported T-DN gels made of xanthan gum (XG) and methylcellulose (MC) from aqueous solution.<sup>57</sup> At room temperature, the XG/MC blend solution could flow and became injectable under applied stress owing to the shear thinning property of XG. At 37°C the samples formed a gel due to the thermal gelation property of MC. The T-DN gels had good biocompatibility and biodegradability as well, which indicated that

these T-DN gels had the potential to serve as injectable drug carriers to realize temperature controlled drug delivery.

For a PNIPAM SN gel, the response rate to temperature change is slow due to the formation of a dense skin layer at the shrinking course.<sup>64</sup> To achieve more rapid response rate to temperature change, Li et al. studied T-DN gels consisting of guar gum (GG) and PNIPAM.<sup>58</sup> By introducing hydrophilic GG component into the PNIPAM network, the temperature sensitivity and permeability of the thermoresponsive hydrogel was improved, which could allow the T-DN gel to be used for establishing controlled drug delivery system for specific-colonic drug release.

Lu et al. fabricated T-DN gels consisting of poly(methyl methacrylate) (PMMA) and PNIPAM.<sup>59</sup> This type of DN gels exhibited good thermosensitivity and lower final water retention at 37°C, as well as slower methylene blue release rate compared with the crosslinked PNIPAM SN gel.

Wang et al. investigated both the semi-IPNs consisting of glutaraldehyde crosslinked chitosan with non-crosslinked PNIPAM,<sup>60</sup> and the full-IPNs composed of formaldehyde crosslinked chitosan and methylene bis-acrylamide crosslinked PNIPAM.<sup>61</sup> Both the semi-IPNs and the full-IPNs were sensitive to the temperature change, but unlike other PNIPAM-based hydrogels which would shrink above volume transition temperature, their thermosensitivity resulted in the change of transparency, i.e., they kept transparent at low temperatures while turned opaque above their transition temperatures (32°C for semi-IPNs and 30°C for full-IPNs); as with other properties (e.g., swelling behavior of hydrogels), the incorporation of the PNIPAM had significant influence in that

of the full-IPNs but little influence in that of semi-IPNs; these IPNs may have the potential to be applied in hydrogel devices or soft robotics.<sup>60,61</sup>

J. Zhang et al. fabricated semi-IPNs by the combination of non-crosslinked poly(vinyl alcohol) (PVA) with crosslinked PNIPAM to make hydrogels with extremely high temperature response rate which could be very important for the performance of chemical sensors and artificial organs. The incorporation of PVA endowed these semi-IPNs with higher equilibrium swelling, significant faster response rate, and full deswelling in one minute above LCST of PNIPAM.

Käfer et al. designed T-DN gels by the combination of thermophilic poly(*N*-acryloyl glycinamide) (PNAGA) and thermophobic PNIPAM.<sup>63</sup> By increasing the weight ratio of PNIPAM to NAGA, the thermoresponsive behavior of these T-DN gels changed from thermophilic volume phase transition to double thermoresponsive behavior (i.e., the temperature-dependent volume change curve was determined by the co-contribution of the thermoresponsiveness of PNAGA and PNIPAM).

Moreover, various characterization methods were used to improve the understanding of structures and properties of T-DN gels as well as establish theoretical models for them. 65-73

Furthermore, temperature- and pH- dual responsive DN gels were prepared for more versatile applications. <sup>74-77</sup>

Above all, tens of different combinations of materials have been investigated to produce T-DN gels, but still many issues remain to be solved, in particular, only limited

pairs of combinations of polymers have been studied, and the thermoresponsive networks were mainly PNIPAM or its modified type (e.g., copolymers containing NIPAM units).

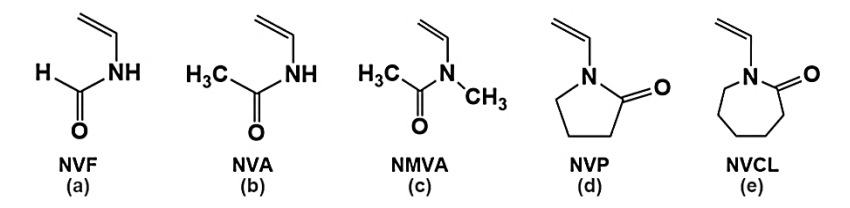
However, it has been proved that PNIPAM is potentially cytotoxic,<sup>78</sup> and the cytotoxicity of PNIPAM could be attributed to the potentially existing low molecular weight amino compounds resulted by hydrolysis.<sup>79</sup> Therefore, new thermoresponsive polymers are strongly desired for T-DN gels designed for biomedical applications.

#### 2.4 Thermoresponsive *N*-alkylated poly(*N*-vinylamide)s

Poly(*N*-vinylamide)s, a class of water-soluble carbon chain polymers with amide groups in side substitutes, are expected to serve as the alternatives of polyacrylamides for possessing the isomeric structures, and be used as models of natural polyamides (e.g., proteins). Rolling Polyvinylpyrrolidone (PVP), which was first developed by Walter Reppe and his colleagues in BASF during the 1930s and used as blood plasma substitute in World War II, is probably the most well-known poly(*N*-vinylamide) and has been used in diverse fields including but not limited to pharmaceuticals, cosmetics, and textiles. Poly(*N*-vinylcaprolactam) (PNVCL) is another popular poly(*N*-vinylamide), which has also been broadly investigated for biomedical applications owing to its thermoresponsive behavior with an LCST which is close to body temperature (ranging from 32°C to 35°C) and can be manipulated by varying the degree of polymerization or concentration.

Structures of representative *N*-vinylamide monomers are shown in **Scheme 2**. The large-scale synthesis of *N*-vinylamide monomers are challenging: for instance, it took researchers years to solve the problem in purifying NVF by distillation on large scale, until a special chaser was invented and adopted in the system,<sup>84</sup> and NMVA monomer

was the only N-vinylamide monomer that had been produced on industrial scale till the year of 1998.  $^{80}$ 



**Scheme 2.** Structures of representative *N*-vinylamide monomers. (a) *N*-vinylformamide (NVF); (b) *N*-vinylacetamide (NVA); (c) *N*-methyl-*N*-vinylacetamide (NMVA); (d) *N*-vinylpyrrolidone (NVP); (e) *N*-vinylcaprolactam (NVCL).

Among the representative *N*-vinylamide monomers, only *N*-vinylacetamide (NVA) and *N*-vinylformamide (NVF) are able to be readily modified by *N*-substitution at the amide position, therefore we are particularly interested in their corresponding polymers, PNVA and PNVF, both of which are of good biocompatibility. <sup>85, 86</sup> Functional groups can be linked with PNVA or PNVF by direct *N*-substitution at the amide position or reactions with the *N*-vinylamine units which can be obtained by hydrolysis of PNVA or PNVF. <sup>81,87</sup> Some of alkylated PNVAs and PNVFs have been proved as LCST-type polymers, <sup>88-91</sup> therefore, they are expected to work as ideal alternatives for PNIPAM to make T-DN gels with enhanced mechanical performance.

#### 2.5 References

[1] Kopeček, J. Swell gels. Nature 2002, 417 (6887), 389-391. DOI: 10.1038/417388a.

[2] Li, J.; Mooney, D. J. Designing hydrogels for controlled drug delivery. *Nature Reviews Materials* **2016**, *1* (12), 16071. DOI: 10.1038/natrevmats.2016.71.

[3] Brumberg, V.; Astrelina, T.; Malivanova, T.; Samoilov, A. Modern Wound Dressings: Hydrogel Dressings. *Biomedicines* **2021**, *9* (9), 1235. DOI: 10.3390/biomedicines9091235.

- [4] Lee, K. Y.; Mooney, D. J. Hydrogels for Tissue Engineering. *Chemical Reviews* **2001**, *101* (7), 1869-1880. DOI: 10.1021/cr000108x.
- [5] Li, Z.; Cheng, H.; Ke, L.; Liu, M.; Wang, C.-G.; Jun Loh, X.; Li, Z.; Wu, Y.-L. Recent Advances in New Copolymer Hydrogel-Formed Contact Lenses for Ophthalmic Drug Delivery. *ChemNanoMat* **2021**, *7* (6), 564-579. DOI: 10.1002/cnma.202100008.
- [6] Mistry, P. A.; Konar, M. N.; Latha, S.; Chadha, U.; Bhardwaj, P.; Eticha, T. K. Chitosan Superabsorbent Biopolymers in Sanitary and Hygiene Applications. *International Journal of Polymer Science* **2023**, 2023, 4717905. DOI: 10.1155/2023/4717905.
- [7] Sun, X.; Agate, S.; Salem, K. S.; Lucia, L.; Pal, L. Hydrogel-Based Sensor Networks: Compositions, Properties, and Applications—A Review. *ACS Applied Bio Materials* **2021**, *4* (1), 140-162. DOI: 10.1021/acsabm.0c01011.
- [8] Liu, X.; Liu, J.; Lin, S.; Zhao, X. Hydrogel machines. *Materials Today* **2020**, *36*, 102-124. DOI: 10.1016/j.mattod.2019.12.026.
- [9] Lee, Y.; Song, W. J.; Sun, J. Y. Hydrogel soft robotics. *Materials Today Physics* **2020**, *15*, 100258. DOI: 10.1016/j.mtphys.2020.100258.
- [10] Sánchez-Cid, P.; Jiménez-Rosado, M.; Romero, A.; Pérez-Puyana, V. Novel Trends in Hydrogel Development for Biomedical Applications: A Review. *Polymers* **2022**, *14* (15), 3023. DOI: 10.3390/polym14153023.
- [11] Cascone, S.; Lamberti, G. Hydrogel-based commercial products for biomedical applications: A review. *International Journal of Pharmaceutics* **2020**, *573*, 118803. DOI: 10.1016/j.ijpharm.2019.118803.
- [12] Thakur, S.; Thakur, V. K.; Arotiba, O. A. History, Classification, Properties and Application of Hydrogels: An Overview. In *Hydrogels: Recent Advances*, Thakur, V. K., Thakur, M. K. Eds.; Springer Singapore, 2018; pp 29-50. DOI: 10.1007/978-981-10-6077-9\_2.
- [13] Du, J.; Zhang, Y.; Huang, Y.; Zhang, Q.; Wang, W.; Yu, M.; Xu, L.; Xu, J. Dual-Cross-Linked Chitosan-Based Antibacterial Hydrogels with Tough and Adhesive Properties for Wound Dressing. *Macromolecular Rapid Communications* **2023**, *44* (23), 2300325. DOI: 10.1002/marc.202300325.

- [14] Chen, G.; Huang, J.; Gu, J.; Peng, S.; Xiang, X.; Chen, K.; Yang, X.; Guan, L.; Jiang, X.; Hou, L. Highly tough supramolecular double network hydrogel electrolytes for an artificial flexible and low-temperature tolerant sensor. *Journal of Materials Chemistry A* **2020**, *8* (14), 6776-6784. DOI: 10.1039/D0TA00002G.
- [15] Kuang, X.; Arıcan, M. O.; Zhou, T.; Zhao, X.; Zhang, Y. S. Functional Tough Hydrogels: Design, Processing, and Biomedical Applications. *Accounts of Materials Research* **2023**, *4* (2), 101-114. DOI: 10.1021/accountsmr.2c00026.
- [16] Gong, J. P. Why are double network hydrogels so tough? *Soft Matter* **2010**, *6* (12), 2583-2590. DOI: 10.1039/B924290B.
- [17] Na, Y. H. Double network hydrogels with extremely high toughness and their applications. *Korea-Australia Rheology Journal* **2013**, *25* (4), 185-196. DOI: 10.1007/s13367-013-0020-y.
- [18] Dou, C.; Li, Z.; Luo, Y.; Gong, J.; Li, Q.; Zhang, J.; Zhang, Q.; Qiao, C. Bio-based poly (γ-glutamic acid)-gelatin double-network hydrogel with high strength for wound healing. *International Journal of Biological Macromolecules* **2022**, *202*, 438-452. DOI: 10.1016/j.ijbiomac.2022.01.057.
- [19] He, Y.; Li, Y.; Sun, Y.; Zhao, S.; Feng, M.; Xu, G.; Zhu, H.; Ji, P.; Mao, H.; He, Y.; et al. A double-network polysaccharide-based composite hydrogel for skin wound healing. *Carbohydrate Polymers* **2021**, *261*, 117870. DOI: 10.1016/j.carbpol.2021.117870.
- [20] Guo, Z.; Liu, W.; Tang, A. Stretchable, adhesive, antifreezing and 3D printable double-network hydrogel for flexible strain sensors. *European Polymer Journal* **2022**, *164*, 110977. DOI: 10.1016/j.eurpolymj.2021.110977.
- [21] Ling, Q.; Ke, T.; Liu, W.; Ren, Z.; Zhao, L.; Gu, H. Tough, Repeatedly Adhesive, Cyclic Compression-Stable, and Conductive Dual-Network Hydrogel Sensors for Human Health Monitoring. *Industrial & Engineering Chemistry Research* **2021**, *60* (50), 18373-18383. DOI: 10.1021/acs.iecr.1c03358.
- [22] Zhalmuratova, D.; Chung, H.-J. Reinforced Gels and Elastomers for Biomedical and Soft Robotics Applications. *ACS Applied Polymer Materials* **2020**, *2* (3), 1073-1091. DOI: 10.1021/acsapm.9b01078.

- [23] Haraguchi, K.; Takehisa, T. Nanocomposite Hydrogels: A Unique Organic–Inorganic Network Structure with Extraordinary Mechanical, Optical, and Swelling/Deswelling Properties. *Advanced Materials* **2002**, *14* (16), 1120-1124. DOI: 10.1002/1521-4095(20020816)14:16<1120::AID-ADMA1120>3.0.CO;2-9.
- [24] Okumura, Y.; Ito, K. The Polyrotaxane Gel: A Topological Gel by Figure-of-Eight Cross-links. *Advanced Materials* **2001**, *13* (7), 485-487. DOI: 10.1002/1521-4095(200104)13:7<485::AID-ADMA485>3.0.CO;2-T.
- [25] Jiang, H.; Duan, L.; Ren, X.; Gao, G. Hydrophobic association hydrogels with excellent mechanical and self-healing properties. *European Polymer Journal* **2019**, *112*, 660-669. DOI: 10.1016/j.eurpolymj.2018.10.031.
- [26] Gong, J. P.; Katsuyama, Y.; Kurokawa, T.; Osada, Y. Double-Network Hydrogels with Extremely High Mechanical Strength. *Advanced Materials* **2003**, *15* (14), 1155-1158. DOI: 10.1002/adma.200304907.
- [27] Kempson, G. E. 5 The Mechanical Properties of Articular Cartilage. In *The Joints and Synovial Fluid*, Sokoloff, L. Ed.; Academic Press, 1980; pp 177-238. DOI: 10.1016/B978-0-12-655102-0.50011-4.
- [28] Muir, H. The chondrocyte, architect of cartilage. Biomechanics, structure, function and molecular biology of cartilage matrix macromolecules. *BioEssays* **1995**, *17* (12), 1039-1048. DOI: 10.1002/bies.950171208.
- [29] Mansour, J. M. Biomechanics of cartilage. *Kinesiology: the mechanics and pathomechanics of human movement* **2003**, *2*, 66-79.
- [30] Sophia Fox, A. J.; Bedi, A.; Rodeo, S. A. The Basic Science of Articular Cartilage: Structure, Composition, and Function. *Sports Health* **2009**, *1* (6), 461-468. DOI: 10.1177/1941738109350438.
- [31] Nonoyama, T.; Gong, J. P. Double-network hydrogel and its potential biomedical application: A review. *Proceedings of the Institution of Mechanical Engineers, Part H: Journal of Engineering in Medicine* **2015**, 229 (12), 853-863. DOI: 10.1177/0954411915606935.
- [32] Xin, H. Double-Network Tough Hydrogels: A Brief Review on Achievements and Challenges. In *Gels*, 2022; Vol. 8.

- [33] Nakajima, T.; Sato, H.; Zhao, Y.; Kawahara, S.; Kurokawa, T.; Sugahara, K.; Gong, J. P. A Universal Molecular Stent Method to Toughen any Hydrogels Based on Double Network Concept. *Advanced Functional Materials* **2012**, *22* (21), 4426-4432. DOI: 10.1002/adfm.201200809.
- [34] Dragan, E. S. Advances in interpenetrating polymer network hydrogels and their applications. *Pure and Applied Chemistry* **2014**, *86* (11), 1707-1721. DOI: doi:10.1515/pac-2014-0713.
- [35] Zoratto, N.; Matricardi, P. 4 Semi-IPNs and IP*N*-based hydrogels. In *Polymeric Gels*, Pal, K., Banerjee, I. Eds.; Woodhead Publishing, 2018; pp 91-124. DOI: 10.1016/B978-0-08-102179-8.00004-1.
- [36] Klouda, L. Thermoresponsive hydrogels in biomedical applications: A seven-year update. *European Journal of Pharmaceutics and Biopharmaceutics* **2015**, *97*, 338-349. DOI: 10.1016/j.ejpb.2015.05.017.
- [37] Koetting, M. C.; Peters, J. T.; Steichen, S. D.; Peppas, N. A. Stimulus-responsive hydrogels: Theory, modern advances, and applications. *Materials Science and Engineering: R: Reports* **2015**, *93*, 1-49. DOI: 10.1016/j.mser.2015.04.001.
- [38] Brazel, C. S. Magnetothermally-responsive Nanomaterials: Combining Magnetic Nanostructures and Thermally-Sensitive Polymers for Triggered Drug Release. *Pharmaceutical Research* **2009**, *26* (3), 644-656. DOI: 10.1007/s11095-008-9773-2.
- [39] Wang, L.; Li, B.; Xu, F.; Xu, Z.; Wei, D.; Feng, Y.; Wang, Y.; Jia, D.; Zhou, Y. UV-crosslinkable and thermo-responsive chitosan hybrid hydrogel for NIR-triggered localized on-demand drug delivery. *Carbohydrate Polymers* **2017**, *174*, 904-914. DOI: 10.1016/j.carbpol.2017.07.013.
- [40] Fei, R.; Means, A. K.; Abraham, A. A.; Locke, A. K.; Coté, G. L.; Grunlan, M. A. Self-Cleaning, Thermoresponsive P(NIPAAm-co-AMPS) Double Network Membranes for Implanted Glucose Biosensors. *Macromolecular Materials and Engineering* **2016**, *301* (8), 935-943. DOI: 10.1002/mame.201600044.
- [41] Zheng, W. J.; An, N.; Yang, J. H.; Zhou, J.; Chen, Y. M. Tough Al-alginate/Poly(*N*-isopropylacrylamide) Hydrogel with Tunable LCST for Soft Robotics. *ACS Applied Materials & Interfaces* **2015**, *7* (3), 1758-1764. DOI: 10.1021/am507339r.

- [42] Zhang, X.-Z.; Wu, D.-Q.; Chu, C.-C. Synthesis, characterization and controlled drug release of thermosensitive IPN–PNIPAAm hydrogels. *Biomaterials* **2004**, *25* (17), 3793-3805. DOI: 10.1016/j.biomaterials.2003.10.065.
- [43] Guo, J.; Zhang, R.; Zhang, L.; Cao, X. 4D Printing of Robust Hydrogels Consisted of Agarose Nanofibers and Polyacrylamide. *ACS Macro Letters* **2018**, *7* (4), 442-446. DOI: 10.1021/acsmacrolett.7b00957.
- [44] Gutowska, A.; Bae, Y. H.; Jacobs, H.; Feijen, J.; Kim, S. W. Thermosensitive Interpenetrating Polymer Networks: Synthesis, Characterization, and Macromolecular Release. *Macromolecules* **1994**, *27* (15), 4167-4175. DOI: 10.1021/ma00093a018.
- [45] Krakovský, I.; Kouřilová, H.; Hrubovský, M.; Labuta, J.; Hanyková, L. Thermoresponsive double network hydrogels composed of poly(*N*-isopropylacrylamide) and polyacrylamide. *European Polymer Journal* **2019**, *116*, 415-424. DOI: 10.1016/j.eurpolymj.2019.04.032.
- [46] Muniz, E. C.; Geuskens, G. Influence of temperature on the permeability of polyacrylamide hydrogels and semi-IPNs with poly(*N*-isopropylacrylamide). *Journal of Membrane Science* **2000**, *172* (1), 287-293. DOI: 10.1016/S0376-7388(00)00346-X.
- [47] Muniz, E. C.; Geuskens, G. Compressive Elastic Modulus of Polyacrylamide Hydrogels and Semi-IPNs with Poly(*N*-isopropylacrylamide). *Macromolecules* **2001**, *34* (13), 4480-4484. DOI: 10.1021/ma0011921.
- [48] Boon-in, S.; Theerasilp, M.; Crespy, D. Temperature-Responsive Double-Network Cooling Hydrogels. *ACS Applied Polymer Materials* **2023**, *5* (4), 2562-2574. DOI: 10.1021/acsapm.2c02189.
- [49] Means, A. K.; Ehrhardt, D. A.; Whitney, L. V.; Grunlan, M. A. Thermoresponsive Double Network Hydrogels with Exceptional Compressive Mechanical Properties. *Macromolecular Rapid Communications* **2017**, *38* (20), 1700351. DOI: 10.1002/marc.201700351.
- [50] Li, X.; Wang, Y.; Li, D.; Shu, M.; Shang, L.; Xia, M.; Huang, Y. High-strength, thermosensitive double network hydrogels with antibacterial functionality. *Soft Matter* **2021**, *17* (28), 6688-6696. DOI: 10.1039/D1SM00689D.
- [51] Guo, H.; Sanson, N.; Marcellan, A.; Hourdet, D. Thermoresponsive Toughening in LCST-Type Hydrogels: Comparison between Semi-Interpenetrated and Grafted

- Networks. *Macromolecules* **2016**, *49* (24), 9568-9577. DOI: 10.1021/acs.macromol.6b02188.
- [52] Fei, R.; Hou, H.; Munoz-Pinto, D.; Han, A.; Hahn, M. S.; Grunlan, M. A. Thermoresponsive Double Network Micropillared Hydrogels for Controlled Cell Release. *Macromolecular Bioscience* **2014**, *14* (9), 1346-1352. DOI: 10.1002/mabi.201400172.
- [53] Fei, R.; George, J. T.; Park, J.; Grunlan, M. A. Thermoresponsive nanocomposite double network hydrogels. *Soft Matter* **2012**, *8* (2), 481-487. DOI: 10.1039/C1SM06105D.
- [54] Fei, R.; George, J. T.; Park, J.; Means, A. K.; Grunlan, M. A. Ultra-strong thermoresponsive double network hydrogels. *Soft Matter* **2013**, *9* (10), 2912-2919. DOI: 10.1039/C3SM27226E.
- [55] Liu, C.; Tan, Y.; Xu, K.; Hua, M.; Huo, X.-H.; Sun, Y.-S. A novel designed high strength and thermoresponsive double network hydrogels cross-linked by starch-based microspheres. *Iranian Polymer Journal* **2018**, *27* (11), 889-897. DOI: 10.1007/s13726-018-0662-1.
- [56] Hanyková, L.; Krakovský, I.; Šťastná, J.; Ivaniuzhenkov, V.; Labuta, J. Thermal response of double network hydrogels with varied composition. *e-Polymers* **2023**, *23* (1). DOI: 10.1515/epoly-2023-0044.
- [57] Liu, Z.; Yao, P. Injectable thermo-responsive hydrogel composed of xanthan gum and methylcellulose double networks with shear-thinning property. *Carbohydrate Polymers* **2015**, *132*, 490-498. DOI: 10.1016/j.carbpol.2015.06.013.
- [58] Li, X.; Wu, W.; Liu, W. Synthesis and properties of thermo-responsive guar gum/poly(*N*-isopropylacrylamide) interpenetrating polymer network hydrogels. *Carbohydrate Polymers* **2008**, *71* (3), 394-402. DOI: 10.1016/j.carbpol.2007.06.005.
- [59] Lu, X.; Zhai, M.; Li, J.; Ha, H. Radiation preparation and thermo-response swelling of interpenetrating polymer network hydrogel composed of PNIPAAm and PMMA. *Radiation Physics and Chemistry* **2000**, *57* (3), 477-480. DOI: 10.1016/S0969-806X(99)00475-2.
- [60] Wang, M.; Qiang, J.; Fang, Y.; Hu, D.; Cui, Y.; Fu, X. Preparation and properties of chitosan-poly(*N*-isopropylacrylamide) semi-IPN hydrogels. *Journal of Polymer Science*

- *Part A: Polymer Chemistry* **2000**, *38* (3), 474-481. DOI: 10.1002/(SICI)1099-0518(20000201)38:3<474::AID-POLA12>3.0.CO;2-B.
- [61] Wang, M.; Fang, Y.; Hu, D. Preparation and properties of chitosan-poly(*N*-isopropylacrylamide) full-IPN hydrogels. *Reactive and Functional Polymers* **2001**, *48* (1), 215-221. DOI: 10.1016/S1381-5148(01)00057-8.
- [62] Zhang, J.-T.; Cheng, S.-X.; Zhuo, R.-X. Poly(vinyl alcohol)/poly(*N*-isopropylacrylamide) semi-interpenetrating polymer network hydrogels with rapid response to temperature changes. *Colloid and Polymer Science* **2003**, *281* (6), 580-583. DOI: 10.1007/s00396-002-0829-2.
- [63] Käfer, F.; Hu, Y.; Wang, Y. J.; Wu, Z. L.; Agarwal, S. Interpenetrating thermophobic and thermophilic dual responsive networks. *Journal of Polymer Science Part A: Polymer Chemistry* **2019**, *57* (4), 539-544. DOI: 10.1002/pola.29292.
- [64] Zhang, X.-Z.; Zhuo, R.-X. Dynamic Properties of Temperature-Sensitive Poly(*N*-isopropylacrylamide) Gel Cross-Linked through Siloxane Linkage. *Langmuir* **2001**, *17* (1), 12-16. DOI: 10.1021/la000170p.
- [65] Krakovský, I.; Hanyková, L.; Paladini, G.; Almásy, L. SANS and NMR study on nanostructure of thermoresponsive double network hydrogels. *European Polymer Journal* **2020**, *137*, 109929. DOI: 10.1016/j.eurpolymj.2020.109929.
- [66] Hanyková, L.; Spěváček, J.; Radecki, M.; Zhigunov, A.; Šťastná, J.; Valentová, H.; Sedláková, Z. Structures and interactions in collapsed hydrogels of thermoresponsive interpenetrating polymer networks. *Colloid and Polymer Science* **2015**, *293* (3), 709-720. DOI: 10.1007/s00396-014-3455-x.
- [67] Radecki, M.; Spěváček, J.; Zhigunov, A.; Sedláková, Z.; Hanyková, L. Temperature-induced phase transition in hydrogels of interpenetrating networks of poly(*N*-isopropylacrylamide) and polyacrylamide. *European Polymer Journal* **2015**, *68*, 68-79. DOI: 10.1016/j.eurpolymj.2015.04.019.
- [68] Šťastná, J.; Hanyková, L.; Sedláková, Z.; Valentová, H.; Spěváček, J. Temperature-induced phase transition in hydrogels of interpenetrating networks poly(*N*-isopropylmethacrylamide)/poly(*N*-isopropylacrylamide). *Colloid and Polymer Science* **2013**, *291* (10), 2409-2417. DOI: 10.1007/s00396-013-2992-z.

- [69] Hanyková, L.; Spěváček, J.; Radecki, M.; Zhigunov, A.; Kouřilová, H.; Sedláková, Z. Phase transition in hydrogels of thermoresponsive semi-interpenetrating and interpenetrating networks of poly(N,N-diethylacrylamide) and polyacrylamide. *European Polymer Journal* **2016**, *85*, 1-13. DOI: 10.1016/j.eurpolymj.2016.10.010.
- [70] Zhang, J.; Peppas, N. A. Molecular interactions in poly(methacrylic acid)/poly(*N*-isopropyl acrylamide) interpenetrating polymer networks. *Journal of Applied Polymer Science* **2001**, *82* (5), 1077-1082. DOI: 10.1002/app.1942.
- [71] Tarashi, S.; Nazockdast, H.; Bandegi, A.; Shafaghsorkh, S.; Sodeifian, G.; Foudazi, R. Large amplitude oscillatory shear behavior of thermoresponsive hydrogels: Single versus double network. *Journal of Rheology* **2023**, *67* (1), 15-33. DOI: 10.1122/8.0000457.
- [72] Dhara, D.; Rathna, G. V. N.; Chatterji, P. R. Volume Phase Transition in Interpenetrating Networks of Poly(*N*-isopropylacrylamide) with Gelatin. *Langmuir* **2000**, *16* (6), 2424-2429. DOI: 10.1021/la990065j.
- [73] Dong, P.; Schott, B. J.; Means, A. K.; Grunlan, M. A. Comb Architecture to Control the Selective Diffusivity of a Double Network Hydrogel. *ACS Applied Polymer Materials* **2020**, *2* (11), 5269-5277. DOI: 10.1021/acsapm.0c00987.
- [74] Ju, H. K.; Kim, S. Y.; Lee, Y. M. pH/temperature-responsive behaviors of semi-IPN and comb-type graft hydrogels composed of alginate and poly(*N*-isopropylacrylamide). *Polymer* **2001**, *42* (16), 6851-6857. DOI: 10.1016/S0032-3861(01)00143-4.
- [75] Kelmanovich, S. G.; Parke-Houben, R.; Frank, C. W. Competitive swelling forces and interpolymer complexation in pH- and temperature-sensitive interpenetrating network hydrogels. *Soft Matter* **2012**, *8* (31), 8137-8148, 10.1039/C2SM25389E. DOI: 10.1039/C2SM25389E.
- [76] Chen, Y.; Song, G.; Yu, J.; Wang, Y.; Zhu, J.; Hu, Z. Mechanically strong dual responsive nanocomposite double network hydrogel for controlled drug release of asprin. *Journal of the Mechanical Behavior of Biomedical Materials* **2018**, *82*, 61-69. DOI: 10.1016/j.jmbbm.2018.03.002.
- [77] Kim, A. R.; Lee, S. L.; Park, S. N. Properties and in vitro drug release of pH- and temperature-sensitive double cross-linked interpenetrating polymer network hydrogels based on hyaluronic acid/poly (*N*-isopropylacrylamide) for transdermal delivery of

- luteolin. *International Journal of Biological Macromolecules* **2018**, *118*, 731-740. DOI: 10.1016/j.ijbiomac.2018.06.061.
- [78] Vihola, H.; Laukkanen, A.; Valtola, L.; Tenhu, H.; Hirvonen, J. Cytotoxicity of thermosensitive polymers poly(*N*-isopropylacrylamide), poly(*N*-vinylcaprolactam) and amphiphilically modified poly(*N*-vinylcaprolactam). *Biomaterials* **2005**, *26* (16), 3055-3064. DOI: 10.1016/j.biomaterials.2004.09.008.
- [79] Kan, K.; Ajiro, H. Switchable Thermal Responsive Interpenetrated Polymer Network Gels of Poly(*N*-vinylacetamide) and Poly(*N*-vinylisobutyramide). *Chemistry Letters* **2018**, *47* (4), 591-593. DOI: 10.1246/cl.171191.
- [80] Kirsh, Y. E. Water Soluble Poly-*N*-Vinylamides: Synthesis and Physicochemical Properties. 1998; John Wiley & Sons, Inc.: 1998.
- [81] Pelton, R. Polyvinylamine: A Tool for Engineering Interfaces. *Langmuir* **2014**, *30* (51), 15373-15382. DOI: 10.1021/la5017214.
- [82] Luo, Y.; Hong, Y.; Shen, L.; Wu, F.; Lin, X. Multifunctional Role of Polyvinylpyrrolidone in Pharmaceutical Formulations. *AAPS PharmSciTech* **2021**, *22* (1), 34. DOI: 10.1208/s12249-020-01909-4.
- [83] Liu, J.; Debuigne, A.; Detrembleur, C.; Jérôme, C. Poly(*N*-vinylcaprolactam): A Thermoresponsive Macromolecule with Promising Future in Biomedical Field. *Advanced Healthcare Materials* **2014**, *3* (12), 1941-1968. DOI: 10.1002/adhm.201400371.
- [84] Pinschmidt Jr, R. K. Polyvinylamine at last. *Journal of Polymer Science Part A:* Polymer Chemistry **2010**, 48 (11), 2257-2283. DOI: 10.1002/pola.23992.
- [85] Ajiro, H.; Watanabe, J.; Akashi, M. Cell Adhesion and Proliferation on Poly(*N*-vinylacetamide) Hydrogels and Double Network Approaches for Changing Cellular Affinities. *Biomacromolecules* **2008**, *9* (2), 426-430. DOI: 10.1021/bm701221c.
- [86] Marhefka, J. N.; Marascalco, P. J.; Chapman, T. M.; Russell, A. J.; Kameneva, M. V. Poly(*N*-vinylformamide)A Drag-Reducing Polymer for Biomedical Applications. *Biomacromolecules* **2006**, *7* (5), 1597-1603. DOI: 10.1021/bm060014i.
- [87] Pinschmidt Jr, R. K.; Renz, W. L.; Carroll, W. E.; Yacoub, K.; Drescher, J.; Nordquist, A. F.; Chen, N. *N*-Vinylformamide Building Block for Novel Polymer Structures. *Journal of Macromolecular Science, Part A* **1997**, *34* (10), 1885-1905. DOI: 10.1080/10601329708010315.

- [88] Ajiro, H.; Takemoto, Y.; Akashi, M.; Chua, P. C.; Kelland, M. A. Study of the Kinetic Hydrate Inhibitor Performance of a Series of Poly(*N*-alkyl-*N*-vinylacetamide)s. *Energy & Fuels* **2010**, *24* (12), 6400-6410. DOI: 10.1021/ef101107r.
- [89] Kelland, M. A.; Abrahamsen, E.; Ajiro, H.; Akashi, M. Kinetic Hydrate Inhibition with *N*-Alkyl-*N*-vinylformamide Polymers: Comparison of Polymers to n-Propyl and Isopropyl Groups. *Energy & Fuels* **2015**, *29* (8), 4941-4946. DOI: 10.1021/acs.energyfuels.5b01251.
- [90] Kawatani, R.; Kan, K.; Kelland, M. A.; Akashi, M.; Ajiro, H. Remarkable Effect on Thermosensitive Behavior Regarding Alkylation at the Amide Position of Poly(*N*-vinylamide)s. *Chemistry Letters* **2016**, *45* (6), 589-591. DOI: 10.1246/cl.160145.
- [91] Zhang, Q.; Kawatani, R.; Ajiro, H.; Kelland, M. A. Optimizing the Kinetic Hydrate Inhibition Performance of *N*-Alkyl-*N*-vinylamide Copolymers. *Energy & Fuels* **2018**, *32* (4), 4925-4931. DOI: 10.1021/acs.energyfuels.8b00251.

# 3 Hydrophobic interaction within sparsely *N*-alkylated poly(*N*-vinylacetamide)s enables versatile formation of reversible hydrogels

## 3.1 Introduction

Hydrogels formed by biocompatible polymers, which get crosslinked by physical bonds, such as ionic interaction, hydrophobic association, or hydrogen-bonding, have gained wide interest for application in biology and medicine.<sup>1, 2</sup> Typically, their crosslinking elements aggregate to small domains or clusters, so that the crosslinks gain strength by multiplicity.<sup>3</sup> In the case that the binding energy  $\varepsilon$  of the associating group is strong,  $\varepsilon \gg kT$ , the lifetime of the clusters or crosslinks is practically infinite. If  $\varepsilon$  approaches kT, associating groups can be dynamically exchanged between clusters; the lifetime and strength of a crosslinking cluster depends also on the number of associating groups that form this crosslink.<sup>4,5</sup> Strain caused disruption of such a crosslinking cluster is not an irreversible catastrophic event but a sequence of rearrangements during which single cluster-constituting elements may get exchanged between adjacent clusters. This spreads the fracture stress and thus the fracture energy can be dissipated.<sup>6</sup> As a consequence, physical hydrogels can demonstrate high toughness and large strain at break.<sup>7</sup>

Multiple reversible bonding within one cluster yields another characteristic feature of such networks. When a cluster gets disrupted by strain, the driving force for its recovery serves like a memory of the original structure as long as the interacting groups do not assemble and relax in a new structure of similarly low free energy.<sup>5, 8, 9</sup> In particular in networks consisting of strong and weak crosslinks, this memory causes self-healing properties so that a deformation or even the formation of micro-cracks can be reversed. Breaking weaker crosslinks allows some yielding, while the stronger crosslinks can recover the shape of the hydrogel and direct the weaker bonds to reorganize in the original topology.<sup>5, 10</sup>

Synthetic hydrogels crosslinked by hydrophobic interactions can be classified into three groups. The first group comprises hydrogels in which water swollen domains are interpenetrated by hydrophobic domains that account for a large volume fraction  $\phi$  of the material,  $\phi > 0.2$ . These are typically statistical copolymers with amphiphilic segments. Here soft water swollen domains get held together by extended or even continuous domains and the swelling ratio is limited to a factor below 2.7, 10-12 A second group comprises triblock structures with a hydrophilic center block. In this case, the hydrophobic end blocks associate to discrete domains which act as the crosslinks. The lengths of the hydrophobic end blocks determine their size and strength of interaction. 10, 13 It is a characteristic feature of such triblock copolymers that the end groups can associate in dilute solution to form flower-like soluble micelles, while intermolecular association to gelled structures is favored at higher concentration. <sup>14</sup> As a third group, copolymers with block-wise sequences of the alkyl-substituted monomers have been achieved by a technique called micellar copolymerization where the hydrophobic monomers get pre-clustered by addition of surfactant. In all these cases, the strength of the crosslinks gets fortified significantly by crystallization for longer hydrophobic alkylsegments.15

In this work, we address reversibly crosslinked hydrogels with a small fraction of hydrophobic alkyl-substituents, which are stochastically distributed along the water soluble polymer backbone. Hydrophobic association of the alkyl substituents will be strongly confined by the topological constrictions exerted by their linkage to the polymer backbone and only few alkyl chains can assemble in a single cluster. Yet the small volume fraction of hydrophobic side chains ensures their full separation by the hydrophilic matrix as finite size crosslinks. Very small numbers of association should also suppress crystalline ordering in the case of longer side chains. Even for relatively long *n*-alkyl side chains like octadecyl substituents, the network will be connected by amorphous and thus liquid hydrophobic clusters, i.e., the side chains are sticky attachments to the hydrophilic polymer backbone, whose stickiness is systematically increased by their length.

In order to synthesize reversibly linked hydrogels as described above, we focused on poly(*N*-vinylacetamide), a structural isomer to poly(*N*-methylacrylamide) known for its excellent water solubility. The circumstance that the amine function is directly bound to the backbone opens wide possibilities for functionalization and substitution after partial hydrolysis or by direct *N*-substitution of the amide. Thus, *n*-alkyl side chains can be attached to the preformed polymer backbone. This way we avoid block formation caused by unfavorable copolymerization parameters and differences in monomer solubility, and we could alkylate only a small fraction of the monomer units (3 mol%). We could study the side chain length dependence of the strength of the hydrophobic crosslinks without interference by crystallization. We believe that these gel-forming

polymers present rather well-defined building blocks for more advanced heterogeneous hydrogel structures as exemplified in nature.

## 3.2 Experimental section

#### 3.2.1 Materials

*N*-vinylacetamide (NVA), sodium hydride (NaH) dispersed in paraffin liquid (60%), and 2,2'-azobis[2-(2-imidazolin-2-yl)propane]dihydrochloride (VA-044) were purchased from Tokyo Chemical Industry Co., Ltd. Anhydrous dimethylformamide (DMF),2,2'-azobis(2-methylpropionitrile) (AIBN, 98%), and alkyl bromides (H–(CH<sub>2</sub>)<sub>n</sub>–Br, n = 10, 12, 14, 16, 18) were bought from Sigma-Aldrich. Anhydrous tetrahydrofuran (THF) was a product of Acros Organics. Deuterated methanol and water were purchased from Deutero GmbH. P.a. level ethanol, methanol and dichloromethane were obtained from VWR. AIBN was purified by recrystallization from methanol. Deionized water (DI water) was used for all experiments.

## 3.2.2 Sample denotation

The following denotation was used for polymers:  $P_62$  and  $P_8$  represent 1.6 wt.% and 11.1 wt.% aqueous solution of the poly (*N*-vinylacetamide) (PNVA) with degree of polymerisation (DP) = 4500. PNVA<sub>xxx</sub>-C<sub>n</sub>-y represents poly(N- alkyl-N-vinylacetamide) with DP = xxx, n-alkyl side chains consisting of n methylene units,  $-(CH_2)_n$ -H, at a degree of substitution (DS) of y.

#### 3.2.3 Synthesis of poly(*N*-vinylacetamide)

Poly(N-vinylacetamide)s (PNVA) were synthesized through free radical polymerization. For PNVA with  $M_n > 50$  kDa, NVA was dissolved in water to 0.1 g/mL

at room temperature and degassed by three freeze-thaw cycles. Subsequently, the solution was heated to 60°C, and VA-044 (0.01 mol% of [NVA]) was added. The mixture was stirred at 60°C for 18 hours and precipitated in a tenfold volume of acetone. Finally, the polymer was redissolved in water and dried by lyophilisation.

For PNVA with  $M_{\rm n}$  < 50 kDa, NVA was dissolved in ethanol with AIBN (3 mol% of [NVA]) used as initiator, and the same conditions and procedure were applied.

## 3.2.4 *N*-alkylation of poly(*N*-vinylacetamide)

N-alkylation of PNVA was carried out under nitrogen gas atmosphere at water-free conditions. Firstly, PNVA was dissolved in anhydrous DMF at 60°C (60 mL/g) and cooled to room temperature for further use. NaH (60%, dispersed in paraffin liquid) was washed twice with anhydrous THF and subsequently by anhydrous DMF, and finally suspended in anhydrous DMF (30 mL/g). The suspension was kept cool in an ice bath and the DMF-solution of PNVA was added in a dropwise manner controlled by a precision syringe pump (to avoid vigorous foaming or explosion). The alkyl bromide was added either by injection (for liquid alkyl bromides) or putting in the powder directly after 30 minutes. Reaction time, temperature and stoichiometric ratios used in the synthesis procedure are listed in **Table S1**.

For work-up, methanol was added dropwisely to quench remaining NaH. Solvents were removed by rotary evaporator; the residue was re-dissolved in methanol/dichloromethane mixture (the ratios of the two solvents varied according to the hydrophobicity of the polymers), and then precipitated in a tenfold volume of acetone. The precipitate was purified by dialysis against water and dried via lyophilisation.

# 3.2.5 Nuclear magnetic resonance

High resolution  $^1$ H NMR (400 MHz) spectra were measured by a Bruker Avance III-400 spectrometer (Bruker Corporation, Billerica, MA, USA). For NMR sample preparation, the PNVA and PNVA-C<sub>n</sub>-0.03 polymers were dissolved in deuterated methanol (CD<sub>3</sub>OD), while the PNVA-C<sub>n</sub>-y ( $y \ge 0.1$ ) samples were dissolved in CD<sub>3</sub>OD/CDCl<sub>3</sub>, the ratios of the two solvents varied according to the hydrophobicity of the samples.

<sup>13</sup>C high-resolution NMR spectra were measured at T = 23°C on a wide bore AVIII500 Bruker NMR spectrometer operating at a frequency of 125.721 MHz. <sup>13</sup>C-<sup>1</sup>H cross-polarization under magic angle spinning (CP-MAS) with a rotor frequency of 5 kHz and direct polarization (DP-MAS) were used for both dry polymers and hydrogels prepared by swelling the polymers in D<sub>2</sub>O. For CP-MAS and DP-MAS measurements, <sup>13</sup>C-<sup>1</sup>H heteronuclear decoupling was employed by applying a spinal 64 pulse sequence at the proton frequency.<sup>17</sup> The <sup>13</sup>C NMR spectra were referenced externally to adamantane. The recycle delay was 10 s for DP-MAS experiments, the <sup>13</sup>C pulse length was 4 s, while the dwell time was 10 s, and the number of scans was 4096. The time domain data were 4k, and the zero filling was done with 32k. For CP-MAS experiments the contact pulses had duration of 4 ms and the recycle delay was set to 5 s. The spectral integral intensities of <sup>13</sup>C NMR spectra were determined using the Bruker software TopSpin 3.2.6. The <sup>13</sup>C spectral decomposition was processed using MestReNova (2018, Mestrelab Research S.L.) program.

## 3.2.6 Size exclusion chromatography

The size exclusion chromatography (SEC) system was equipped with a HPLC pump (1260 Infinity, Agilent), a dual refractive index/viscosity detector (ETA-200, WGE), an UV-detector (VWD, 1290 Infinity II, Agilent). SEC was performed using DMF ( $\geq$  99.9%, HPLC grade, VWR) containing 1mg/mL of LiBr ( $\geq$  99%, Sigma-Aldrich) as an eluent and 2  $\mu$ L/mL toluene ( $\geq$  99%, Sigma-Aldrich) as internal standard at a flow rate of 1 mL/min at 60°C. For separation, a precolumn (8 × 50 mm²) was combined with three GRAM gel columns (8 × 300 mm² with nominal pore widths of 30, 100, and 1000 Å, Polymer Standards Service). Narrowly distributed poly(methyl methacrylate) standards (Polymer Standards Service) were used for calibration of molecular weight. PSS WinGPC UniChrom software (Version 8.3.2) was used for the evaluation of molecular weights.

#### 3.2.7 Differential scanning calorimetry

Differential scanning calorimetry (DSC) traces were recorded with a DSC 8500 (PerkinElmer, Waltham) in the range of -30 to 230°C with a heating/cooling rate of 10°C/min in aluminum crucibles.

#### 3.2.8 Hydrogel preparation

All hydrogel samples were prepared by solution casting. Polymers were firstly dissolved in ethanol and the solution was poured into a flat-bottomed petri dish (for rheological measurements) or into glass vial (for swelling ratio measurement). After complete evaporation of the ethanol, the polymer film was immersed into large amount of water to swell.

#### 3.2.9 Swelling

To measure the degree of swelling, 100 mg of each polymer was dissolved in ethanol at 20 mg/mL in a glass vial, ethanol was removed by evaporation in a vacuum drying oven at 65°C for 48 h, and then 50 mL of deionized water was added. The vial was kept at room temperature (25°C) or 60°C for further observation and measurements. At predetermined time points, the water phase was removed and residue water was blotted by a precision wipe (Kimtech<sup>TM</sup> Science). The mass of the swollen hydrogel was determined by weighing, and mass of polymers extracted to the sol phase was weighed after freeze drying. The swelling ratio (*SR*) is calculated by **Equation 1**:

$$SR = \frac{M_{gel} - M_p}{M_p} \tag{1}$$

Where  $M_{gel}$  represents the mass of gel phase,  $M_p$  is the mass of polymer in gel phase.

We also measured the apparent swelling of the same series of polymers at  $60^{\circ}$ C. Apparent swelling ratio (ASR) is calculated by **Equation 2**:

$$ASR = \frac{M_{gel} - M_{p\_total}}{M_{p\ total}} \tag{2}$$

Where  $M_{gel}$  represents the mass of the gel phase and  $M_{p\_total}$  is the mass of the initial amount of polymer (total polymer mass in the gel phase and sol phase).

## 3.2.10 Rheology

Measurements were conducted with a shear rheometer (DHR-3, TA Instruments, USA) using a cone-plate geometry (diameter 40 mm, angle 2° and truncation 57μm) equipped with a water trap. Excess amount of hydrogels were loaded on the centre of the plate to fill up the gap space, and the hydrogels were resting and equilibrated at room

temperature until the normal axial force became negligible, then the extra amount of hydrogel was removed before measurement.

- (a) Creep recovery. At the predetermined temperature, a fixed shear stress was applied to the hydrogel samples for 180 s, followed by the relaxation period of 300 s. The strain was recorded with respect to time. No slippage or breakage of the hydrogels was observed during the test.
- (b) Stress relaxation. At the predetermined temperature a fixed strain was applied to the hydrogel sample for 200 s and the relaxation modulus was recorded with respect to time.
- (c) Shear rate sweeps were measured within the shear rate range of  $10^{-4}$  to  $10^3$  s<sup>-1</sup> at different temperatures.
- (d) Frequency sweeps were measured from  $10^{-3}$  to  $10^2$  Hz at fixed strain and at different temperatures.

#### 3.2.11 Cytotoxicity and cell adherence studies

Gel films were cast from ethanol solution, dried and subsequently swollen in water. For evaluation of the cytotoxicity of the hydrogels extract, the film of PNVA<sub>4500</sub>-C<sub>18</sub>-0.03 was immersed in culture medium (DMEM) for 36 h and the conditioned culture media was collected. Then primary human fibroblasts (NHDF) (passage 8) were seeded together with the conditioned culture medium and cultivated for 24 h and 72 h. XTT assay (ATCC) was performed to evaluate the cell viability according to the manufacturer's protocol. <sup>18</sup> Cell viability was determined by measuring the absorbance (at 490 and 630 nm) with microplate reader (SpectraMaxM3, Molecular devices, Germany).

For the evaluation of cell adherence and viability of NHDF directly seeded on the hydrogel, live-dead fluorescent assay was performed. 0.4 mg or 4 mg of the respective PNVA<sub>4500</sub>-C<sub>n</sub>-0.03 polymers were dissolved in ethanol and added to 48-well plate in fourfold implementation; ethanol was removed by evaporation in a vacuum drying oven at 65°C for 48 h. After sterilization by UV irradiation for 2 h, samples were soaked in 0.4 mL DMEM cell culture media for 48 h for further experiments. The media was collected after 48 h. 3×10<sup>4</sup> of NHDF (passage 8) were seeded on top of the hydrogel and subsequently cultured with the previously collected media. Live/dead staining was performed after 36 h of cell culture on all hydrogel samples using live/dead cell assay (Live/dead cell double staining kit, 04511-1KT-F).

## 3.3 Results and discussion

#### 3.3.1 Synthesis of polymers

PNVA- $C_n$  polymers were synthesized by *N*-alkylation of PNVAs, which were prepared by free radical polymerization (**Figure 1a**). <sup>1</sup>H NMR was used to determine the degree of alkyl side chain substitution (*DS*) of the PNVA- $C_n$  polymers, examples of peak assignments in the spectra (PNVA<sub>4500</sub> and PNVA<sub>4500</sub>- $C_{10}$ -0.03) are shown in **Figure 1b-c**. The *DS* was determined as the ratio of alkylated NVA units to all NVA units from the ratio of the total integrated peak area from 1.2 ppm to 2.2 ppm to the integrated peak area from 0.8 ppm to 1.0 ppm, denoted as *K*, and *n* is the number of carbon atom in the alkyl side chain, as shown in **Equation 3**:

$$DS = \frac{5}{3K - 2n + 4} \tag{3}$$

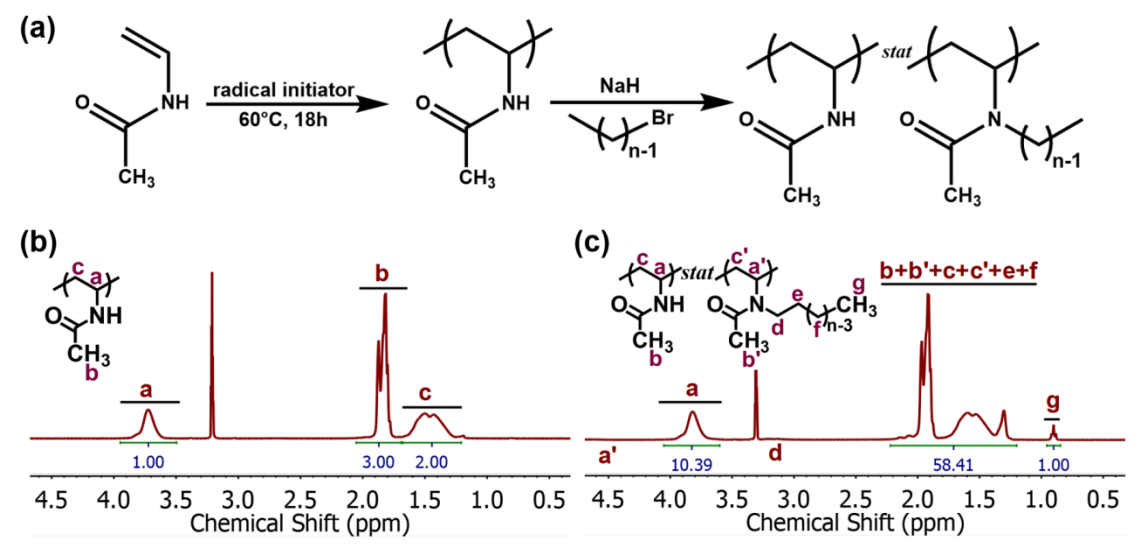


**Figure 1.** (a) Synthesis procedure of PNVA and poly(N-alkyl-N-vinylacetamide)s; (b) and (c) are  $^{1}$ H NMR spectra of PNVA<sub>4500</sub> and PNVA<sub>4500</sub>-C<sub>10</sub>-0.03 in deuterated methanol. (Signal peaks a' and d marked in (c) are not visible due to the very low DS.)

Molecular weight distributions of PNVA and poly(*N*-alkyl-*N*-vinylacetamide)s were checked by SEC (see **Figure S1**, Supporting Information). The elution curves show that PNVA and the *N*-alkylated polymers all have unimodal molecular weight distributions and confirms that the post-polymerization *N*-alkylation route yielded a stochastical substitution of the alkyl side chains along the PNVA backbone. Copolymers with such a small fraction of *n*-alkyl side chains cannot be prepared easily by copolymerization because of unfavourable copolymerization parameters and segregation.

#### 3.3.2 Gel formation

In order to prepare homogeneous hydrogels from PNVA<sub>4500</sub>-C<sub>n</sub>-0.03 (n = 10, 12, 14, 16, 18), the polymers were firstly dissolved in ethanol. From this solution, a solid film was cast by evaporation of the solvent in a flat-bottomed mould. We obtained clear transparent films, which could be immersed in water for swelling (**Figure 2a**). Irrespective of the length of the alkyl side chains, all polymers swelled to a finite degree of swelling.

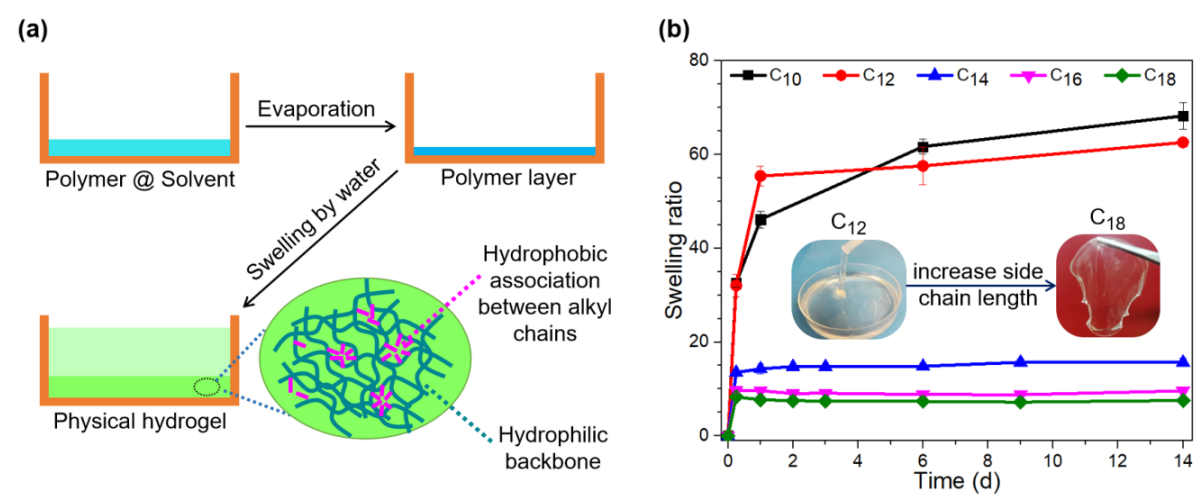


**Figure 2.** (a) Schematic illustration of hydrogel preparation process; (b) Swelling ratio (SR) of PNVA<sub>4500</sub>-C<sub>n</sub>-0.03 hydrogels (denoted as C<sub>n</sub> in the legend) for 14 days at 25°C. The insets show PNVA<sub>4500</sub>-C<sub>12</sub>-0.03 hydrogel and PNVA<sub>4500</sub>-C<sub>18</sub>-0.03 hydrogel after swelling for 14 days at 25°C. For the swelling rate measurement, 100 mg of PNVA<sub>4500</sub>-C<sub>n</sub>-0.03 polymer and 50 mL of deionized water was used (replicates = 3).

Figure 2b and Table 1 show the swelling as recorded for 14 days at 25°C after the ethanol cast polymer films were immersed in water. PNVA<sub>4500</sub>-C<sub>n</sub>-0.03 (n = 10, 12) hydrogels showed high degrees of swelling and could slowly flow. In contrast, PNVA<sub>4500</sub>-C<sub>n</sub>-0.03 (n = 14, 16, 18) hydrogels were elastic and mechanically strong, and they reached an equilibrium degree of swelling of 8 to 16. Such degrees of swelling are expected for a high degree of crosslinking at a high functionality of the crosslinks. Here the degree of substitution corresponds to an average of 32 monomer units between two crosslinks, while the functionality of a crosslink can exceed 4, as it is formed by association of the alkyl side chains.

**Table1.** Extracted polymer fraction and swelling ratio of PNVA<sub>4500</sub>-C<sub>n</sub>-0.03 polymers immersed in water for indicated days at constant temperature.

Entry	25°C, 14 days		60°C, 24 days	
	Extracted polymer fraction (%)	Swelling ratio (SR)	Extracted polymer fraction (%)	Swelling ratio (SR)
PNVA <sub>4500</sub> -C <sub>10</sub> -0.03	16 ± 3	68 ± 3	100	/
PNVA <sub>4500</sub> -C <sub>12</sub> -0.03 <sup>(a)</sup>	9 ± 1	63 ± 1	15 ± 1	57 ± 2
PNVA <sub>4500</sub> -C <sub>14</sub> -0.03	0	16 ± 1	4 ± 1	$20\pm1$
PNVA <sub>4500</sub> -C <sub>16</sub> -0.03	0	$10\pm0.2$	$7 \pm 0.5$	15 ± 1
PNVA <sub>4500</sub> -C <sub>18</sub> -0.03	0	$8 \pm 0.1$	5 ± 1	$9 \pm 0.4$

<sup>&</sup>lt;sup>(a)</sup> There is no significant change of DS (within the accuracy of the <sup>1</sup>H NMR determination  $3\% \pm 1\%$ ) between the originally employed polymer (PNVA<sub>4500</sub>-C<sub>12</sub>-0.03) and the polymer that has been extracted in water

To investigate the effects of temperature on the swelling behaviour of PNVA<sub>4500</sub>- $C_n$ -0.03 polymers, we also recorded an apparent swelling ratio (ASR, not corrected for the extracted fraction of polymer) over a longer period of time (24 days) at higher temperature (60°C) (see **Figure S2** and **Table 1**).

The ASR of PNVA<sub>4500</sub>-C<sub>10</sub>-0.03 reached its peak value rapidly after 1 day and successively decreased during the following 9 days. Hence, PNVA<sub>4500</sub>-C<sub>10</sub>-0.03 polymers could be fully extracted to the sol phase at elevated temperature (i.e., 60°C or higher). We explain this by rearrangement of the hydrophobic clusters favoured by the high temperature and the long time. Association of the alkyl side chains to domains yielded originally a network structure, rearrangement of the alkyl side chains between domains allowed formation of microgels and flower-like micelles driven by the osmotic pressure.

A systematic study of the degree of association of molecules in the sol phases will be subject of further studies.

For PNVA<sub>4500</sub>-C<sub>n</sub>-0.03 (n = 12, 14, 16, 18), the extracted polymer fraction only increased slightly by 4% to 7% at  $60^{\circ}$ C. PNVA<sub>4500</sub>-C<sub>n</sub>-0.03 (n = 14, 16, 18) showed higher swelling ratio at  $60^{\circ}$ C compared to  $25^{\circ}$ C, which would be expected for a quasi-permanent network when the interaction with the solvent is improved by temperature.

# 3.3.3 Biocompatibility

Biocompatibility of the PNVA<sub>4500</sub>-C<sub>n</sub>-0.03 hydrogels was evaluated firstly by incubating NHDF together with supernatant sol fraction of the PNVA<sub>4500</sub>-C<sub>18</sub>-0.03 hydrogel (for testing cytotoxicity) and secondly by direct cultivation on the gel surface (for testing adherence and viability via live-dead staining). Viability of cells was tested by live-dead staining whereby dead cells were fluorescently stained (red) and living cells were stained with green. When NHDFs were seeded on top of the hydrogels, we monitored whether cells could adhere and spread on the hydrogel surface. Typically, the NHDFs adhere on an adsorbed protein layer and protein repellent surfaces will not allow cell adherence, preventing cellular spreading. Thus, if the NHDF cannot adhere on the hydrogel surface, it is an indication of protein repellency of the hydrogel surface.

Figure 3a depicts the viability (24 and 72 hours) of NHDF cultured in PNVA<sub>4500</sub>-C<sub>18</sub>-0.03 hydrogel extract (conditioned medium). We observed no significant differences in cellular viability between the hydrogel extract and control media. Also, NHDF cultivation on hydrogel films as demonstrated in Figure 3b did not indicate a significant fraction of dead cells (red fluorescence labeled) irrespective of the length of the *n*-alkyl substituents and thus the gel strength. However, even after 36 h, the NHDF showed a

rounded morphology indicating lack of strong adherence and spreading (See also the bright field micrographs in **Figure S3**, Supporting Information). Hence, the experiments give a first indication of the biocompatibility and protein repellency of the polyvinylamide hydrogels.

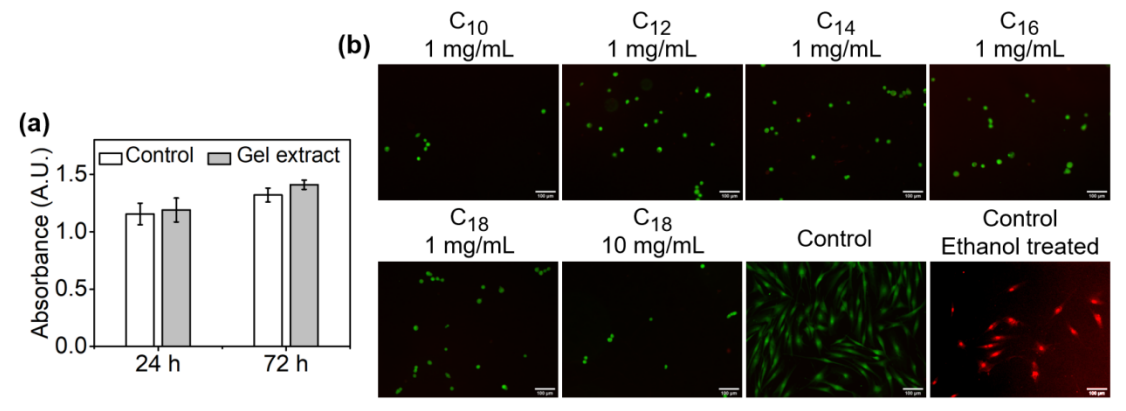


**Figure 3.** (a) Cell viability test by XTT assay of NHDF cells in the presence of PNVA<sub>4500</sub>-C<sub>18</sub>-0.03 extract after 24 h and 72 h incubation time (replicates = 4). The control was treated with DMEM medium only; (b) Live (green) and dead (red) fluorescence images of NHDF cells after cultivation on hydrogel films of PNVA<sub>4500</sub>-C<sub>n</sub>-0.03 (denoted as C<sub>n</sub>) for 36 h (replicates = 3) with indicated polymer concentration in DMEM. The scale bars represent 100 μm.

#### 3.3.4 Structural characterization of the hydrogels

An important aspect of our concept to prepare a series of reversible hydrogels, for which the gel strength depends merely on the hydrophobicity of the side chains, i.e., stickiness, has been that we wanted to exclude side chain crystallization also for relatively long alkyl substituents. Comb-like polymers with relatively long alkyl side chains can crystallize at ambient temperature, when the length of the alkyl chains exceeds 14 methylene groups. <sup>19-21</sup> In the case of the sparely but evenly substituted polymers described here, domain sizes of *n*-alkyl aggregates are expected to be very limited and the question arises, whether side chain crystallization can be excluded for relatively long alkyl substituents.

DSC heating diagrams were recorded for PNVA<sub>4500</sub>-C<sub>n</sub>-0.03 (n = 10, 12, 14, 16, 18), PNVA<sub>4500</sub>-C<sub>n</sub>-1 (n = 10, 12, 14, 16) and PNVA<sub>220</sub>-C<sub>18</sub>-1. DSC data of all other polymers are summarized in **Table S2** (Supporting Information). For most of the samples we could observe a glass transition in the range from 170°C to 200°C.

**Figure 4** demonstrates a comparison for 1-bromooctadecane, PNVA<sub>220</sub>-C<sub>18</sub>-1 (full substitution) and PNVA<sub>4500</sub>-C<sub>18</sub>-0.03 (3 mol% substitution). For PNVA<sub>220</sub>-C<sub>18</sub>-1, side chain crystallization is indicated by the melting endotherm at 58.1 °C with  $\Delta H = 61$  J/g and recrystallization upon cooling,  $T_{cryst}^{onset} = 57$ °C. As it is expected by the reduced melting entropy for the polymer tethered side chains, the melting temperature is higher than that of the corresponding 1-bromooctadecane. No evidence on side chain crystallization was found for the slightly alkylated PNVA<sub>4500</sub>-C<sub>18</sub>-0.03. Inhibition of side chain crystallization for the low degree of substitution was confirmed by thermooptical studies between crossed polarizers (see **Figure S4**, Supporting Information). As expected, we observed a strong birefringence and spherulite formation for the fully substituted polymers but no birefringence for a film of PNVA<sub>4500</sub>-C<sub>18</sub>-0.03 as prepared from the melt.

\_

<sup>&</sup>lt;sup>1</sup> From the melting entropy  $\Delta S$  per CH<sub>2</sub>-unit in the side chains compared to  $\Delta S^{\circ}$  of an ideal  $-(\text{CH}_2)_n$ -crystal, one can estimate the degree of crystallinity for the side chains to be not more than 30% (see Supporting Information)

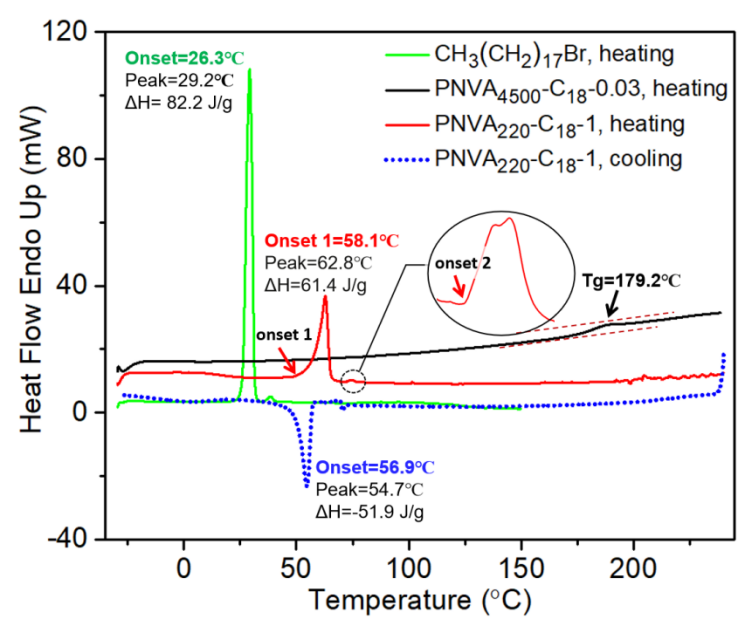


**Figure 4.** DSC curves of 1-bromooctadecane and PNVA-C<sub>18</sub> (second heating or cooling), heating/cooling rate is 10°C/min.

It must be noted that we observed another, although very weak transition between T = 66°C and T = 71°C for most of the samples, irrespective of whether they were fully or only slightly substituted (see **Table S2**, Supporting Information). Because this transition is at higher temperature than the side chain melting transition of the fully *N*-alkylated polyvinylamides and independent of the degree of substitution we assign it tentatively to the breakdown of small hydrogen-bonded clusters formed from short stereoregular segments of the *N*-vinylamide monomers.

In order to obtain more insight into the side chain ordering, we performed <sup>13</sup>C-MAS (magic angle spinning) NMR experiments on the PNVA<sub>4500</sub>-C<sub>18</sub>-0.03 hydrogel and the PNVA<sub>220</sub>-C<sub>18</sub>-1 bulk sample. Because of the so-called γ-gauche effect for the chemical shift, –(CH<sub>2</sub>)<sub>n</sub>– segments in the all-anti zig-zag conformation yield a signal at 32.6 ppm, while –(CH<sub>2</sub>)<sub>n</sub>– segments adjacent to gauche-arrangements in the disordered amorphous state give a signal at 30.0 ppm.<sup>22</sup> We performed <sup>13</sup>C-MAS with and without cross polarisation, i.e., CP-MAS and DP-MAS. By the CP-MAS experiments, the

"crystalline"  $-(CH_2)_n$ — signal is significantly overestimated, while by experiments without cross polarisation it has been underestimated because of its long  $T_1$ -relaxation time and too short sampling times.<sup>23, 24</sup> Yet the spectra allowed to discriminate a crystalline and an amorphous  $-(CH_2)_n$ — signal for the hydrogels and confirmed semi-quantitatively that side chain crystallization can be neglected in the case of the PNVA<sub>4500</sub>-C<sub>18</sub>-0.03 hydrogel (see **Figure S5**, Supporting Information).

# 3.3.5 Mechanical characterization of hydrogels

For the rheological characterization of the hydrogels, we firstly employed creep recovery experiments with a shear rheometer. The shear stress was set to a minimum as enabled by the rheometer and the creep period was 3 min. Hydrogels were soaked in water for 6 days before they were transferred to the rheometer. (See **Figure S6**, Supporting Information)

Figure 5 depicts exemplary creep-recovery experiments with the hydrogels from PNVA<sub>4500</sub>-C<sub>12</sub>-0.03 and PNVA<sub>4500</sub>-C<sub>18</sub>-0.03 in comparison to aqueous solutions of PNVA<sub>4500</sub> at concentrations which correspond to degree of swelling of C<sub>12</sub>- and C<sub>18</sub>-hydrogels. The elastic contribution increased significantly when the length and the hydrophobic stickiness of the side chains were increased. Within the time frame of the experiment, the PNVA<sub>4500</sub>-C<sub>12</sub>-0.03 hydrogel exhibited a strong temperature dependence of the viscous flow and the recoverable creep, while the PNVA<sub>4500</sub>-C<sub>18</sub>-0.03 hydrogel behaved like a permanently crosslinked gel.

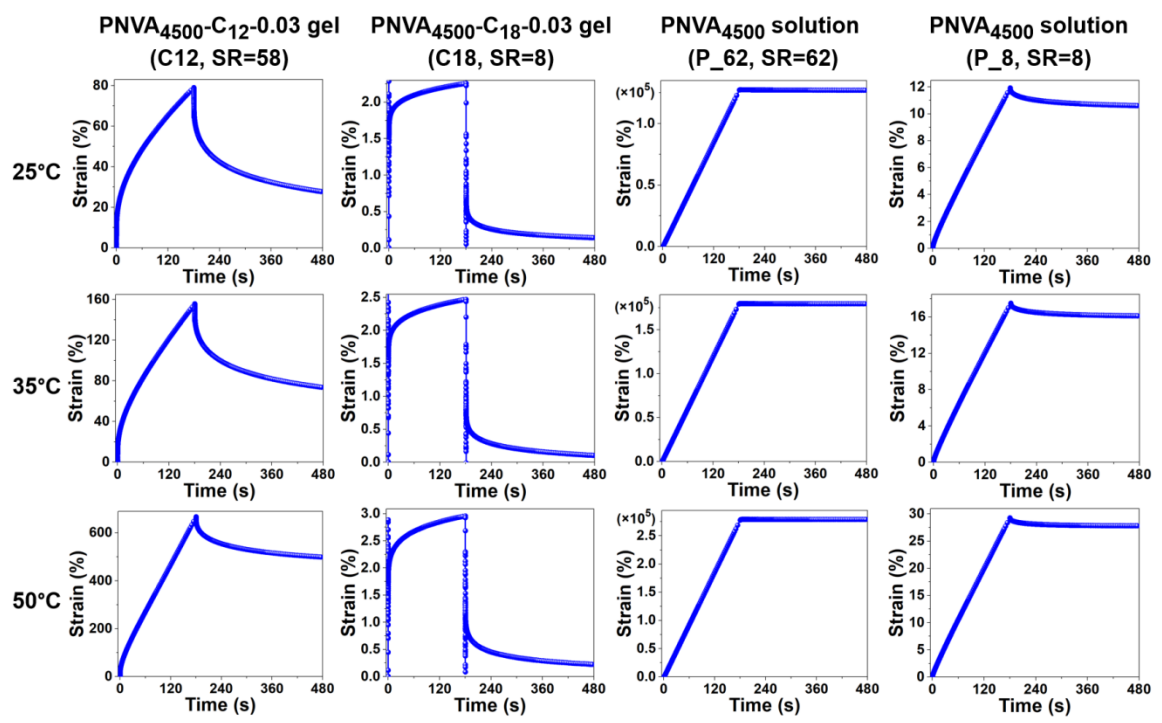


**Figure 5.** Representative creep recovery curves for PNVA<sub>4500</sub>-C<sub>12</sub>-0.03 and PNVA<sub>4500</sub>-C<sub>18</sub>-0.03 hydrogel in comparison to PNVA<sub>4500</sub> aqueous solutions of the corresponding concentration at 25, 35, and 50°C. Stresses were set to 20, 160, and 1 Pa, for PNVA<sub>4500</sub>-C<sub>12</sub>-0.03, PNVA<sub>4500</sub>-C<sub>18</sub>-0.03, and the PNVA<sub>4500</sub> solutions respectively.

From the temperature dependence of the low shear viscosity, we attempted to evaluate an activation energy for the release of the associations. In the case of the shorter side chains  $C_{10}$  and  $C_{12}$  we determined values of 27 kT (at 1.6 w/v%) and 26 kT (at 1.7 w/v%) at 298 K as shown in the supporting information (see **Figure S7** and **Table S3**). These values are within the same order of magnitude as the activation energy reported before for a telechelic polyethyleneoxide polymer with hexadecyl endgroups,  $E_a = 28$  kT.<sup>25</sup> However, we do not think that the structures are comparable. While in the case of alkyl groups at the chain end, the authors consider crosslinks in the form of small micelles of about 10 alkyl chains, we assume smaller and much more disordered associates which are in close proximity. This should correspond to a smaller activation energy for the disengagement or hoping of the alkyl chains. At the same time each chain

is linked to a larger number of the clusters and this multiplicity of links is expected to retard the flow compared to an endgroup-substituted polymer. The situation is even less comparable for the polymers with longer side chains because their gelation yields much higher concentrations.

Figure 6 demonstrates a comparative evaluation of creep recovery experiments regarding the nonelastic strain, the viscosity and relaxation times derived thereof (see method used for calculation in Figure S6, Supporting Information). For PNVA<sub>4500</sub>-C<sub>12</sub>-0.03 hydrogel at 2°C, the recoverable creep corresponded to 80% of the strain, and we determined a viscosity value nearly five orders of magnitude higher than the one measured for the parent PNVA<sub>4500</sub> at about the same concentration (P\_62). Upon raising the temperature to 70°C the viscosity as well as the recoverable strain of PNVA<sub>4500</sub>-C<sub>12</sub>-0.03 decreased approaching the properties of the PNVA<sub>4500</sub> solution. For PNVA<sub>4500</sub>-C<sub>18</sub>-0.03 with 18 methylene units in the side chains, the viscous strain contribution was only 5% at 2°C and increased to only 8% at 70°C. Figures 6d-f depict a comparison of poly(*N*-vinylacetamide) substituted by side chains of different length in dependence of the swelling ratio or polymer concentration. Longer side chains cause more dense networks which swell less, are more elastic and exhibit longer relaxation times.

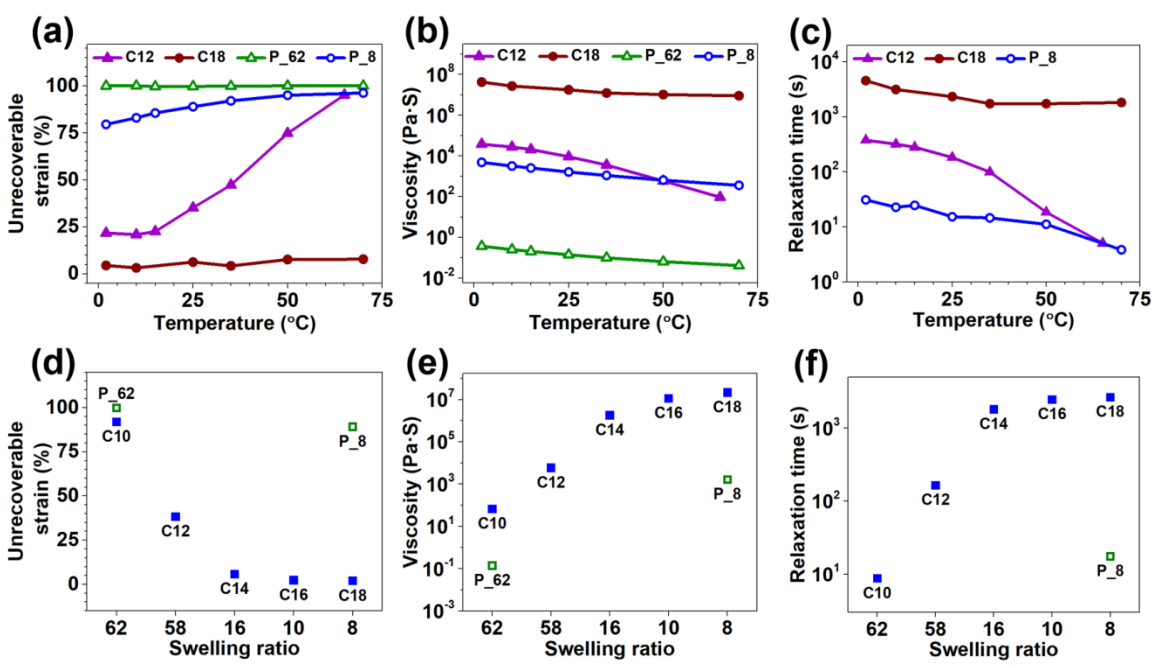


**Figure 6.** (a-c) Comparative evaluation of creep recovery experiments of the PNVA<sub>4500</sub>-C<sub>n</sub>-0.03 hydrogels and PNVA<sub>4500</sub> aqueous solutions with a concentration corresponding to the degree of swelling at temperatures from 2°C up to 70°C: (a) unrecoverable strain, (b) apparent viscosity after t-180 sec ( $\eta = \sigma/\dot{\gamma}$ ), (c) relaxation times ( $\tau = \eta \times J_{eq}$ ); (d-f) comparison of different hydrogels at 25°C for unrecoverable strain (d), viscosity (e) and relaxation time (f). (Note: the data of P\_62 in (c) and (f) are not displayed in the graph because its relaxation times are so short that it cannot be measured by the rheometer using this method.)

Figures 7a-b depict shear rate dependent viscosities of the soft PNVA<sub>4500</sub>-C<sub>10</sub>-0.03 hydrogel in comparison to the equally concentrated PNVA<sub>4500</sub> solution (P<sub>62</sub>). For both samples, we observed Newtonian behaviour at low shear rates, however with a roughly three orders of magnitude higher viscosity of the PNVA<sub>4500</sub>-C<sub>10</sub>-0.03 hydrogel at low temperature (e.g., 2°C), irrespective of the same degree of polymerisation. The difference dropped to two orders of magnitude, when the temperature was raised to 50°C. Shear rate dependent viscosities of PNVA<sub>4500</sub>-C<sub>16</sub>-0.03 and PNVA<sub>4500</sub>-C<sub>18</sub>-0.03 at higher concentration respectively lower degree of swelling are shown in Figures 7c-d. When shear rates were decreased stepwisely for the PNVA<sub>4500</sub>-C<sub>16</sub>-0.03 hydrogel, which was at rest before, the low shear rate viscosity was by an order of magnitude higher than when

the experiment was started at low shear rates. Going from low to high shear rates yielded an apparent  $\eta_0$  value around  $10^6\,\mathrm{Pa}\cdot\mathrm{s}$  for both PNVA<sub>4500</sub>-C<sub>16</sub>-0.03 and PNVA<sub>4500</sub>-C<sub>18</sub>-0.03 hydrogels. **Figure 7d** includes also viscosity data determined at very low shear rates and long creep times. The comparison demonstrates a significant dependence of the Newtonian shear regime on the pre-treatment of the sample. Experimental  $\eta_0$  values increased by a factor of 12 to 35 at low shear rates and long equilibration time.

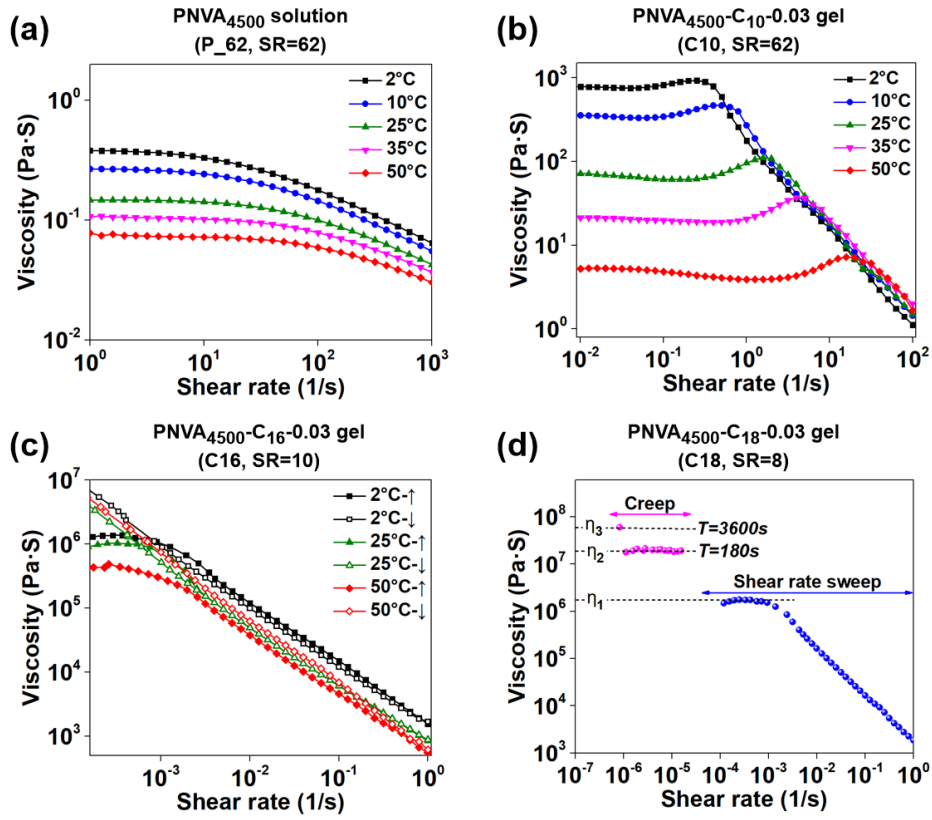


**Figure 7.** Shear rate dependent viscosities of (a) PNVA<sub>4500</sub>, (b) PNVA<sub>4500</sub>-C<sub>10</sub>-0.03, (c) PNVA<sub>4500</sub>-C<sub>16</sub>-0.03 and (d) PNVA<sub>4500</sub>-C<sub>18</sub>-0.03. Data were measured by shear rate sweeps. In (c), viscosities were first measured starting at low shear rates (filled symbols) with a sample kept for over 12 hours at rest and afterwards also from high to low shear rates (open symbols). Only in the former case a plateau of  $\eta_0$  could be observed at low shear rates. The purple points at ultra-low shear rates in (d) were determined from  $\sigma/\dot{\gamma}$  after 3 and 60 minutes.

The data in Figure 7c demonstrate anti-thixotropy (negative thixotropy) for the polymers with relatively long alkyl side chains, i.e., associations are improved by long

lasting shearing and cannot re-equilibrate within the time of the experiment. This behaviour might be expected because association linkages are not uniform consisting of larger and smaller clusters of alkyl chains whose topological arrangement and size distribution is certainly effected by shearing. The anti-thixotropic effect corresponds to shear thickening observed for the polymers with shorter side chains and in a more pronounced way at higher temperatures, when rearrangement of the associations could take place within the time scale of the experiment. Clearly, the rheology data demonstrate a transient character of the crosslinks with an enormous range of relaxation times.

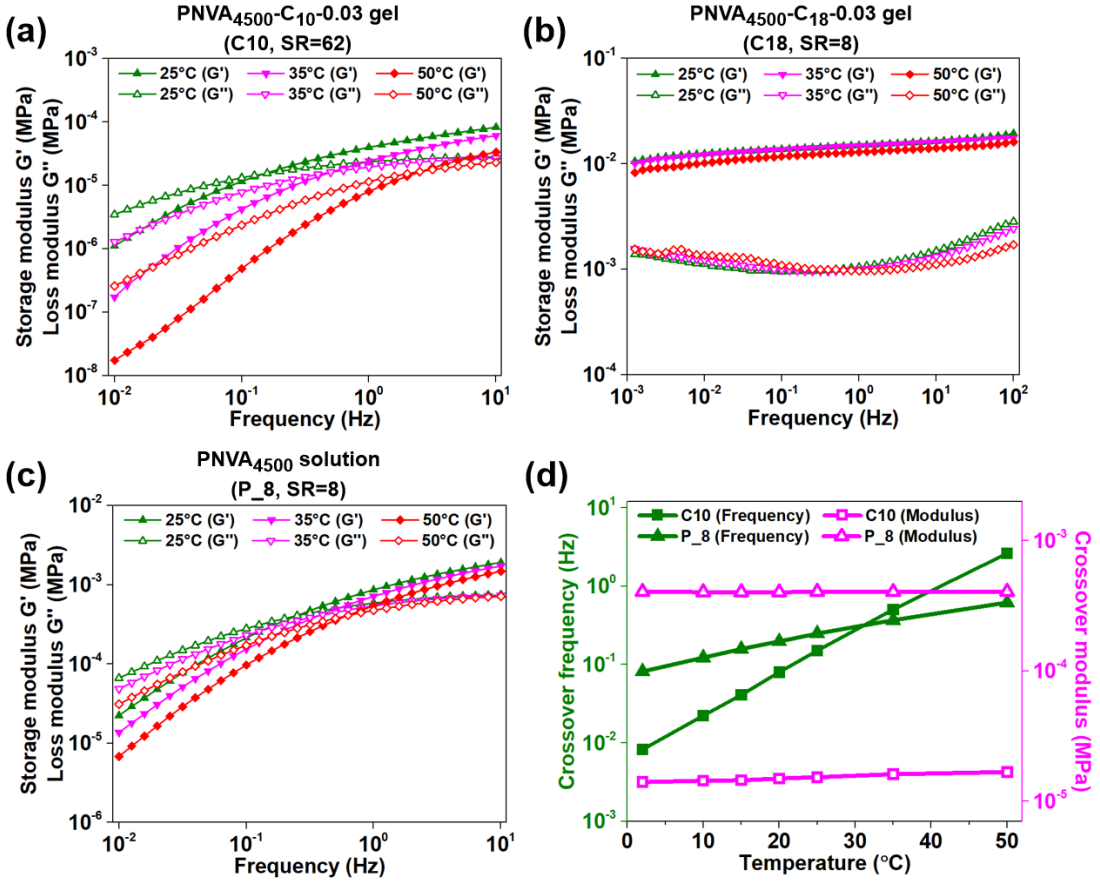


**Figure 8.** (a-c) are frequency dependence of G' and G'' for indicated hydrogels and  $PNVA_{4500}$  aqueous solution deformed by strain of 2%, 1% and 2%, respectively; (d) crossover frequency and modulus of  $PNVA_{4500}$ - $C_{10}$ -0.03 hydrogel and  $PNVA_{4500}$  aqueous solution obtained from frequency sweep.

We also performed dynamic shear experiments for comparison. **Figure 8a** demonstrates the frequency dependence of the storage and loss modulus for the highly swollen soft PNVA<sub>4500</sub>-C<sub>10</sub>-0.03 hydrogel (equilibrated for 6 days) at different temperatures. We observed a strong temperature dependence of the frequency at which G' crossed G'', while for an eight times higher concentration of the same polymer without alkyl side chains, the crossover frequency changed significantly less between 2° and 50°C (**Figure 8c**). For the PNVA<sub>4500</sub>-C<sub>18</sub>-0.03 hydrogel, we observed a wide rubber elastic plateau within the frequency/temperature window of the experiment (**Figure 8b**).

Overall, the data show a remarkable continuity of the effects caused by the stepwise increase of the length of the side chains. This confirms our initial expectation that the side chains will serve as sticky attachments to the hydrophilic backbone, whose stickiness is systematically increased by their length. If the increased hydrophobic interaction causes merely an increased stickiness, we expect a thermorheological uniform flow mechanism common to all samples, manifested in a time-temperature-stickiness master curve. This is indeed the case as shown in **Figure 9**.

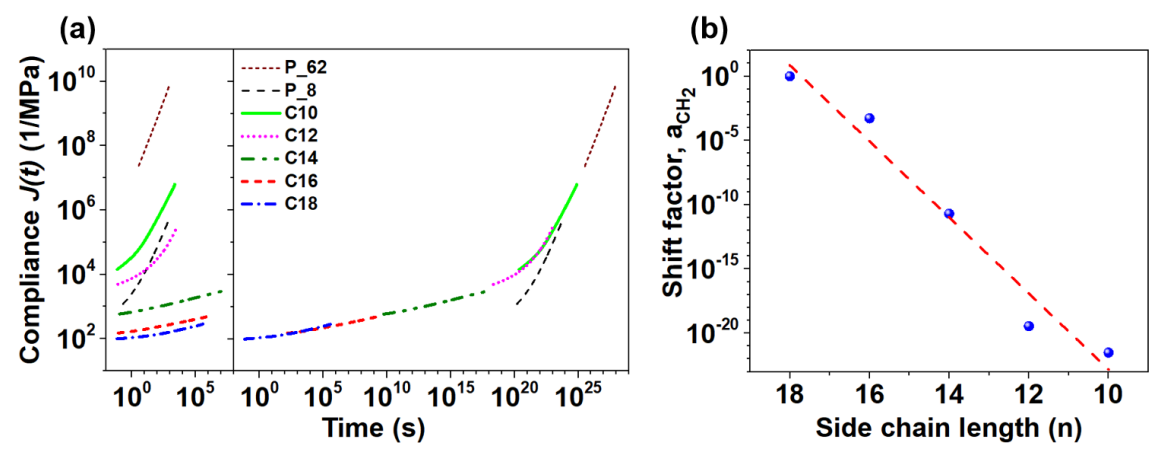


**Figure 9.** (a) Time-temperature-stickiness master curve (on the right side) generated by horizontally shifting time-temperature superposition master curves of PNVA<sub>4500</sub>-C<sub>n</sub>-0.03 hydrogels and PNVA<sub>4500</sub> aqueous solutions (on the left side) according to creep experiments (conditions for measurements, see **Table S4**, Supporting Information); (b) Side chain length dependence of shift factor ( $a_{CH_2}$ ) for PNVA<sub>4500</sub>-C<sub>n</sub>-0.03 hydrogels, the red dash line show the linear fitting of shift factor with respect to side chain length.

Figure 9a depicts a time-temperature-stickiness superposition master curve constructed from the time-temperature master curves of the compliance data from creep experiments (see Figure S8, Supporting Information). In Figure 9b we plotted the shift factor  $a_{CH_2}$  as a function of the length of the side chains. Roughly we found that the extension by one CH<sub>2</sub>-group corresponded to a time shift by 2.6 orders of magnitude. In Figure 9a we also added compliance data for the 1.6 wt.% and the 11.1 wt.% solutions of poly(N-vinylacetamide) (see results of PNVA<sub>4500</sub> aqueous solutions (P\_62 and P\_8) in Figures 5 and 6). For the low concentrations, their compliance data fit to the time-temperature-stickiness superposition master curve at the end when the stickiness effect is small and negligible. For the high concentrations when entanglements control the flow behaviour of the PNVA and the hydrophobic stickiness of the alkyl-substituted polymers, we find a significant deviation. We also found significant deviations from a common master curve when we probed the time-temperature-stickiness superposition for data from

stress relaxation experiments (see **Figures S9** and **S10**, Supporting Information), whereby the relaxation started from states in the nonlinear deformation regime.

#### 3.4 Conclusion

PNVAs are biocompatible hydrophilic polymers which enable versatile substitution to introduce particular functionalities either via the amine groups after hydrolysation or by direct addition to the amide group. We took advantage from the fact that the long alkyl chains could be substituted to the preformed macromolecules ensuring a stochastical distribution along the backbone even at low degrees of substitution. The low degree of substitution ensured preservation of the hydrophilic character of the PNVAs irrespective of the variation in length of the side chains while at the same time, we could tailor the strength of the hydrophobic interaction.

We could shape geometrically defined objects from the polymers by casting their ethanol solutions into a mould. When such objects were brought into contact with water, PNVAs with shorter alkyl substituents yielded soft hydrogels, which flow upon shearing but still segregate from excess water, i.e., they showed syneresis; while PNVAs with longer alkyl substituents yielded hydrogels with mechanical properties as if permanently crosslinked.

Figure 10 presents an idealized qualitative model to explain the gelation and the flow behaviour of the polymers in water: The alkyl groups act as sticky sites distributed along the polymer backbone. Each sticky interaction can be considered a transient crosslink. Their stickiness is determined by the rates by which they attach and detach from each other. These rates depend on the length and respective hydrophobicity of the alkyl chains. Shorter alkyl chains exchange more quickly than longer alkyl chains and the

exchange rate is strongly dependent on temperature. Hence, as shorter the alkyl chains and as higher the temperature, the more transient are these crosslinks. Longer alkyl side chains and lower temperatures cause smaller rates of the exchange processes by which a polymer chain can change its position. Smaller rates of this exchange processes result in dramatically increased terminal relaxation times. In this respect the flow behaviour resembles that of ionomers, where the ionic substituents serve as sticky substituents within the hydrophobic bulk.<sup>26</sup> However, the scope of applications of the present hydrogel system is entirely different.

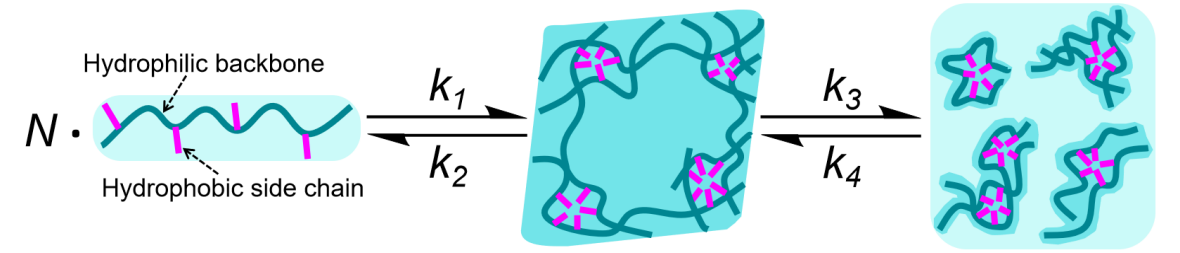


**Figure 10.** Schematic illustration of an idealized qualitative model for dynamics of PNVA-C<sub>n</sub>-0.03 hydrogel system (association and dissociation in water).

We consider the fact, that we could tailor the rheological properties over an enormous range as a speciality of the presented system. Time-temperature superposition and our successful attempt to construct a time-temperature-stickiness superposition master curve demonstrate the coherent flow mechanism for all hydrogel samples irrespective of the length of the alkyl side chains. We consider the *N*-alkylated polyvinylamides not only of interest as a biocompatible hydrogel with tailored mechanical properties, but also a basis for more advanced rheology investigations.

## 3.5 References

[1] Creton, C. 50th Anniversary Perspective: Networks and Gels: Soft but Dynamic and Tough. *Macromolecules* **2017**, *50* (21), 8297-8316. DOI: 10.1021/acs.macromol.7b01698.

- [2] Peppas, N. A.; Hilt, J. Z.; Khademhosseini, A.; Langer, R. Hydrogels in Biology and Medicine: From Molecular Principles to Bionanotechnology. *Advanced Materials* **2006**, *18* (11), 1345-1360. DOI: 10.1002/adma.200501612.
- [3] Tanaka, F.; Stockmayer, W. H. Thermoreversible Gelation with Junctions of Variable Multiplicity. *Macromolecules* **1994**, *27* (14), 3943-3954. DOI: 10.1021/ma00092a039.
- [4] Kumar, S. K.; Douglas, J. F. Gelation in Physically Associating Polymer Solutions. *Physical Review Letters* **2001**, *87* (18), 188301. DOI: 10.1103/PhysRevLett.87.188301.
- [5] Tanaka, F.; Ishida, M. Elastically Effective Chains in Transient Gels with Multiple Junctions. *Macromolecules* **1996**, *29* (23), 7571-7580. DOI: 10.1021/ma960604g.
- [6] Sun, T. L.; Kurokawa, T.; Kuroda, S.; Ihsan, A. B.; Akasaki, T.; Sato, K.; Haque, M. A.; Nakajima, T.; Gong, J. P. Physical hydrogels composed of polyampholytes demonstrate high toughness and viscoelasticity. *Nature Materials* **2013**, *12* (10), 932-937. DOI: 10.1038/nmat3713.
- [7] Abdurrahmanoglu, S.; Can, V.; Okay, O. Design of high-toughness polyacrylamide hydrogels by hydrophobic modification. *Polymer* **2009**, *50* (23), 5449-5455. DOI: 10.1016/j.polymer.2009.09.042.
- [8] Cui, K.; Sun, T. L.; Liang, X.; Nakajima, K.; Ye, Y. N.; Chen, L.; Kurokawa, T.; Gong, J. P. Multiscale Energy Dissipation Mechanism in Tough and Self-Healing Hydrogels. *Physical Review Letters* **2018**, *121* (18), 185501. DOI: 10.1103/PhysRevLett.121.185501.
- [9] Tuncaboylu, D. C.; Argun, A.; Sahin, M.; Sari, M.; Okay, O. Structure optimization of self-healing hydrogels formed via hydrophobic interactions. *Polymer* **2012**, *53* (24), 5513-5522. DOI: 10.1016/j.polymer.2012.10.015.
- [10] Murakami, T.; Kawamori, T.; Gopez, J. D.; McGrath, A. J.; Klinger, D.; Saito, K. Synthesis of PEO-based physical gels with tunable viscoelastic properties. *Journal of Polymer Science Part A: Polymer Chemistry* **2018**, *56* (10), 1033-1038. DOI: 10.1002/pola.28992.
- [11] Pan, J.; Gao, L.; Sun, W.; Wang, S.; Shi, X. Length Effects of Short Alkyl Side Chains on Phase-Separated Structure and Dynamics of Hydrophobic Association Hydrogels. *Macromolecules* **2021**, *54* (13), 5962-5973. DOI: 10.1021/acs.macromol.1c00471.

- [12] Zhao, L.; Wang, S.; Yang, Z.; Tian, L.; Gao, L.; Shi, X. Structural evolution of dispersed hydrophobic association in a hydrogel analyzed by the tensile behavior. *Soft Matter* **2020**, *16* (35), 8245-8253, 10.1039/D0SM01211D. DOI: 10.1039/D0SM01211D.
- [13] Verkoyen, P.; Dreier, P.; Bros, M.; Hils, C.; Schmalz, H.; Seiffert, S.; Frey, H. "Dumb" pH-Independent and Biocompatible Hydrogels Formed by Copolymers of Long-Chain Alkyl Glycidyl Ethers and Ethylene Oxide. *Biomacromolecules* **2020**, *21* (8), 3152-3162. DOI: 10.1021/acs.biomac.0c00576.
- [14] Mao, H.; Pan, P.; Shan, G.; Bao, Y. In Situ Formation and Gelation Mechanism of Thermoresponsive Stereocomplexed Hydrogels upon Mixing Diblock and Triblock Poly(Lactic Acid)/Poly(Ethylene Glycol) Copolymers. *The Journal of Physical Chemistry B* **2015**, *119* (21), 6471-6480. DOI: 10.1021/acs.jpcb.5b03610.
- [15] Geng, Y.; Lin, X. Y.; Pan, P.; Shan, G.; Bao, Y.; Song, Y.; Wu, Z. L.; Zheng, Q. Hydrophobic association mediated physical hydrogels with high strength and healing ability. *Polymer* **2016**, *100*, 60-68. DOI: 10.1016/j.polymer.2016.08.022.
- [16] Ajiro, H.; Watanabe, J.; Akashi, M. Cell Adhesion and Proliferation on Poly(*N*-vinylacetamide) Hydrogels and Double Network Approaches for Changing Cellular Affinities. *Biomacromolecules* **2008**, *9* (2), 426-430. DOI: 10.1021/bm701221c.
- [17] Belthle, T.; Demco, D. E.; Pich, A. Nanostructuring the Interior of Stimuli-Responsive Microgels by *N*-Vinylimidazoles Quaternized with Hydrophobic Alkyl Chains. *Macromolecules* **2022**, *55* (3), 844-861. DOI: 10.1021/acs.macromol.1c02276.
- [18] Kamiloglu, S.; Sari, G.; Ozdal, T.; Capanoglu, E. Guidelines for cell viability assays. *Food Frontiers* **2020**, *I* (3), 332-349. DOI: 10.1002/fft2.44.
- [19] López-Carrasquero, F.; Martínez de Ilarduya, A.; Cárdenas, M.; Carrillo, M.; Luisa Arnal, M. a.; Laredo, E.; Torres, C.; Méndez, B.; Müller, A. J. New comb-like poly(n-alkyl itaconate)s with crystalizable side chains. *Polymer* **2003**, *44* (17), 4969-4979. DOI: 10.1016/S0032-3861(03)00470-1.
- [20] Greenberg, S. A.; Alfrey, T. Side Chain Crystallization of n-Alkyl Polymethacrylates and Polyacrylates 1. *Journal of the American Chemical Society* **1954**, 76 (24), 6280-6285. DOI: 10.1021/ja01653a015.
- [21] Xu, H.; Wang, H.; Mao, H.; Li, L.; Shi, H. Crystallization and thermal performance of poly(acrylonitrile-co-alkyl acrylate) comb-like polymeric phase change materials with

- various side-chain lengths. *CrystEngComm* **2020**, *22* (35), 5799-5808, 10.1039/D0CE00929F. DOI: 10.1039/D0CE00929F.
- [22] Pursch, M.; Brindle, R.; Ellwanger, A.; Sander, L. C.; Bell, C. M.; Händel, H.; Albert, K. Stationary interphases with extended alkyl chains: A comparative study on chain order by solid-state NMR spectroscopy. *Solid State Nuclear Magnetic Resonance* **1997**, *9* (2), 191-201. DOI: 10.1016/S0926-2040(97)00058-1.
- [23] Vanderhart, D. L. Natural-abundance 133C \(\sigma\) 3C spin exchange in rigid crystalline organic solids. *Journal of Magnetic Resonance (1969)* **1987**, 72 (1), 13-47. DOI: 10.1016/0022-2364(87)90173-9.
- [24] Schmidt-Rohr, K.; Spiess, H. W. *Multidimensional solid-state NMR and polymers*; Academic Press, 1994. DOI: 10.1016/C2009-0-21335-3.
- [25] Annable, T.; Buscall, R.; Ettelaie, R.; Whittlestone, D. The rheology of solutions of associating polymers: Comparison of experimental behavior with transient network theory. *Journal of Rheology* **1993**, *37* (4), 695-726. DOI: 10.1122/1.550391.
- [26] Leibler, L.; Rubinstein, M.; Colby, R. H. Dynamics of reversible networks. *Macromolecules* **1991**, *24* (16), 4701-4707. DOI: 10.1021/ma00016a034.

# 3.6 Supporting information

# Size exclusion chromatography (SEC)

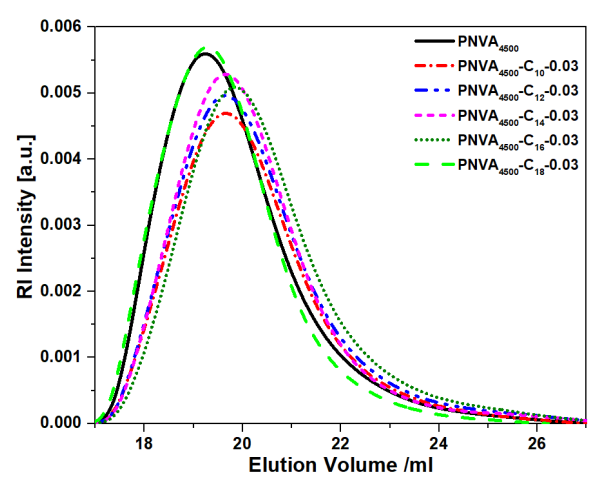


**Figure S1**. SEC elution curves of PNVA and poly(N-alkyl-N-vinylacetamide)s in DMF (DP = 4500 for all samples).

# **Apparent swelling dynamics**

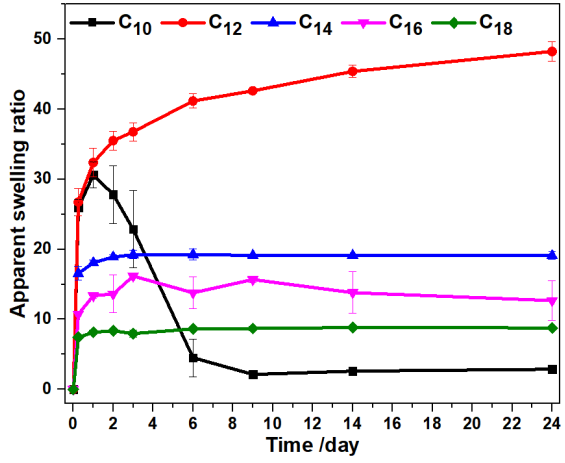


**Figure S2.** Apparent swelling dynamics of PNVA<sub>4500</sub>- $C_n$ -0.03 hydrogels (denoted as  $C_n$  in the legend) at 60°C for 24 days.

# Bright field microscopy of cells on hydrogels

Contrary to the NHDF seeded on tissue culture polystyrene, where the cells displayed elongated morphology, cells seeded on the hydrogel surface exhibited rounded morphology with a tendency to form cellular clusters (**Figure S3 a, b**). The clustering of the NHDF can be attributed to their low attachment to the hydrogel surface, inducing enhanced cell-cell interaction. It is also known that cell-cell interactions lead to improved cellular viability and survival. Therefore, the ability of the fabricated polyvinylamide hydrogels to maintain cellular viability as well as initiate cellular cluster formation could be useful in biomedical applications such as the construction of multicellular spheroids and organoids. A

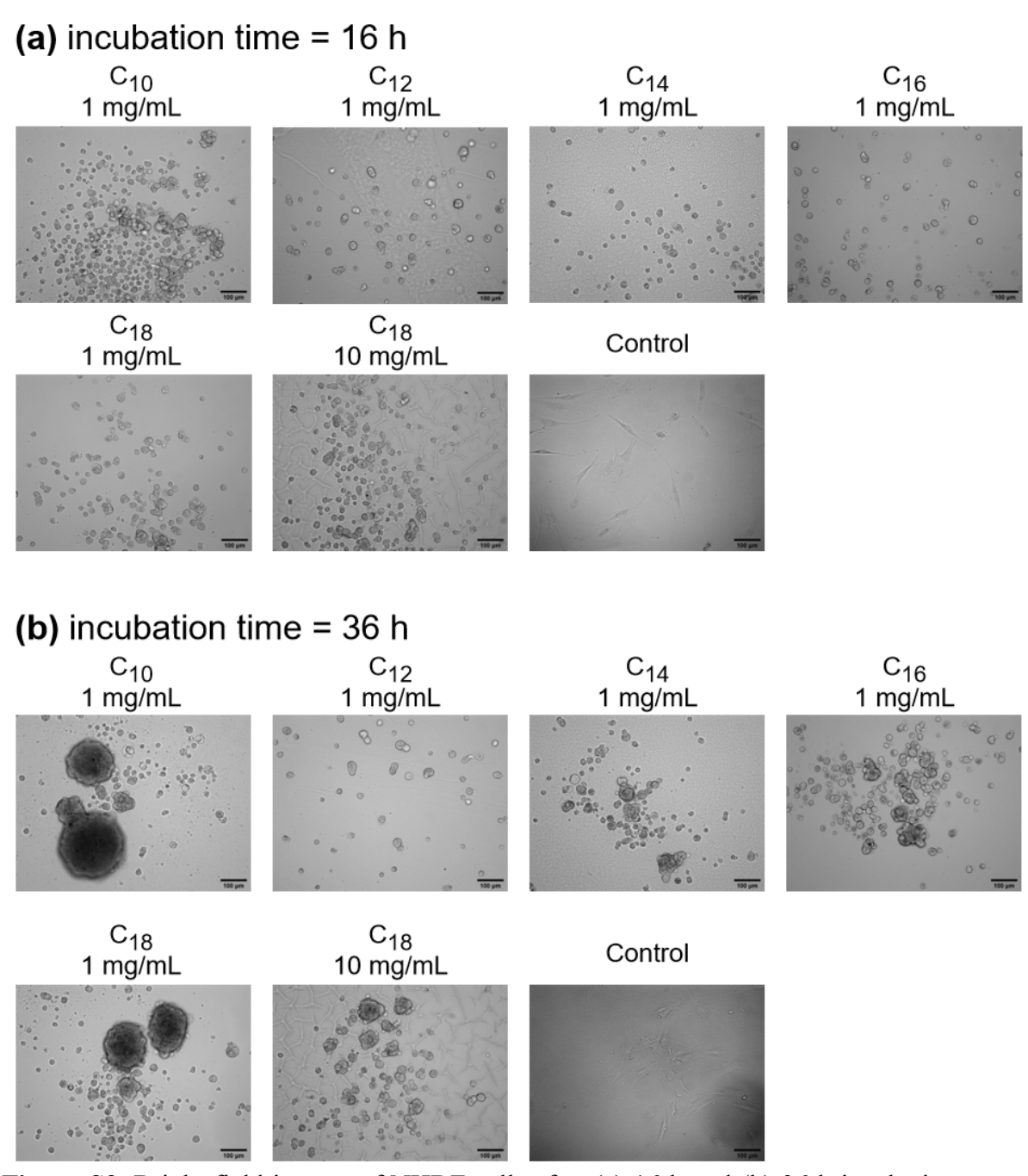


**Figure S3.** Bright field images of NHDF cells after (a) 16 h and (b) 36 h incubation on the PNVA<sub>4500</sub>-C<sub>n</sub>-0.03 hydrogels with indicated polymer concentration in DMEM. Scale bars represent  $100~\mu m$ .

## Polarized light microscopy

Polarized light microscopy was performed using a Zeiss Axioplan 2 optical microscope equipped with crossed polarizers and a Mettler Toledo FP82HT hot stage. Sample powder was loaded between a glass slide and a cover slide, and pressed to form a thin film rightly after being heated above its melting point. The heating/cooling rate was set to 5°C/min. A red retardation plate (retardation = 550nm) was applied to create a color image for white light illumination based on Newtonian subtraction colors.

As shown in **Figure S4**, spherulites were observed at 25°C for PNVA<sub>220</sub>-C<sub>18</sub>-1, the fully substituted polymer. When the temperature was raised to 60°C, the spherulites gradually began to melt and disappeared at 61.6°C, indicating the phase change to the amorphous state. Upon cooling, the crystalline texture started to form at around 57°C and finished at 56.6°C. No birefringence was observed for PNVA<sub>4500</sub>-C<sub>18</sub>-0.03 indicating its side chains could not crystallize.

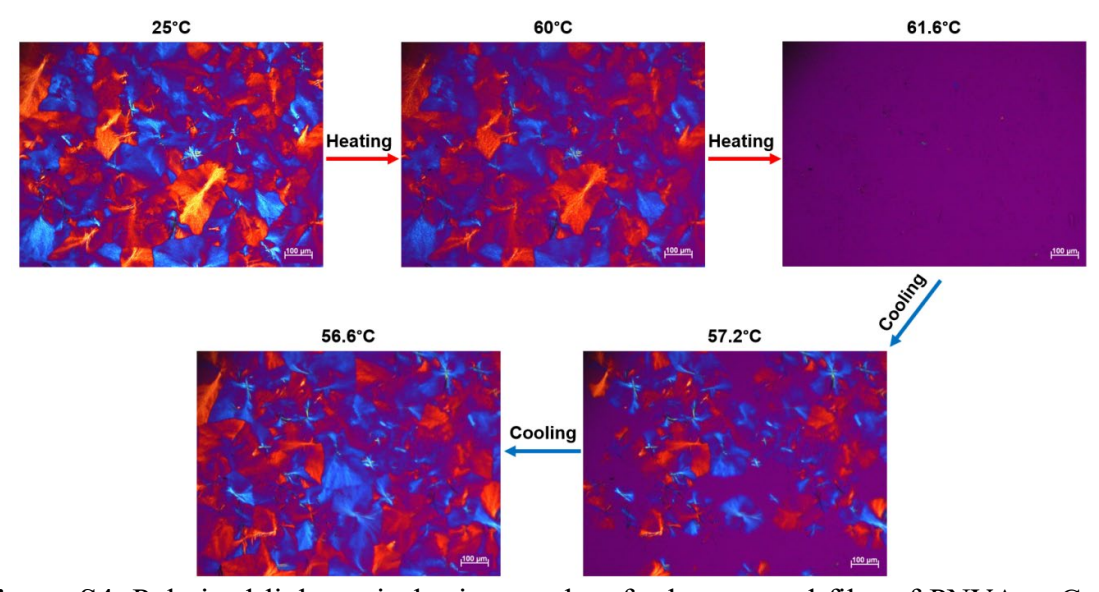


**Figure S4.** Polarized light optical micrographs of a hot-pressed film of PNVA<sub>220</sub>-C<sub>18</sub>-1 captured with a red retardation plate in front of the analyser. Sample was heated from 25°C to 70°C and cooled at heating/cooling rate of 5°C/min to 25°C.

## Magic angle spinning (MAS) NMR

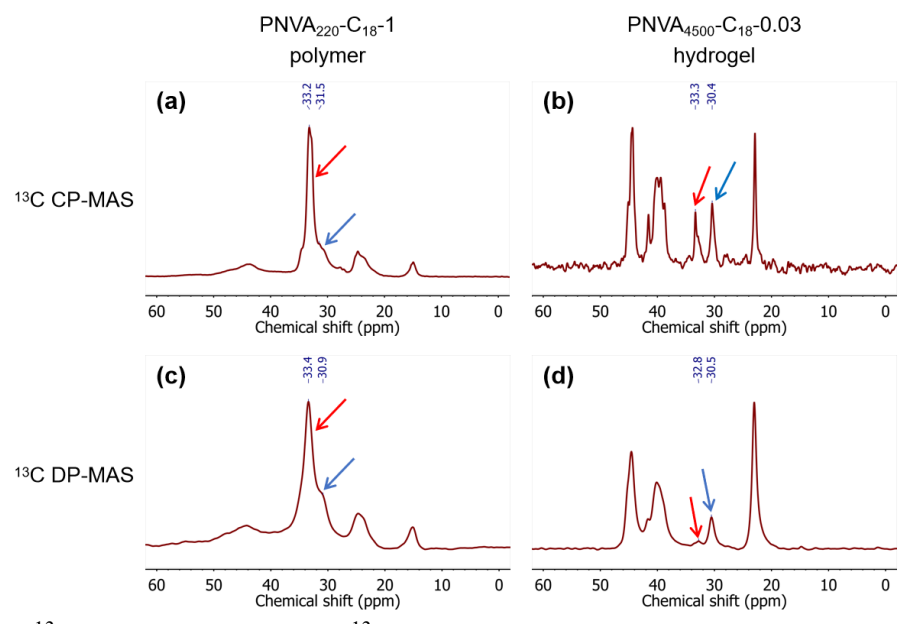


**Figure S5.** <sup>13</sup>C CP-MAS (a, b) and <sup>13</sup>C DP-MAS (c, d) NMR spectra of PNVA<sub>220</sub>-C<sub>18</sub>-1 polymer (a, c) and PNVA<sub>4500</sub>-C<sub>18</sub>-0.03 hydrogel (b, d) measured at 23°C. Arrows in the spectra indicate peaks relevant to *trans* conformations (at around 32.6 ppm, red arrows) and *gauche* conformations (at around 30.0 ppm, blue arrows) of the alkyl side chains.

#### Experimental setup and calculation for creep recovery measurements

The last terminal part of creep curve was fitted using linear regression (as shown in **Figure S6**). The strain rate  $(\dot{\gamma})$  was determined as the slope of the linear fit (k), and shear compliance  $(J_{eq})$  was calculated from the intercept of the linear fit (b) divided by shear stress  $(\sigma_0)$ . Viscosity  $(\eta)$  and relaxation time  $(\tau)$  were calculated by **Equations S1-4:** 

$$J_{eq} = \frac{b}{\sigma_0} \tag{S1}$$

$$\dot{\gamma} = k \tag{S2}$$

$$\eta = \frac{\sigma_0}{\dot{\gamma}} \tag{S3}$$

$$\tau = \eta \times J_{eq} \tag{S4}$$

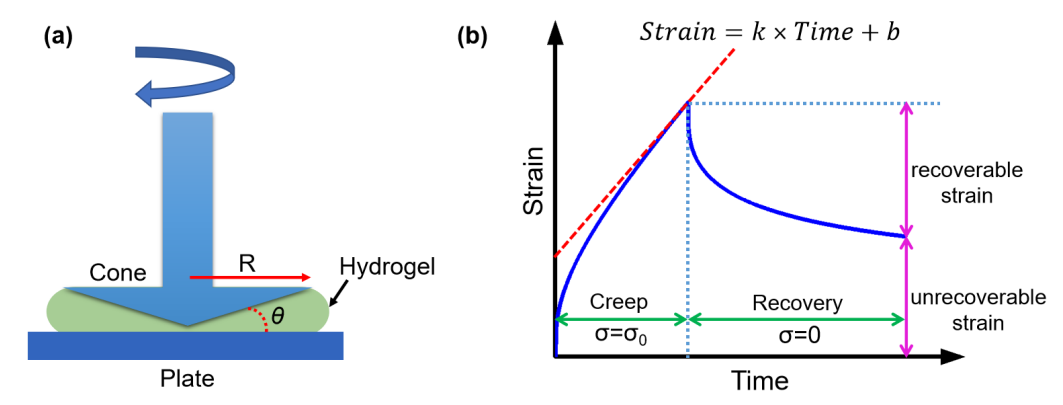


**Figure S6.** (a) Schematic diagram of creep recovery experiments using cone-plate geometry; (b) viscosity, relaxation time and unrecoverable strain (%) determined from creep recovery curves.

# Activation energy calculated from creep experiments by Arrhenius plot

The activation energy of  $PNVA_{4500}$ - $C_n$ -0.03 hydrogels (see **Table S3**) was calculated by Arrhenius plot using **Equations S5** and **S6** according to literature<sup>5, 6</sup>:

$$\ln\left(\frac{\eta}{\eta_{ref}}\right) = \frac{E_a}{R} \left(\frac{1}{T} - \frac{1}{T_{ref}}\right) \tag{S5}$$

$$\ln a_T = \frac{E_a}{R} \left( \frac{1}{T} - \frac{1}{T_{ref}} \right) \tag{S6}$$

The viscosity and shift factor of hydrogels were obtained from creep experiments (parameters used for measurements, see **Table S4**, supporting information).

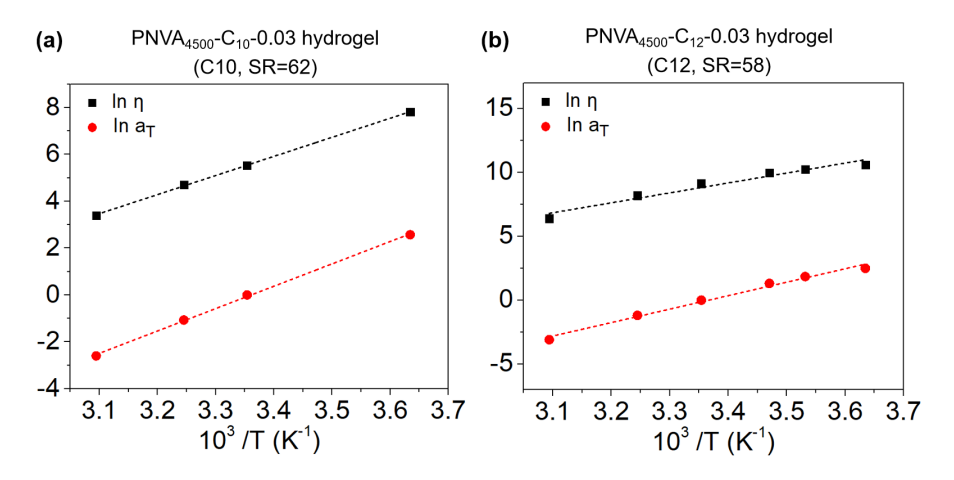


**Figure S7.** Arrhenius plots of viscosity and shift factor for (a)  $PNVA_{4500}$ - $C_{10}$ -0.03 hydrogel and (b)  $PNVA_{4500}$ - $C_{12}$ -0.03 hydrogel.

# Master curve generated from creep compliance

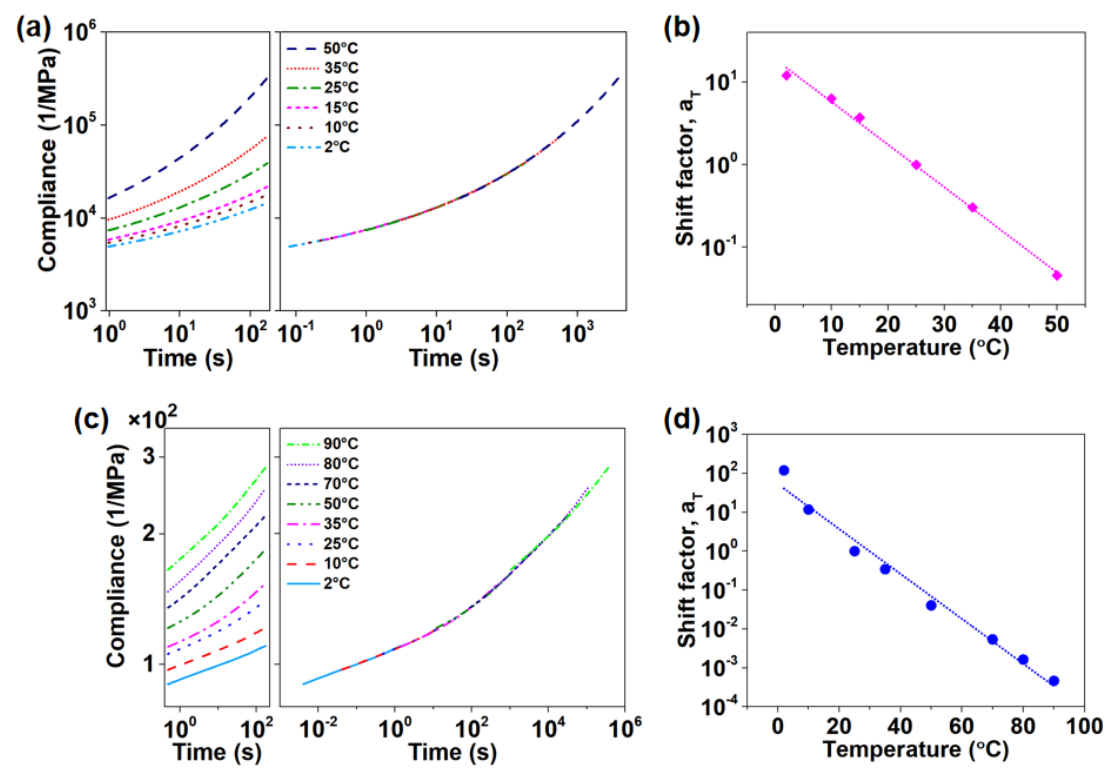


**Figure S8.** (a, c) Creep compliance master curves of (a)  $PNVA_{4500}$ - $C_{12}$ -0.03 and (c)  $PNVA_{4500}$ - $C_{18}$ -0.03 hydrogel generated at 25°C by time-temperature superposition; (b, d) Temperature dependence of shift factor (a<sub>T</sub>) for (b)  $PNVA_{4500}$ - $C_{12}$ -0.03 and (d)  $PNVA_{4500}$ - $C_{18}$ -0.03 hydrogel, the lines are linear fitting of the respective data.

### Master curve generated from stress relaxation

Figure S9 shows representative stress relaxation experiments for the PNVA<sub>4500</sub>- $C_{12}$ -0.03 and PNVA<sub>4500</sub>- $C_{18}$ -0.03 samples at different temperatures. For each of the samples we could construct a master curve as demonstrated in Figure S9c, hence the time-temperature superposition is valid, indicating that there is no change in the flow mechanism within the investigated time-temperature window.

When we also attempted to construct a master curve from the master curves for the  $PNVA_{4500}$ - $C_n$ -0.03 hydrogels with n = 12, 14, 16 and 18 in order to demonstrate a coherent flow mechanism irrespective of the length of the alkyl substituents, we found a

remarkable convergence to one common mater curve, as shown in **Figure S10**. Experiments were based on an initial fast deformation which actually affects the hydrophobic association structures. The certainly significant misfit is actually to be expected considering that the stress relaxation started form different structural states caused by nonlinear deformation.

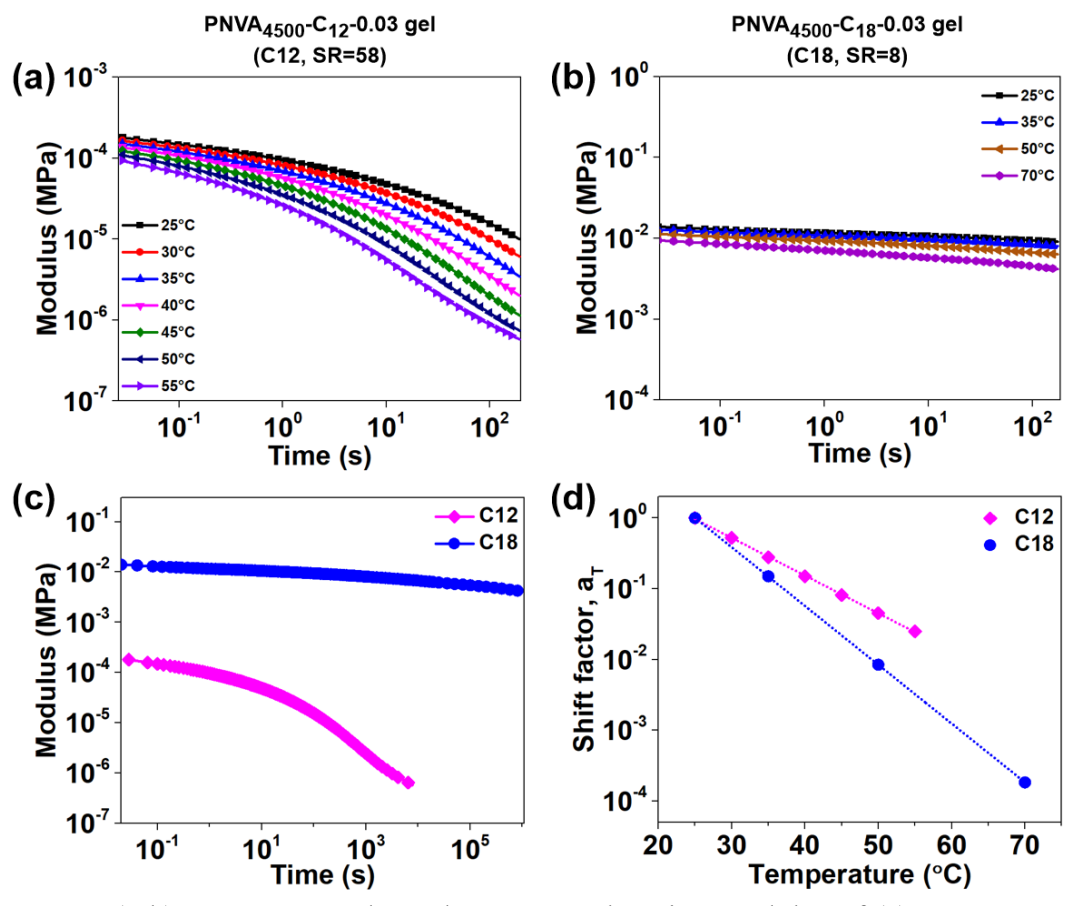


**Figure S9.** (a-b) Temperature dependent stress relaxation modulus of (a) PNVA<sub>4500</sub>-C<sub>12</sub>-0.03 and (b) PNVA<sub>4500</sub>-C<sub>18</sub>-0.03 hydrogels deformed by initial strain of 20% and 2%, respectively; (c) Stress relaxation master curves of PNVA<sub>4500</sub>-C<sub>n</sub>-0.03 hydrogels (n = 12, 18) generated at 25°C by time-temperature superposition; (d) Temperature dependence of shift factor (a<sub>T</sub>) for PNVA<sub>4500</sub>-C<sub>n</sub>-0.03 hydrogels (n = 12, 18), the lines are linear fitting of the respective data.

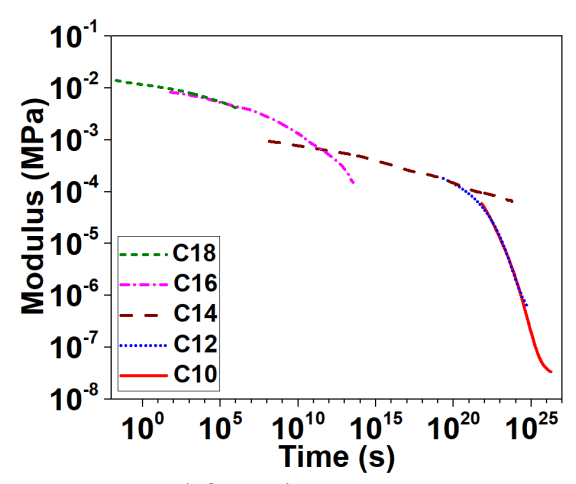


**Figure S10.** Master curve generated from time-temperature superposition master curves of PNVA<sub>4500</sub>-C<sub>n</sub>-0.03 hydrogels according to stress relaxation experiments, shear induced changes of the association structures affect the time-temperature-stickiness superposition (conditions for measurements, see **Table S5**, Supporting Information).

#### Estimation of the extent of side chain ordering in $C_{18}$ side chains

As a reference we take  $\Delta S^0 = 7.8 \text{ J/K/mol}$  as the melting per CH<sub>2</sub> group in polyethylene.<sup>7</sup>  $\Delta S$  for PNVA<sub>220</sub>-C<sub>18</sub>-1 (full substitution) was calculated using the data of second heating shown in **Figure 4** according to **Equation S7**.

$$\Delta G = \Delta H - T \times \Delta S \tag{S7}$$

For each repeat unit (NVA- $C_{18}$ ):

$$M_w = 337.59 \text{ g/mol}$$

$$T_{onset} = 58$$
°C = 331K

$$\Delta S_1 = \Delta H \div T_{onset} = 61.4 \text{ J/g} \div 331 \text{K} = 0.1855 \text{ J/g/K} = 62.6 \text{ J/K/mol}$$
 (Entropy change per monomer)

$$\Delta S_{CH_2}^{PNVA-C_{18}} = 62.6 J/K/mol \div 18 = 3.48 J/K/mol$$

For disordering a CH<sub>2</sub> group in an ideal crystal of polyethylene (PE),

 $\Delta S_{CH_2}^{PE} = 7.8 \ J/K/mol$ , the ratio of  $\Delta S_{CH_2}^{PNVA-C_{18}}/\Delta S_{CH_2}^{PE}$  indicates a significantly lower degree of ordering (< 45%) for the side chain crystallization.

**Table S1.** Parameters for synthesis of poly(*N-n*-alkyl-*N*-vinylacetamide)s.

Sample	PNVA M <sub>n</sub> (PDI) by SEC [kDa]	H(CH <sub>2</sub> ) <sub>n</sub> Br	Molar ratio of Bromide to monomer unit	Molar ratio of NaH to monomer unit	Reaction temperature, time	DS by <sup>1</sup> H NMR [mol%]	Yield (%)
PNVA <sub>4500</sub> -C <sub>10</sub> -0.03	380 (2.7)	n = 10	0.3	0.5	25°C, 18 h	3%	82
PNVA <sub>4500</sub> -C <sub>12</sub> -0.03	380 (2.7)	n = 12	0.3	0.5	25°C, 18 h	3%	78
PNVA <sub>4500</sub> -C <sub>14</sub> -0.03	380 (2.7)	n = 14	0.3	0.5	25°C, 18 h	3%	89
PNVA <sub>4500</sub> -C <sub>16</sub> -0.03	380 (2.7)	n = 16	0.3	0.5	25°C, 18 h	3%	82
PNVA <sub>4500</sub> -C <sub>18</sub> -0.03	380 (2.7)	n = 18	0.3	0.5	25°C, 18 h	3%	90
PNVA <sub>220</sub> -C <sub>18</sub> -1	19 (2.2)	n = 18	2.0	2.4	50°C, 65 h	100%	75

Table S2. DSC results of PNVA $_{4500}$ -C $_n$ -0.03 and PNVA-C $_n$ -1 (all data measured in second heating at a heating rate of  $10^{\circ}$ C/min).

	$1-C_nH_{2n+2}$	$1-C_nH_{2n+1}Br$	$PNVA_{4500}-C_n-0.03 \qquad \qquad PNVA-C_n-1$				$C_n$ -1			
Side chain length (n)	m.p.	m.p.	PNVA  M <sub>n</sub> [kDa]	Onset 1	Onset 2	$T_{g}$	PNVA M <sub>n</sub> [kDa]	Onset 1	Onset 2	$T_{g}$
10	-29.7°C	-29.2°C	380	-	-	189°C	380	-	68°C	-
12	-9.6°C	-9.5°C	380	-	68°C	174°C	380	-	67°C	173°C
14	5.8°C	5.6°C	380	-	67°C	177°C	380	-	65°C	197°C
16	18.1°C	18.0°C	380	-	64°C	182°C	380	-	-	-
18	28.2°C	28.2°C	380	-	72°C	179°C	19	58°C	71°C	-

Table S3. Activation energy obtained from creep experiments by Arrhenius plot

PNVA <sub>4500</sub> -C <sub>n</sub> -0.03 hydrogel	$E_a$ from $\eta$ (kJ/mol)	$E_a$ from $a_T$ (kJ/mol)	E <sub>a</sub> from η (kT)	E <sub>a</sub> from a <sub>T</sub> (kT)	Polymer concentration in hydrogel or aqueous solution
$C_{10}$	67.7	79.3	27	32	1.6 w/v%
$C_{12}$	64.6	87.6	26	35	1.7 w/v%
$C_{14}$	61.4	-	25	-	6.3 w/v%
$C_{16}$	40.4	-	16	-	10 w/v%
$C_{18}$	14.2	-	6	-	12.5 w/v%
P_8	30.0	30.8	12	12	12.5 w/v%
P_62	26.4	24.7	11	10	1.6 w/v%

**Table S4.** Experimental conditions used for creep experiments for master curves of  $PNVA_{4500}$ - $C_n$ -0.03 (creep time = 180 s).

Hydrogel PNVA <sub>4500</sub> -C <sub>n</sub> -0.03 (swelling time = 6 days)	Stress (Pa)	Temperatures measured for master curve (°C)
$C_{10}$	1	2, 25, 35, 50
$C_{12}$	20	2, 10, 15, 25, 35, 50
C <sub>14</sub>	10	25, 35, 50
C <sub>16</sub>	160	10, 25, 35, 50
$C_{18}$	160	2, 10, 25, 35, 50, 70, 80, 90
P_8	1	2, 10, 15, 25, 35, 50, 70
P_62	1	2, 10, 15, 25, 35, 50, 70, 90

**Table S5.** Experimental conditions used for stress relaxation experiments for master curves of  $PNVA_{4500}$ - $C_n$ -0.03 (time = 200 s).

Hydrogel PNVA <sub>4500</sub> -C <sub>n</sub> -0.03 (swelling time = 6 days)	Strain	Temperatures measured for master curve (°C)
$C_{10}$	20%	25, 30, 35, 40, 45, 50, 55
$C_{12}$	20%	25, 30, 35, 40, 45, 50, 55
$C_{14}$	2%	25, 35, 50, 70
$C_{16}$	2%	25, 35, 50, 70
$C_{18}$	2%	25, 35, 50, 70

## References

[1] Thissen, H.; Koegler, A.; Salwiczek, M.; Easton, C. D.; Qu, Y.; Lithgow, T.; Evans, R. A. Prebiotic-chemistry inspired polymer coatings for biomedical and material science applications. *NPG Asia Materials* **2015**, *7* (11), e225-e225. DOI: 10.1038/am.2015.122.

[2] Yen, B. L.; Hsieh, C.-C.; Hsu, P.-J.; Chang, C.-C.; Wang, L.-T.; Yen, M.-L. Three-dimensional spheroid culture of human mesenchymal stem cells: Offering

- therapeutic advantages and in vitro glimpses of the in vivo state. *Stem Cells Translational Medicine* **2023**, *12* (5), 235-244. DOI: 10.1093/stcltm/szad011.
- [3] Kim, S. j.; Kim, E. M.; Yamamoto, M.; Park, H.; Shin, H. Engineering multicellular spheroids for tissue engineering and regenerative medicine. *Advanced Healthcare Materials* **2020**, *9* (23), 2000608. DOI: 10.1002/adhm.202000608.
- [4] Kapałczyńska, M.; Kolenda, T.; Przybyła, W.; Zajączkowska, M.; Teresiak, A.; Filas, V.; Ibbs, M.; Bliźniak, R.; Łuczewski, Ł.; Lamperska, K. 2D and 3D cell cultures—a comparison of different types of cancer cell cultures. *Archives of Medical Science* **2018**, *14* (4), 910-919. DOI: 10.5114/aoms.2016.63743.
- [5] Dharmaraj, V. L.; Godfrin, P. D.; Liu, Y.; Hudson, S. D. Rheology of clustering protein solutions. *Biomicrofluidics* **2016**, *10* (4). DOI: 10.1063/1.4955162.
- [6] Ahmed, J. Chapter 9 Time-Temperature Superposition Principle and its Application to Biopolymer and Food Rheology. In *Advances in Food Rheology and Its Applications*, Ahmed, J., Ptaszek, P., Basu, S. Eds.; Woodhead Publishing, 2017; pp 209-241. DOI: 10.1016/B978-0-08-100431-9.00009-7.
- [7] Wunderlich, B.; Czornyj, G. A study of equilibrium melting of polyethylene. *Macromolecules* **1977**, *10* (5), 906-913. DOI: 10.1021/ma60059a006.

# 4 Synthesis and thermoresponsive properties of *N*-alkylated poly(*N*-vinylamide)s and their hydrogels

# 4.1 Introduction

Since the earliest reports on the lower critical solution temperature (LCST) behavior of aqueous poly(N-isopropylacrylamide) (PNIPAM) solutions, the thermoresponsive volume phase transition of hydrogels has attracted increasing attention for applications, e.g., in the field of biomedicine for actuation of drug delivery,<sup>2</sup> tissue engineering,<sup>3</sup> and studies of mechanotransduction in cell biology.<sup>4</sup> Within the wide range of other polymers, which exhibit LCST behavior in aqueous solution,<sup>5</sup> polyacrylamides have certain advantages. For example, the transition temperature of PNIPAM is in the range of the human body temperature, and the concentration dependence of the lower demixing temperature is negligible. The latter is particularly favorable for ensuring a defined volume phase transition in hydrogels. A family of yet little investigated, but promising water soluble and biocompatible polymers are poly(N-vinylformamide) and poly(N-vinylacetamide), 7, 8 which are isomers of polyacrylamides, exhibiting similar or even better water solubility. Their major advantage is their accessibility for chemical modification. N-vinylformamide and N-vinylacetamide can be copolymerized in a stochastic sequence and chemically modified afterwards by N-alkylation or selective hydrolysis of the formamide units.<sup>10</sup> Hydrolysis yields primary amine groups linked to the polymer backbone.11 Nalkylation allows tailoring the water solubility.<sup>12</sup> Most importantly, the amine group can be employed for linking to activated carboxylic acid groups for conjugation with

peptides and other biomolecules. Hence, the polymers listed in **Scheme 1** are intriguing candidates for novel biomaterials. Stochastic copolymerization and subsequent chemical modification by substitution and partial hydrolysis followed by further functionalization can be used to ensure statistical distribution of side chains along the backbone.

**Scheme 1.** Structure of copolymer of poly(*N*-vinylformamide-*stat-N*-vinylacetamide - *stat-N*-alkyl-*N*-vinylacetamide)

In **Chapter 3**, we have described formation of reversible hydrogels of poly(*N*-vinylacetamide)s that were substituted by 3 mol% of longer alkyl chains (C<sub>10</sub>-C<sub>18</sub>).<sup>13</sup> In this chapter, we focus on the LCST behavior of poly(*N*-alkyl-*N*-vinylamide)s with a higher degree of functionalization with short *n*-propyl and *n*-butyl alkyl chains and their hydrogels. So far, LCST behavior has been reported for poly(*N*-alkyl-*N*-vinylamide)s bearing short alkyl side chains at the amide position synthesized by copolymerization of the *N*-alkylated *N*-vinylamide monomers.<sup>12, 14-16</sup> Yet, these studies do not contain detailed information on the concentration and molecular weight dependence of their water solubility and the formation of thermoresponsive hydrogels.

Step 1.

ONH

radical initiator

ONH

$$R_1 = H, CH_3$$

Step 2.

NaH

 $R_2 = Br$ 

ONH

 $R_1 = H, CH_3$ 
 $R_2 = Br$ 

ONH

 $R_1 = H, CH_3$ 
 $R_2 = Br$ 

ONH

 $R_1 = H, CH_3$ 
 $R_2 = Br$ 

ONH

 $R_3 = Br$ 

ONH

 $R_4 = Br$ 

ONH

 $R_5 = Br$ 

ONH

 $R_7 = Br$ 

ONH

 $R_7$ 

**Scheme 2.** Synthesis procedure for poly(*N*-alkyl-*N*-vinylamide)s by *N*-substitution of poly(*N*-vinylamide)s

This chapter focuses on a more detailed study of the LCST behavior of such poly(N-vinylamide)s and the volume phase transition of hydrogels from these polymers. In contrast to the synthetic route reported in literature, <sup>12, 14-16</sup> the polymers investigated in this chapter were prepared by an inverse approach, relying on post-polymerization modification, as shown in Scheme 2. Compared to the polymerization of N-alkylated monomers, modification of the monomer units after polymerization has been considered to provide the following advantages: (i) The degree of polymerization (DP) of polymer backbones can be controlled by variation of the initiator concentration and determined before substitution; (ii) The degree of substitution (DS) of  $R_2$ - can be controlled by the amount of sodium hydride while the alkyl bromide can be employed in excess. Different substituents can be connected to the polymer backbone in one step by incorporating appropriate equivalents of alkyl bromides; (iii) DP and DS of the final products are controlled independently, while in the case of the copolymerization, the substitution pattern along the polymer backbone is controlled by the copolymerization kinetics of the respective N-alkyl-N-vinylamide monomers;12, 14-16 (iv) A broad variety of substituents can be considered, including relatively longer alkyl groups (e.g., chain length n > 10) and substituents with unsaturated bonds (e.g., allyl group). In this chapter, poly(N-vinylamide)s were synthesized through free radical polymerization, then these pre-polymers were N-alkylated by n-propyl or n-butyl groups in order to adjust the LCST.

# 4.2 Experimental section

#### 4.2.1 Materials

N-vinylacetamide (NVA), sodium hydride (NaH) dispersed in paraffin liquid (60%), 2,2'-azobis[2-(2-imidazolin-2-yl)propane]dihydrochloride and (VA-044)were obtained from Tokyo Chemical Industry Co., Ltd. N-vinylformamide (NVF, 98%), anhydrous dimethylformamide (DMF), 1,2-ethanedithiol, and all alkyl bromides were received from Sigma-Aldrich. Anhydrous dimethyl sulfoxide (DMSO) and anhydrous tetrahydrofuran (THF) were products of Acros Organics. Isopropanol and ethanol were purchased from Fischer Chemical. Technical acetone was purchased from Höfer Chemie. 2,2-Dimethoxy-2-phenylacetophenone (DMPA) and technical n-hexane were purchased from VWR. Deuterated methanol, deuterium oxide and 5 mm NMR tubes (ASTM Class-B Type 1, glass) were purchased from Deutero. 2,2'-azobis(2-methylpropionitrile) (AIBN, 98%, Sigma-Aldrich (Merck, Darmstadt, Germany)) was purified by recrystallization from methanol, NVF was purified by distillation at 70 °C under high vacuum. All the other reagents were used as received. Deionized water was used for all experiments. 1000 Da MWCO dialysis membrane was a product of Spectrum Laboratories, Inc.

# 4.2.2 Sample nomenclature

The following denotation was used for polymers: PNVA-x represents PNVA with DP = x; PNVA- $C_n$ -y-x represents poly(N-alkyl-N-vinylacetamide) with DP = x, and n-alkyl side chains consisting of n methylene units at DS of y; PNVA-(allyl- $y_1$ )-( $C_n$ - $y_2$ )-x represents N-substituted PNVA with a backbone DP = x and two types of side chains: allyl at DS of  $y_1$ , and  $C_n$  at DS of  $y_2$ .

# 4.2.3 Synthesis of poly(*N*-vinylamide)s

Poly(*N*-vinylamide)s were prepared by free radical polymerization in alcohol or water solution. The molecular weight was adjusted by the monomer to initiator ratio. Synthetic parameters are shown in **Table S1**. Firstly, NVA or NVF was dissolved, and then the monomer solution was degassed by three freeze-pump-thaw cycles. After that, the solution was heated to reaction temperature and radical initiator was added under nitrogen flow. The mixture was kept at reaction temperature for 18 hours and reaction was terminated by exposure to air. The mixture was precipitated in acetone, and then the precipitate was dialyzed against deionized water using 1000 Da MWCO dialysis membrane. Final products were obtained by lyophilization.

# 4.2.4 Synthesis of poly(*N*-alkyl-*N*-vinylamide)s

As a representative example, 1 gram of PNVA (11.7 mmol) was dissolved in 60 mL of anhydrous DMF. Sodium hydride powder (NaH, dispersed in paraffin liquid), which was successively washed by anhydrous THF and anhydrous DMF, was suspended in 30 mL of anhydrous DMF and cooled in an ice bath for 30 min. The aforementioned PNVA@DMF solution was slowly injected into the NaH suspension

controlled by a syringe pump. The degree of substitution could be controlled by the equivalent of NaH with excess amount of alkyl bromides (as shown in **Figure 1**). The mixture was stirred for 30 min while being kept in an ice bath. The bromide (allyl bromide, *n*-propyl bromide or *n*-butyl bromide) was added and the ice bath was removed. When the reaction finished, the reaction mixture was cooled again by the ice bath for 30 min, and then quenched by methanol. Solvents were removed by rotary evaporation and the residual solids were dissolved in ethanol and precipitated in technical *n*-hexane. The polymer was dialyzed against deionized water using 1000 Da MWCO dialysis membrane. Final products were obtained by lyophilization. Detailed parameters are listed in **Table S2**, Supporting Information.

For the preparation of poly(*N*-alkyl-*N*-vinylformamide)s, 1.67 gram of the parent polymer (PNVF) were dissolved in 30 mL of anhydrous DMSO, sodium hydride (NaH) was washed and suspended in certain volume of anhydrous DMF. The reaction was conducted at 25 °C and stopped after 18 hours, quenched by methanol, then precipitated directly in THF. Detailed parameters are listed in **Table S3**, Supporting Information.

# 4.2.5 Synthesis of poly(*N*-allyl-*N*-vinylacetamide-*stat-N*-alkyl-*N*-vinylacetamide)s

*N*-alkylated polymers with only a small fraction of allyl groups for covalent crosslinking were prepared by first preparing and isolating allyl-functionalized polymers using allyl bromide followed by a second step in which the remaining amides were *N*-alkylated by the *n*-alkyl bromide according to the procedure described

above. Detailed parameters are listed in Table S4, Supporting Information.

# 4.2.6 Hydrogel preparation

DMPA and 1,2-ethanedithiol (0.2 eq and 0.5 eq, respectively; relative to the total amount of allyl groups in each polymer) were added to a solution of PNVA-(allyl-4%)-(C<sub>3</sub>-91%)-176 or PNVA-(allyl-4%)-(C<sub>4</sub>-35%)-176 (300 mg/mL in ethanol). Then the solution was loaded into a 5 mm NMR tube (O.D. =  $4.950 \pm 0.030$  mm, wall thickness = 0.43 mm), sealed by the NMR tube cap, rested still for over an hour until no air bubbles were visible inside the solution, then exposed to UV irradiation (UVP, UVL-56, 6 W, 365 nm wavelength) at  $20 \pm 2$  °C for 8 hours. The distance between the NMR tube and the planar light source was around 2 mm. After crosslinking, the hydrogels were dried at 65 °C in an oven, and then taken out from the NMR tube, extracted and swollen by water at  $20 \pm 2$  °C. Water was changed every 12 hours for one week until the hydrogels reached equilibrium swelling ratio.

#### 4.2.7 Characterization

High resolution <sup>1</sup>H-NMR spectra were recorded on a Bruker Avance III-400 FT-NMR spectrometer at 400 MHz. Deuterated methanol or deuterium oxide was used as solvent.

Molecular weights ( $M_{\rm n}$  and  $M_{\rm w}$ ) were determined by size exclusion chromatography (SEC) either in DMF or in water. The set-up for SEC in DMF consisted of a HPLC pump (1260 Infinity, Agilent), a dual RI-/Visco detector (ETA-2020, WGE), an UV-detector (VWD, 1290 Infinity II, Agilent). One precolumn (8×50 mm) and three GRAM gel columns were applied. The diameter of the

gel particles measured 10 μm, and the nominal pore widths were 30, 100, 1000 Å (8×300 mm², Polymer Standards Service). DMF (≥99.9%, HiPerSolv CHROMANORM® HPLC grade, VWR) with 1 g/L LiBr (≥99%, Sigma-Aldrich) was used as the eluting solvent and 2 μL/mL of toluene (≥99%, Sigma-Aldrich) were added as internal standard. The flow rate and temperature were set to 1 mL/min and 60 °C, respectively. Calibration was carried out using narrowly distributed poly(methyl methacrylate) (PMMA) standards (Polymer Standards Service).

For SEC in water, water (HiPerSolv CHROMANORM® HPLC grade, VWR) containing 0.1 mol/L sodium nitrate (NaNO<sub>3</sub>, p.a. level, Merck KGaA) and 0.01 wt% sodium azide (NaN<sub>3</sub>, extra pure, Merck KGaA) was used as eluent. The set-up consisted of a pre-column (8 × 50 mm) and three Novema Max gel columns (8 × 300 mm, 30, 100, and 1000 Å, Polymer Standards Service) with an Agilent 1200 HPLC pump, a refractive index detector (1200, Agilent), and an UV-detector (VWD, 1200, Agilent). The diameter of the gel particles measured 5 μm. Elution was done at a flow rate of 1.0 mL/min at 40 °C. Ethylene glycol (0.5 μL/mL, 99.5%, Fluka analytical) was added as internal standard. Calibration was performed using narrowly distributed poly(ethylene oxide) standards (Polymer Standards Service). All results were evaluated using the PSS WinGPC UniChrom software (Version 8.3.2).

#### 4.2.8 Cloud point measurements

Polymers measured were dissolved in deionized water at predetermined concentrations then the mixture was pre-cooled at 4°C before measurement. Transmittance-temperature curves of thermoresponsive polymers were recorded by a

Varian Cary 100 Bio UV–Vis spectrophotometer equipped with a thermo-regulator. The heating/cooling rate was 0.5 °C min<sup>-1</sup> unless otherwise mentioned. The cloud point ( $T_{\rm cp}$ ) of a polymer solution was determined as the temperature at the inflection point of its transmittance-temperature curve of the first heating. Here, the inflection point is the minimum value of the first order derivative of the transmittance-temperature curve.

#### 4.2.9 Degree of Swelling and swelling dynamics of hydrogels

The equilibrium swelling ratios of hydrogels  $(SR(T_0))$  at temperature  $T_0$  (20  $\pm$  2°C) were determined according to **Equation 1**.

$$SR(T_0) = \frac{W_s(T_0) - W_d}{W_d} \tag{1}$$

where  $W_s$  ( $T_0$ ) is the mass of the swollen hydrogel and  $W_d$  is the mass of dry lyophilized hydrogel. For the rates of deswelling and reswelling, the respective hydrogel sample was put into 20 mL of deionized water, which was brought to the target temperature ( $T_1$ ) before. After a waiting period during which the sample could adjust to the temperature, it was taken out of the water, water attached to the surface was quickly removed by blotting with a tissue wiper (Kimtech<sup>TM</sup> Science) and the mass of the swollen gel ( $W_s(T_1)$ ) was determined by weighing, and the swelling ratio was calculated by **Equation 2**.

$$SR(T_1) = \frac{W_S(T_1)}{W_S(T_0)} \times (SR(T_0) + 1) - 1 \tag{2}$$

# 4.3 Results and discussion

Molecular weights of the radically polymerized PNVAs and PNVFs were adjusted by altering the initiator to monomer ratio (Table S1, Supporting

Information). This way, we obtained a series of PNVAs and PNVFs with low, middle and high *DP* in the range of 70, 180, and 1000, respectively. According to size exclusion chromatography (SEC), molecular weight distributions of the parent polymers were monomodal (**Figure S1**, Supporting Information). The parent PNVAs and PNVFs were converted to poly(*N*-alkyl-*N*-vinylamide)s by *N*-substitution with allyl bromide, *n*-propyl bromide and *n*-butyl bromide. Samples were analyzed by <sup>1</sup>H NMR for composition. *DS* could be evaluated from the <sup>1</sup>H-NMR signals of the side chains and the polymer backbone. (For details see **Figure S2** and **Figure S3**, Supporting Information).

Both allyl or alkyl bromides as well as NaH as base were used in excess. We found that the DS mostly depends reproducibly on the amount of NaH used in the functionalization reaction. This is demonstrated in **Figure 1** for the substitution of PNVA (DP = 176) by n-butyl bromide, where the DS was varied from 17 mol% to 97 mol%. For high DS exceeding 80%, large excesses of at least 4.5 eq. of NaH were required. Extrapolation to low DS indicates that only a fraction of the excess NaH got consumed by side reactions with the solvent, e.g., remaining traces of water. We propose that the large excess is needed to overcome the reactivity restrictions of the heterogeneous reaction, where the polymer needs to react with NaH particles dispersed in the solvent.

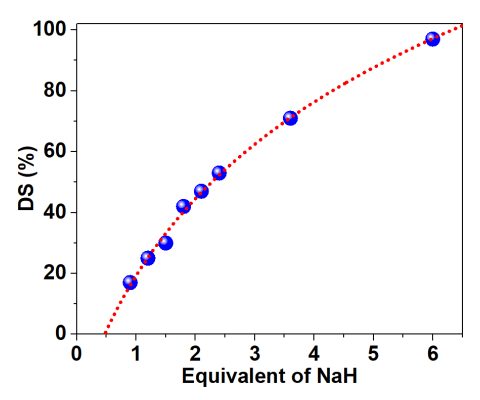


**Figure 1.** Dependence of the degree of substitution of poly(*N*-*n*-butyl-*N*-vinylacetamide) PNVA-C<sub>4</sub>-*DS*-176 on equivalents of sodium hydride per amide group used in the reaction. All polymers were prepared from the same batch of PNVA-176, the molar ratio of *n*-butyl bromide to NaH was kept at 5:6. Red dashed line is the fitting curve according to the fitting equation:  $DS = -0.2273644 + 0.6173327 \cdot \ln(eq_{\text{NaH}} + 0.97469)$  with adjusted  $r^2 = 0.996$ .

**Table 1** lists N-alkylated poly(N-vinylamide)s employed in the following study. Denotation of the samples was chosen to allow direct identification of the degree of polymerization and the substitution. As an example, PNVA-(allyl-4%)-(C<sub>4</sub>-35%)-176 is a poly(N-vinylacetamide) with degree of polymerization DP = 176 where the amide groups were statistically substituted to 35% by n-butyl groups and 4% by allyl groups.

**Table 1.** Thermoresponsive alkylated poly(*N*-vinylamide) derivatives synthesized

Entry	Name	Backbone	$M_{ m n}$ of backbone polymer	$DP^{(a)}$	substituent	DS <sup>(b)</sup>	End group	Approximate  LCST/°C <sup>(c)</sup>
1	PNVA-C <sub>3</sub> -100%-70	PNVA	6 kDa	70	n-propyl	100%	AIBN	53.5
2	PNVA-C <sub>3</sub> -100%-176	PNVA	15 kDa	176	<i>n</i> -propyl	100%	AIBN	57.3
3	PNVA-C <sub>3</sub> -100%-1057	PNVA	90 kDa	1057	n-propyl	100%	VA-044	61.3
4	PNVA-C <sub>4</sub> -37%-70	PNVA	6 kDa	70	<i>n</i> -butyl	37%	AIBN	43.9
5	PNVA-C <sub>4</sub> -25%-176	PNVA	15 kDa	176	<i>n</i> -butyl	25%	AIBN	72.3
6	PNVA-C <sub>4</sub> -30%-176	PNVA	15 kDa	176	<i>n</i> -butyl	30%	AIBN	55.0
7	PNVA-C <sub>4</sub> -45%-176	PNVA	15 kDa	176	<i>n</i> -butyl	45%	AIBN	44.1
8	PNVA-C <sub>4</sub> -47%-176	PNVA	15 kDa	176	n-butyl	47%	AIBN	35.8
9	PNVA-C <sub>4</sub> -53%-176	PNVA	15 kDa	176	<i>n</i> -butyl	53%	AIBN	29.7
10	PNVA-C <sub>4</sub> -71%-176	PNVA	15 kDa	176	n-butyl	71%	AIBN	25.1
11	PNVA-C <sub>4</sub> -97%-176	PNVA	15 kDa	176	n-butyl	97%	AIBN	11.6
12	PNVA-allyl-97%-70	PNVA	6 kDa	70	allyl	97%	AIBN	39.8
13	PNVA-allyl-70%-176	PNVA	15 kDa	176	allyl	70%	AIBN	65.8
14	PNVA-allyl-87%-176	PNVA	15 kDa	176	allyl	87%	AIBN	45.2
15	PNVA-allyl-97%-176	PNVA	15 kDa	176	allyl	97%	AIBN	43.0
16	PNVA-(allyl-4%)-(C <sub>3</sub> -91%)-176	PNVA	15 kDa	176	allyl; n-propyl	4%;	AIBN	60.0 <sup>(d)</sup>
17	PNVA-(allyl-4%)-(C <sub>4</sub> -35%)-176	PNVA	15 kDa	176	allyl; <i>n</i> -butyl	4%;	AIBN	45.6 <sup>(e)</sup>

18	PNVF-C <sub>3</sub> -93%-183	PNVF	13 kDa	183	<i>n</i> -propyl	93%	VA-044	44.7
19	PNVF-C <sub>3</sub> -73%-605	PNVF	43 kDa	605	n-propyl	80%	VA-044	47.3
20	PNVF-C <sub>3</sub> -100%-605	PNVF	43 kDa	605	n-propyl	100%	VA-044	43.0
21	PNVF-C <sub>4</sub> -32%-183	PNVF	13 kDa	183	<i>n</i> -butyl	32%	VA-044	40.3 <sup>(f)</sup>
22	PNVF-allyl-59%-183	PNVF	13 kDa	183	allyl	59%	VA-044	23.4

<sup>(</sup>a) *DP*: degree of polymerization of the backbone polymer; (b) *DS*: degree of substitution of alkyl side chains; (c) The cloud point of 50 mg/mL aqueous polymer solution at inflection point of transmittance-temperature curves is taken as approximate LCST of the corresponding polymer (unless the concentration is specifically mentioned); (d-e) cloud points measured from 100 mg/mL aqueous polymer solution; (f) cloud point measured from 20 mg/mL aqueous polymer solution.

In the last column of **Table 1**, we also listed the approximated LCSTs which were estimated from the concentration dependence of cloud points. The cloud point  $(T_{cp})$  was determined by the temperature of the inflection point of the transmittance-temperature curves during heating. <sup>17</sup> For this method, the observation of the cloud points is highly dependent on the heating rates, and the true value is more closely approached by lower heating rates. For the lack of reference regarding the influence of heating rates in cloud points of alkylated poly(N-vinylamide)s in literature. transmittance-temperature of aqueous solution of curves PNVA-C<sub>3</sub>-100%-176 (50 mg/mL) at three different heating rates were compared and shown in Figure 2a. The cloud points measured were 56.8 °C, 57.4 °C and 60.4 °C, at heating rates of 0.3 °C/min, 0.5 °C/min, and 1.0 °C/min, respectively. Notably, relatively high heating rates (e.g., 1.0 °C/min) would cause considerable error in cloud points, while relatively low heating rates (e.g., 0.3 °C/min) would result in long duration of measurements and consequent change in concentration, therefore 0.5 °C/min was selected as the heating rate for all the cloud point measurements due to the compromise of duration and precision. Furthermore, there is also remarkable hysteresis between heating and cooling curves. The higher the heating rate, the more severe was the hysteresis effect due to retarded segregation.

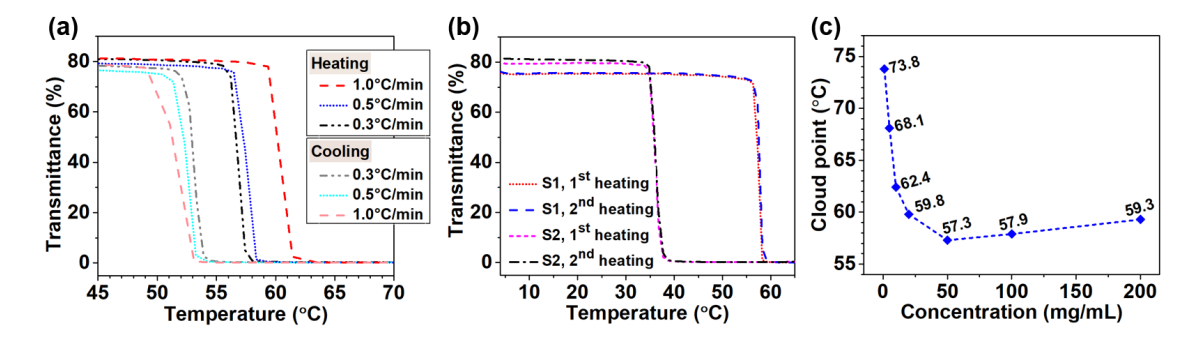


**Figure 2. (a)** Transmittance-temperature curves for PNVA-C<sub>3</sub>-100%-176 (50 mg/mL) measured by firstly heating then cooling at different heating/cooling rates. Transmittance between 4 °C and 70 °C were measured for 0.5 °C/min and 1.0 °C/min groups; while transmittance between 20 °C and 70 °C were measured for 0.3 °C/min

group; **(b)** Transmittance-temperature curves for sample S1 (PNVA-C<sub>3</sub>-100%-176 at 50 mg/mL) and sample S2 (PNVA-C<sub>4</sub>-47%-176 at 50 mg/mL), transmittance-temperature curves from 4 °C to 70 °C were recorded at 0.5 °C/min. First heating: the aqueous solutions were prepared and cooled at 4 °C for 24 h before measurements; second heating: the samples which were used in the first heating were cooled at 4 °C for 24 h and then re-measured; **(c)** Cloud point curve of PNVA-C<sub>3</sub>-100%-176 recorded at heating rate of 0.5 °C/min, the labels (unit: °C) represent cloud points at corresponding concentrations.

**Figure 2b** demonstrates the reversibility of the precipitation/dissolution. After cooling at low temperature for sufficient time (e.g., at 4°C for 24 h), the transmittance-temperature curves in the second heating overlapped well with that of the first heating. This observation indicated that the polymer solution returned to the same state.

For further studies, aqueous solutions for cloud point measurements were kept at 4°C for at least 24 hours. **Figure 2c** summarizes cloud points of PNVA-C<sub>3</sub>-100%-176 at concentrations up to 200 mg/mL. Above 20 mg/mL, the cloud point curve became rather flat like it is known for polyacrylamides.<sup>6</sup> As listed in **Table 1** for the different polymers, we took the cloud points of the 50 mg/mL solutions as an approximate LCST (measured at a heating rate of 0.5 °C/min unless otherwise specified).

Figure 3 depicts variations of the cloud point depending on the molecular weight of PNVAs, which were fully substituted by *n*-propyl groups. Irrespective of the low heating rate, the transition occurred in a narrower temperature window for lower molecular weights. At higher concentrations, the cloud points yielded a flat concentration dependence from which we estimated the LCST as given in Table 1. We observed inverse molecular weight dependence, implying that lower molecular weight polymers showed lower cloud point temperatures. For higher molecular weights, the onset of turbidity was not observed at low concentration, most likely because polymers could not agglomerate to sufficiently large particles to scatter the

light and attenuate transmission. As it will be discussed below, this retardation was attributed to some crosslinking by the formation of clusters of short stereoregular segments. Still, higher molecular weight polymers should exhibit larger miscibility gaps compared with lower molecular weight ones according to the statistical thermodynamics of polymer solutions.<sup>22, 23</sup> In agreement with this, LCST shifting towards lower temperatures with increasing molecular weights has been confirmed for aqueous solutions of poly(ethylene oxide).<sup>24</sup> However, the inverse molecular weight dependence, which we observed for all samples reported here, has been reported also for poly(N-isopropylacrylamide)s and explained by the association of hydrophobic end groups of hydrophilic polymer backbones. 18, 19, 25 The concentration of hydrophobic end groups may exceed the critical association concentration, and the entropy of mixing corresponds to that of a much larger molecular volume than that of the non-associated high molecular weight polymers yielding an apparently lower LCST. 26 This is an additional explanation for our observation. While the two lower molecular weight samples were polymerized with AIBN as an initiator favouring end group association, only PNVA-C<sub>3</sub>-100%-1057 was prepared with the water soluble initiator VA-044.

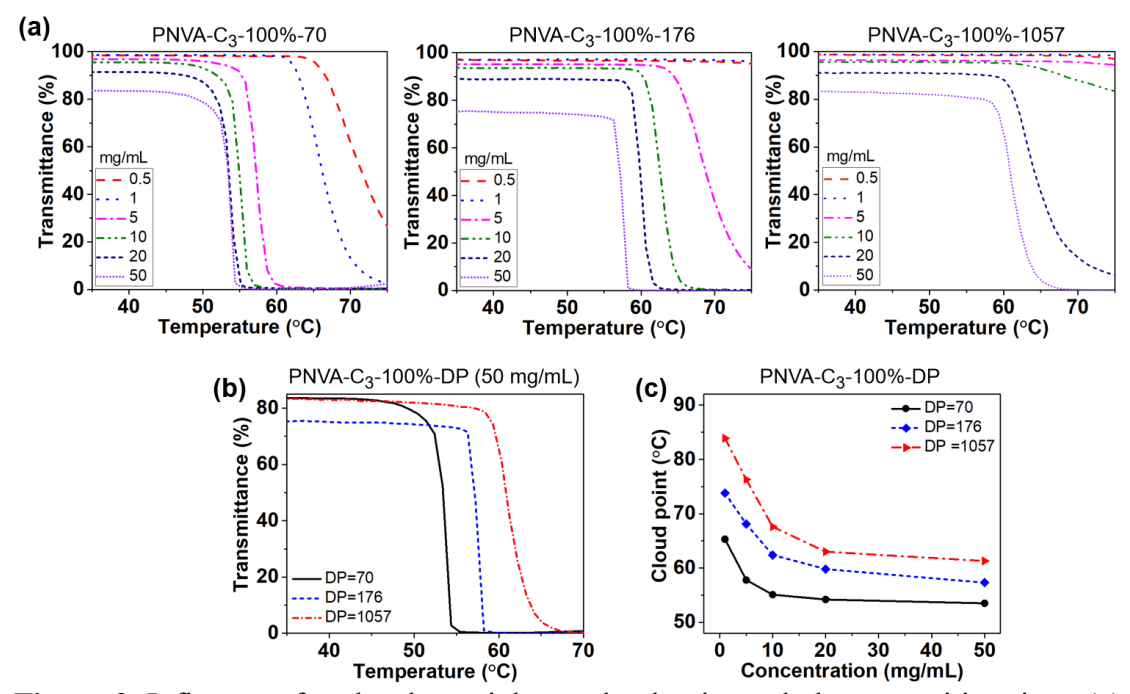


**Figure 3.** Influence of molecular weight on cloud point and phase transition time. (a) temperature-dependent transmittance curves of PNVA-C<sub>3</sub>-100%-70, PNVA-C<sub>3</sub>-100%-176, and PNVA-C<sub>3</sub>-100%-1057 aqueous solution at indicated polymer concentrations (mg/mL); (b) comparison of the temperature-dependent transmittance curves of PNVA-C<sub>3</sub>-100%-DP (DP = 70, 176, and 1057) at identical concentration of 50 mg/mL; (c) comparison of the cloud point curves of PNVA-C<sub>3</sub>-100%-DP (DP = 70, 176, and 1057). Heating rate = 0.5 °C/min.

The cloud point shifted to lower temperature, when the *n*-propyl substituents were replaced by allyl and by *n*-butyl groups indicating an increased hydrophobicity of these substituents (**Figures 4** and **5**). For the allyl substituted PNVAs (**Figure 4**), we observed that the cloud point could be shifted to lower temperature when the fraction of allyl substituted units were increased, and the difference in LCSTs caused by increase of DS became negligible when the DS exceeded a certain value (e.g., DS > 87%).

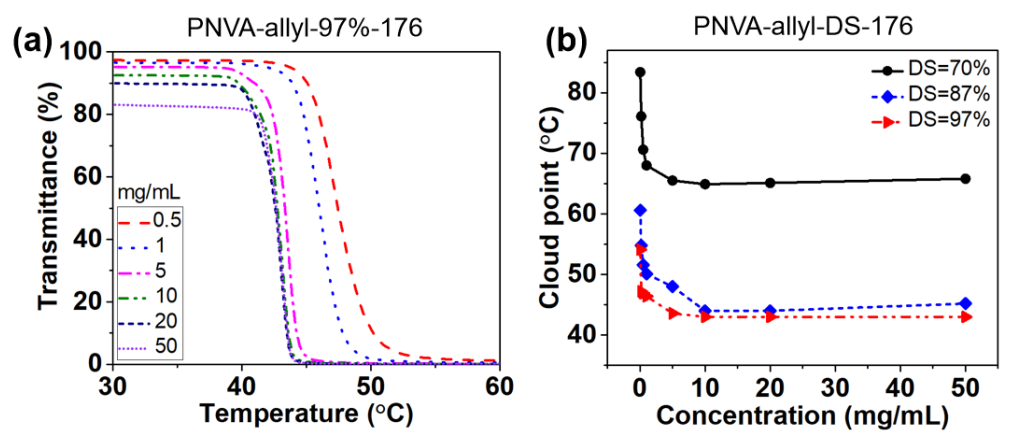


**Figure 4.** (a) Transmittance-temperature curves of PNVA-allyl-97%-176 aqueous solutions at indicated concentrations; (b) Comparison of the cloud point curves of PNVA-allyl-DS-176 (DS = 70%, 87%, and 97%). Heating rate = 0.5 °C/min.

**Figure 5a** depicts cloud point curves of PNVA-176 which was *N*-alkylated by *n*-butyl bromide to different degrees. As shown in **Figure 5b** as an example of the cloud point for the 50 mg/mL solutions, which we took for an estimation of the LCST, the cloud point decreased monotonically with increasing *DS*. This monotonic decrease is expected only for a stochastical substitution of the polymer backbone. **Figure 5c** gives a comparison of the miscibility gap as measured by cloud points for the practically fully *N*-substituted PNVAs with *n*-propyl, allyl and *n*-butyl groups, respectively. **Figure 5d** depicts transmission measurements for the respective highest concentration of the samples in **Figure 5c**, demonstrating a slower onset of the cloudiness at lower temperature at increasing length of the side chains. We consider this an indication that the higher hydrophobicity of the longer alkyl chains causes a stronger amphiphilic character of the monomer unit with its hydrophilic backbone and favours intramolecular association in the early stages of the segregation.

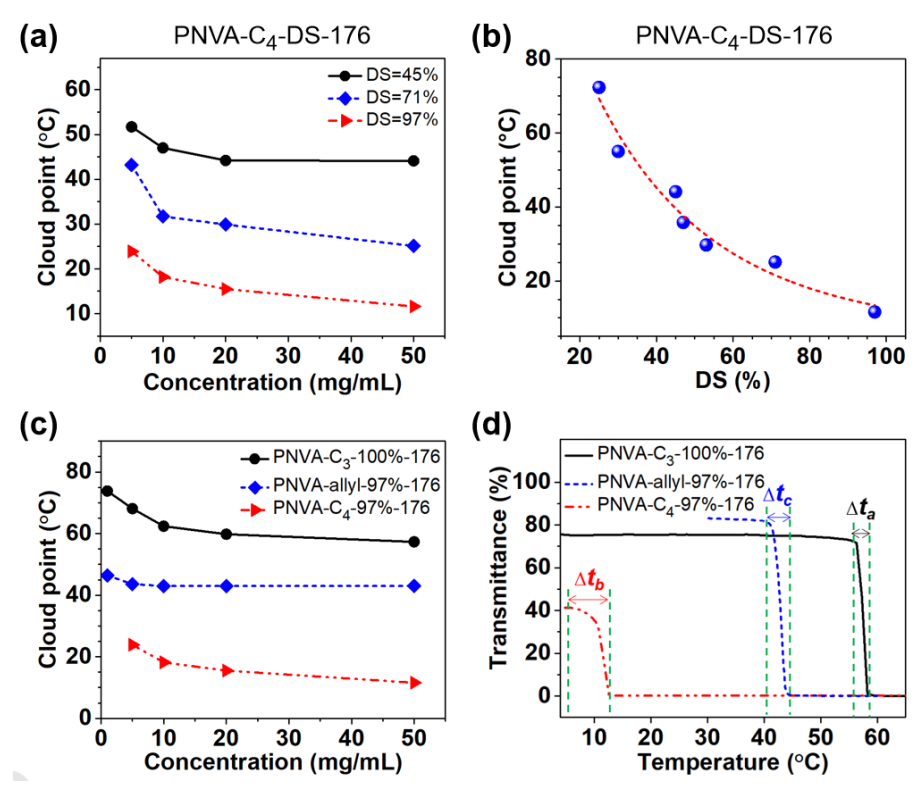


**Figure 5. (a, b)** Cloud point suppression upon increasing *N*-alkylation of PNVA by *n*-butyl groups. **(a)** Cloud point curves of PNVA-176 with 45%, 71% and 97% substitution by *n*-butyl groups (transmittance-temperature curves for all data point are shown in **Figure S4**, Supporting Information); **(b)** monotonic decrease of the cloud points upon increasing degree of substitution, the red dashed curve is the fitting line according to equation:  $LCST = e^{5.04869-3.49\times DS+0.99142\times DS^2}$ , adjusted  $r^2 = 0.95$ ; **(c)** comparison of the cloud point suppression by practically full *n*-propyl, *n*-allyl, and *n*-butyl substitution of PNVAs; **(d)** comparison of the rate by which the cloudiness developed in solutions at 50 mg/mL (the transmittance was measured upon heating at 0.5 °C/min).

Furthermore, we investigated low molecular weight polyvinylamides in which the isobutyronitrile end groups were replaced by water soluble 2-isopropyl-2-imidazoline groups and we replaced the prepolymer PNVA by the presumably more water soluble PNVF. To eliminate the effect of the backbone molecular weights, we prepared polymers from PNVA-176 (15 kDa) and PNVF-183 (13 kDa) with roughly identical monomer units per chain. **Figures 6a-c** depicts the comparison of the cloud point curves of PNVA-C<sub>3</sub>-100%-176 with isobutyronitrile end groups and PNVF-C<sub>3</sub>-93%-183 with 2-isopropyl-2-imidazoline end groups. Opposite to our

expectation, PNVF-C<sub>3</sub>-93%-183 turned out to segregate at lower temperature than the poly(*N*-vinylacetamide) derivative. The same trend is observed by the comparison of PNVA-allyl-70%-176 and PNVF-allyl-59%-183 (**Figures 6d-f**). Because the choice of the end groups would promote the converse effect, the data indicate that the PNVF backbone favours segregation. A tentative explanation may be that the formamide groups tend to form clusters comprising short stereoregular segments. Both this observation and explanation are supported by earlier reports. <sup>12, 14, 15</sup> The atactic polymer configuration contains segments with a different stereo-structure and we assume that short segments with a suitable stereo-structure, can form hydrogen bonded clusters which in turn favour segregation. Such an explanation is supported by the fact that the polymers which precipitated at high temperatures from concentrated aqueous solutions did not quickly re-dissolve when they were cooled below the LCST.

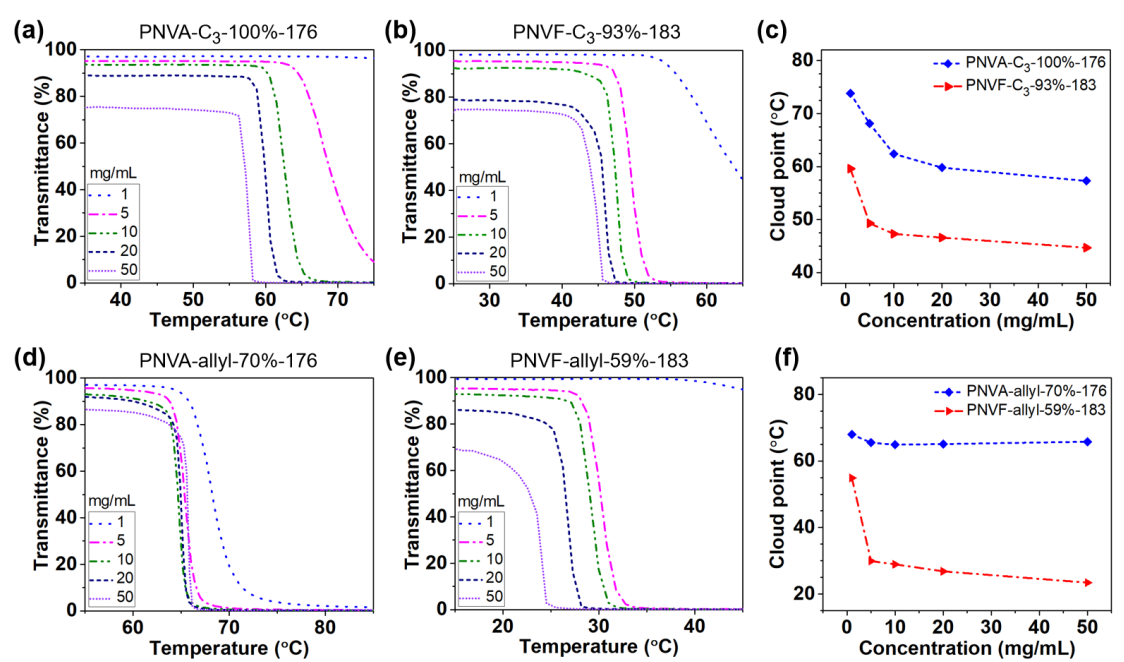
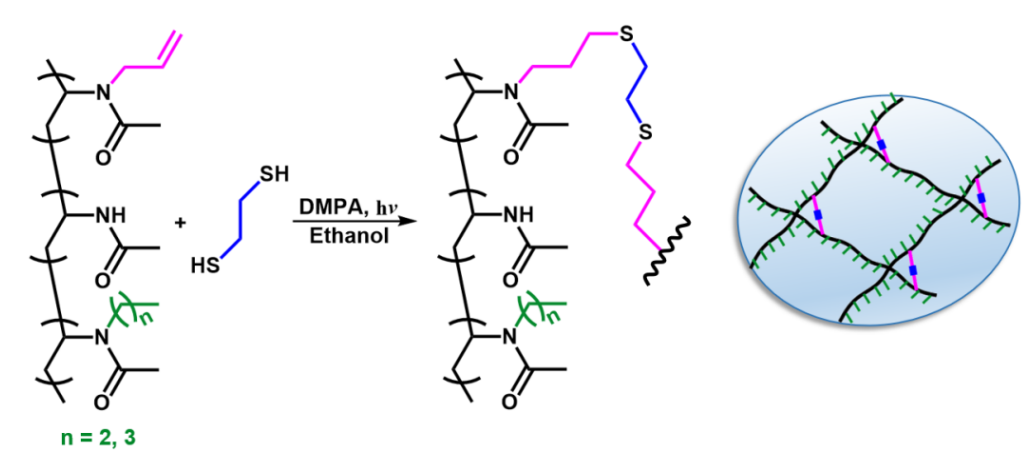


**Figure 6.** Comparison of cloud points of alkylated PNVAs and alkylated PNVFs. (a, b, d, e) are temperature-dependent transmittance curves of (a) PNVA-C<sub>3</sub>-100%-176, (b) PNVF-C<sub>3</sub>-93%-183, (d) PNVA-allyl-70%-176, and (e) PNVF-allyl-59%-183 aqueous solutions at different concentrations. (c, f) are comparison of cloud point curves of (c) PNVA-C<sub>3</sub>-100%-176 and PNVF-C<sub>3</sub>-93%-183, and (f) PNVA-allyl-70%-176 and PNVF-allyl-59%-183.

Formation of small crosslinking clusters favoured by hydrophobic segregation at high temperature, which act as catenations after cooling a sample from a temperature above the LCST to the solubility regime, should become much more obvious with permanently crosslinked gel bodies. In order to do swelling and deswelling experiments with gels from the thermoresponsive alkylated PNVAs, we prepared permanently crosslinked gels from PNVA-(allyl-4%)-(C<sub>3</sub>-91%)-176 and PNVA-(allyl-4%)-(C<sub>4</sub>-35%)-176. Crosslinking was done by the photo-initiated radical reaction of the allyl groups with ethanedithiol (**Scheme 3**).



**Scheme 3.** Synthetic route for the preparation of PNVA-allyl-C<sub>n</sub> hydrogels by UV.

Figure 7 depicts a series of small gel discs, which had been cut from a cylinder prepared by crosslinking of an ethanol solution of the respective polymer in an NMR tube. After drying to remove the ethanol, samples were swollen at  $20 \pm 2$  °C in deionized water. The photographs in Figures 7a and 7b show samples kept in water at target temperatures and photographed immediately after taken out of water. For each of the images, the sample was kept at the respective temperature for three days in order to ensure equilibrium swelling. Figures 7c and 7d demonstrate the collapse of the hydrogels at different temperatures. The geometrically affine shrinkage of the short cylinders demonstrates macroscopically homogeneous crosslinking.

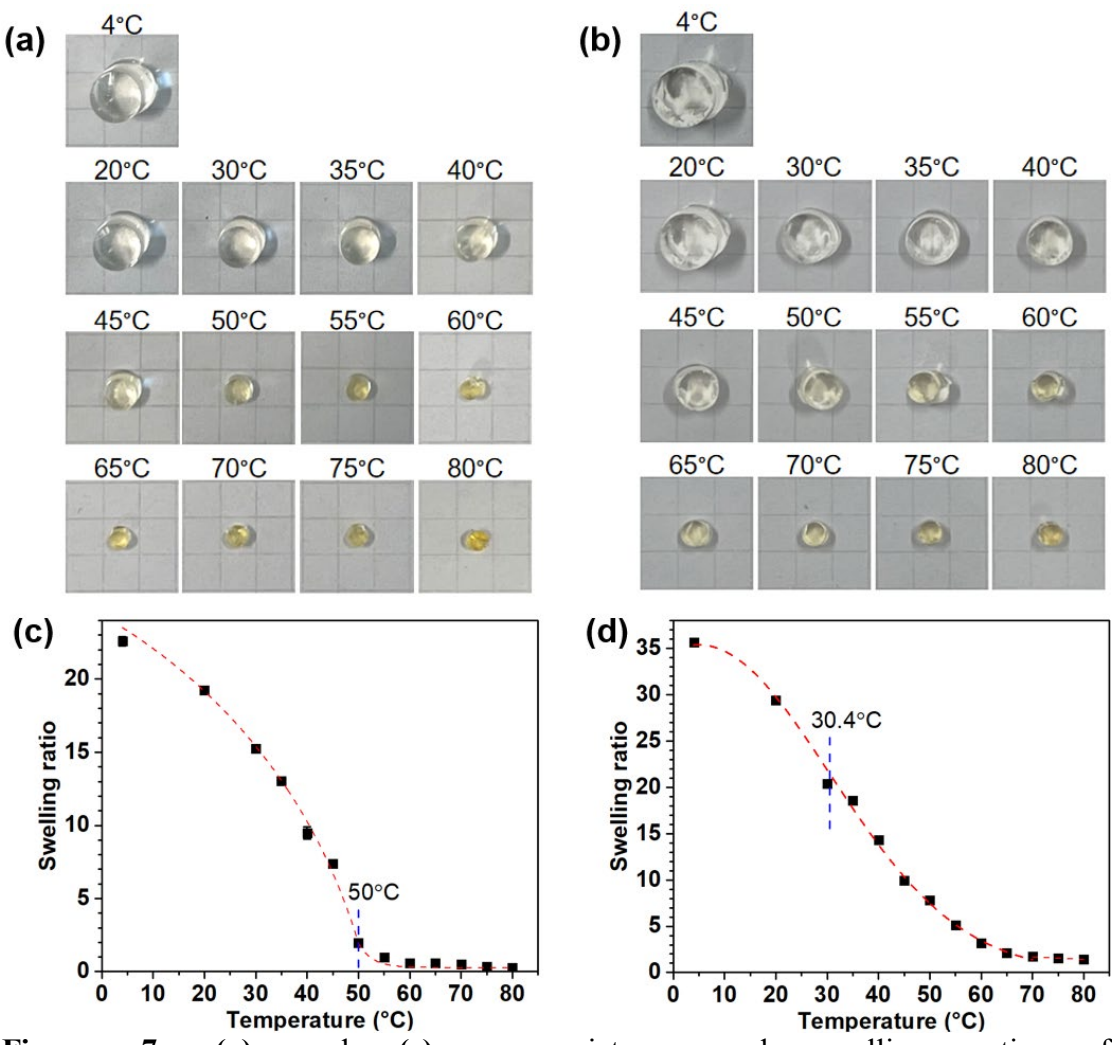


**Figure** pictures 7. (a) and (c) are and swelling ratio PNVA-(allyl-4%)-(C<sub>3</sub>-91%)-176 hydrogels after soaked in water at indicated temperatures for 3 days, respectively. (b) and (d) are pictures and swelling ratio of PNVA-(allyl-4%)-(C<sub>4</sub>-35%)-176 hydrogels after soaked in water at indicated temperatures for 3 days, respectively. The mesh size behind the hydrogels samples in (a) and (b) is 5 mm  $\times$  5 mm. Error bars for the swelling ratios in Figures (c) and (d) represent standard deviation (replicates = 3). The blue dashed lines in Figures (c) and (d) indicate the VPTT of the respective sample calculated by first-order derivation of the exponential fitting line of the swelling-temperature data.

Figure 8 depicts reswelling after the samples were first heated from  $20 \pm 2$  °C to a particular temperature and then brought back to  $20 \pm 2$  °C. After fast initial reswelling, the samples reached a plateau at a degree of swelling significantly smaller than the original degree of swelling (the equilibrium degree of swelling at  $20 \pm 2$  °C before heating). This reduction of the degree of swelling increased with higher temperatures before reswelling. The gradual decrease in swelling depicted in **Figures** 

7c and 7d when the temperature was raised could in principle be homogeneous (described by the increase of a single interaction parameter) or heterogeneous (as polymer segments of slightly different structure which lose solubility at different temperatures). Also in the second case, gels will remain transparent as long as the domains do not exceed a size that can cause scattering. In view of the extremely broad transition regime and the observation of the retarded precipitation of the higher molecular weight polymers (Figure 3a), explanation by heterogeneous loss of solubility is more likely. In this case, the degression of the degree of swelling after the first heating which is stronger at higher temperature or the extend of the collapse was chosen in the pre-treatment can be explained by the formation of crosslinking clusters of different aggregation strength, which do not redissolved within the time of the experiment. When we determined the degree of swelling of samples that were kept in water for more than one year, we found that the original degree of swelling could be recovered partly (Figure 9).

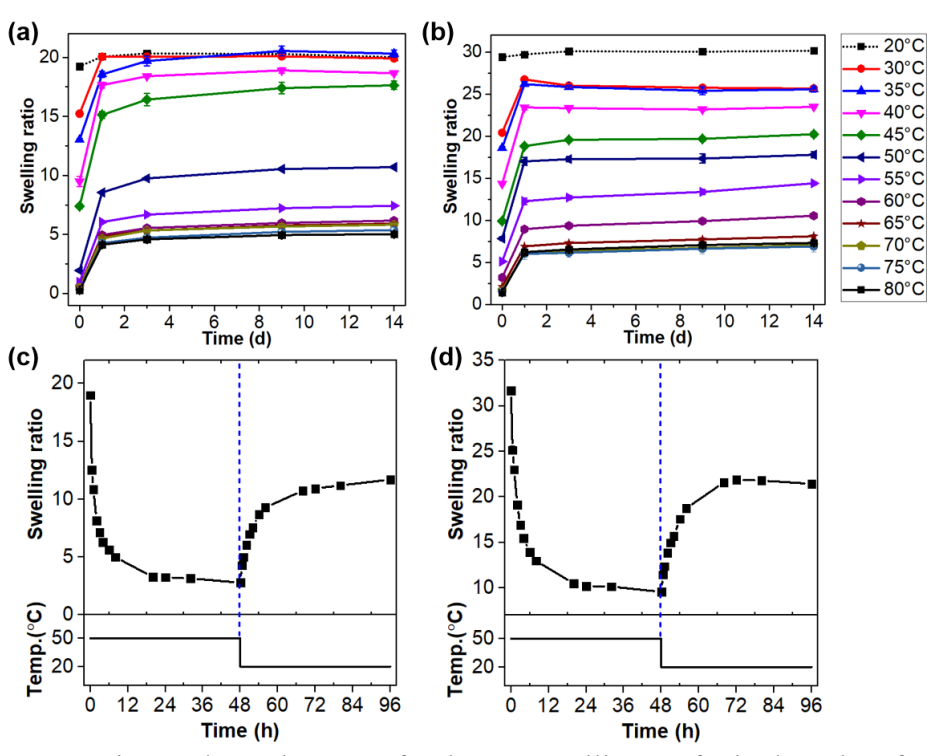


**Figure 8.** Time dependence of the reswelling of hydrogels from **(a)** PNVA-(allyl-4%)-( $C_3$ -91%)-176 and **(b)** PNVA-(allyl-4%)-( $C_4$ -35%)-176. Samples

were first swollen at  $20 \pm 2^{\circ}$ C then brought for 3 days to the temperature indicated by the legend and subsequently monitored for reswelling at  $20 \pm 2^{\circ}$ C after indicated time. Figures (c) PNVA-(allyl-4%)-(C<sub>3</sub>-91%)-176, and (d) PNVA-(allyl-4%)-(C<sub>4</sub>-35%)-176, demonstrate the collapse and reswelling of a sample swollen at equilibrium at 20°C then brought to 50°C for 48 h and subsequently cooled again to 20°C. Reswelling after the sample has been collapsed at a particular temperature turned out to be reversible (see **Figure S5** in supporting information).

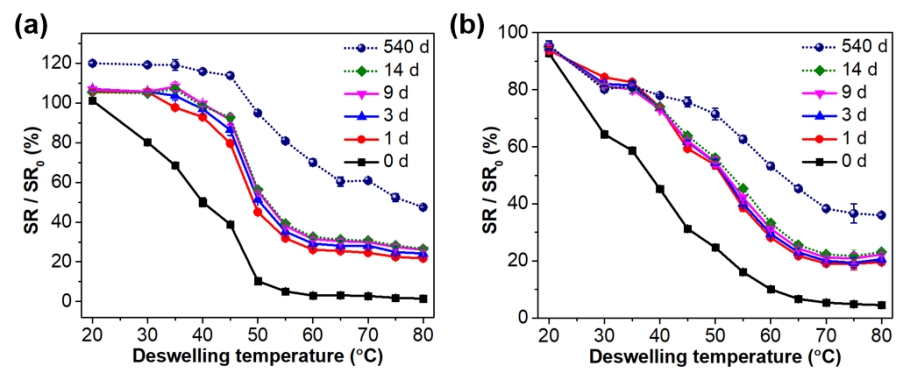


**Figure 9.** Reswelling coefficient (expressed by  $SR/SR_0$  (%)) of hydrogels from (a) PNVA-(allyl-4%)-(C<sub>3</sub>-91%)-176 and (b) PNVA-(allyl-4%)-(C<sub>4</sub>-35%)-176. Samples were first swollen at  $20 \pm 2^{\circ}$ C (initial degree of swelling =  $SR_0$ ), then kept for 3 days at the deswelling temperature, and subsequently brought back to 20°C to monitor the time-dependent reswelling after indicated time in the legend (final degree of swelling = SR).

Formation of additional crosslinks is in agreement with the concept, that short stereoregular segments may form ultra-small but rather strong hydrophobic clusters. Yet, we cannot exclude that additional crosslinking has been caused at least partially by remaining reactive reagents such as ethanedithiol in combination with DMPA and the allyl groups.

# 4.4 Conclusion

Poly(*N*-alkyl-*N*-vinylamide)s do not only present an alternative to other thermoresponsive polymers. These isomers of polyacrylamides are furthermore of significant interest because of the possibilities for chemical modification via the backbone-bound amine function offered by post hydrolysis. The poly(*N*-alkyl-*N*-vinylamide)s with allyl, *n*-propyl, and *n*-butyl substituents prepared in this work demonstrated how the LCST behavior of their aqueous solutions could be

manipulated and tailored by altering the molecular weight, hydrophobic substituent and degree of substitution. As a second point, we noticed that the poly(N-vinylamide)s might undergo secondary bonding with each other. Most importantly, the high molecular weight polymers do not precipitate readily from aqueous solution when the temperature is raised above the LCST. In addition, we found that gels do not reswell to the initial degree, once they have been collapsed by raising the temperature above the VPTT. As a tentative explanation, we consider formation of nanometre-sized clusters between short stereoregular segments within the atactic macromolecules. Such an explanation is analogous to the properties of polyvinylchloride, which can form elastomer composites with an appropriate plasticizer without covalent crosslinking.<sup>27</sup> Certainly this question whether such an associative bond formation or clustering needs to be supported by further evidence of a secondary bonding crosslinking should be subject of further experiments such as light scattering experiments in dilute solution, small angle X-Ray studies on the gels (SAXS) and eventually also neutron scattering. Yet, such studies were beyond the scope of this thesis. So far, we could only explore the field to raise these questions. A first rather simple study suggested here, might be dissolution and swelling studies of samples in water to which different salts are added following the Hofmeister Series.<sup>28</sup>, 29

# 4.5 References

- [1] Heskins, M.; Guillet, J. E. Solution Properties of Poly(*N*-isopropylacrylamide). *Journal of Macromolecular Science: Part A - Chemistry* **1968**, *2* (8), 1441-1455. DOI: 10.1080/10601326808051910.
- [2] Schmaljohann, D. Thermo- and pH-responsive polymers in drug delivery. *Advanced Drug Delivery Reviews* **2006**, *58* (15), 1655-1670. DOI: 10.1016/j.addr.2006.09.020.

- [3] Ward, M. A.; Georgiou, T. K. Thermoresponsive Polymers for Biomedical Applications. *Polymers* **2011**, *3* (3), 1215-1242. DOI: 10.3390/polym3031215.
- [4] Chandorkar, Y.; Castro Nava, A.; Schweizerhof, S.; Van Dongen, M.; Haraszti, T.; Köhler, J.; Zhang, H.; Windoffer, R.; Mourran, A.; Möller, M.; et al. Cellular responses to beating hydrogels to investigate mechanotransduction. *Nature Communications* **2019**, *10* (1), 4027. DOI: 10.1038/s41467-019-11475-4.
- [5] Roy, D.; Brooks, W. L. A.; Sumerlin, B. S. New directions in thermoresponsive polymers. *Chemical Society Reviews* **2013**, *42* (17), 7214-7243. DOI: 10.1039/C3CS35499G.
- [6] Halperin, A.; Kröger, M.; Winnik, F. M. Poly(*N*-isopropylacrylamide) Phase Diagrams: Fifty Years of Research. *Angewandte Chemie International Edition* **2015**, *54* (51), 15342-15367. DOI: 10.1002/anie.201506663.
- [7] Ajiro, H.; Watanabe, J.; Akashi, M. Cell Adhesion and Proliferation on Poly(*N*-vinylacetamide) Hydrogels and Double Network Approaches for Changing Cellular Affinities. *Biomacromolecules* **2008**, *9* (2), 426-430. DOI: 10.1021/bm701221c.
- [8] Marhefka, J. N.; Marascalco, P. J.; Chapman, T. M.; Russell, A. J.; Kameneva, M. V. Poly(*N*-vinylformamide)-A Drag-Reducing Polymer for Biomedical Applications. *Biomacromolecules* **2006**, *7* (5), 1597-1603. DOI: 10.1021/bm060014i.
- [9] Kirsh, Y. E. Water Soluble Poly-*N*-Vinylamides: Synthesis and Physicochemical Properties. 1998; John Wiley & Sons, Inc.: 1998.
- [10] Fischer, T.; Köhler, J.; Keul, H.; Singh, S.; Möller, M. Highly Swellable Hydrogels from Waterborne Poly(Vinylamine-co-Acetamide). *Macromolecular Chemistry and Physics* **2018**, *219* (24), 1800399. DOI: 10.1002/macp.201800399.
- [11] Gu, L.; Zhu, S.; Hrymak, A. N. Acidic and basic hydrolysis of poly(*N*-vinylformamide). *Journal of Applied Polymer Science* **2002**, *86* (13), 3412-3419. DOI: 10.1002/app.11364.
- [12] Kawatani, R.; Kan, K.; Kelland, M. A.; Akashi, M.; Ajiro, H. Remarkable Effect on Thermosensitive Behavior Regarding Alkylation at the Amide Position of Poly(*N*-vinylamide)s. *Chemistry Letters* **2016**, *45* (6), 589-591. DOI: 10.1246/cl.160145.
- [13] Zhang, C.; Demco, D. E.; Rimal, R.; Köhler, J.; Vinokur, R.; Singh, S.; Tenbusch, J.; Möller, M. Hydrophobic Interaction within Sparsely *N*-Alkylated Poly(*N*-vinylacetamide)s Enables Versatile Formation of Reversible Hydrogels. *Macromolecules* **2023**, *56* (23), 9616-9625. DOI: 10.1021/acs.macromol.3c01706.
- [14] Ajiro, H.; Takemoto, Y.; Akashi, M.; Chua, P. C.; Kelland, M. A. Study of the

- Kinetic Hydrate Inhibitor Performance of a Series of Poly(*N*-alkyl-*N*-vinylacetamide)s. *Energy & Fuels* **2010**, *24* (12), 6400-6410. DOI: 10.1021/ef101107r.
- [15] Kelland, M. A.; Abrahamsen, E.; Ajiro, H.; Akashi, M. Kinetic Hydrate Inhibition with *N*-Alkyl-*N*-vinylformamide Polymers: Comparison of Polymers to n-Propyl and Isopropyl Groups. *Energy & Fuels* **2015**, *29* (8), 4941-4946. DOI: 10.1021/acs.energyfuels.5b01251.
- [16] Zhang, Q.; Kawatani, R.; Ajiro, H.; Kelland, M. A. Optimizing the Kinetic Hydrate Inhibition Performance of *N*-Alkyl-*N*-vinylamide Copolymers. *Energy & Fuels* **2018**, *32* (4), 4925-4931. DOI: 10.1021/acs.energyfuels.8b00251.
- [17] Osváth, Z.; Iván, B. The Dependence of the Cloud Point, Clearing Point, and Hysteresis of Poly(*N*-isopropylacrylamide) on Experimental Conditions: The Need for Standardization of Thermoresponsive Transition Determinations. *Macromolecular Chemistry and Physics* **2017**, *218* (4), 1600470. DOI: 10.1002/macp.201600470.
- [18] Tong, Z.; Zeng, F.; Zheng, X.; Sato, T. Inverse Molecular Weight Dependence of Cloud Points for Aqueous Poly(*N*-isopropylacrylamide) Solutions. *Macromolecules* **1999**, *32* (13), 4488-4490. DOI: 10.1021/ma990062d.
- [19] Kawaguchi, T.; Kojima, Y.; Osa, M.; Yoshizaki, T. Cloud Points in Aqueous Poly(*N*-isopropylacrylamide) Solutions. *Polymer Journal* **2008**, *40* (5), 455-459. DOI: 10.1295/polymj.PJ2007227.
- [20] Flory, P.; Orwoll, R.; Vrij, A. Statistical thermodynamics of chain molecule liquids. I. An equation of state for normal paraffin hydrocarbons. *Journal of the American Chemical Society* **1964**, *86* (17), 3507-3514. DOI: 10.1021/ja01071a023.
- [21] Saeki, S.; Kuwahara, N.; Konno, S.; Kaneko, M. Upper and Lower Critical Solution Temperatures in Polystyrene Solutions. *Macromolecules* **1973**, *6* (2), 246-250. DOI: 10.1021/ma60032a020.
- [22] Flory, P. J. Thermodynamics of High Polymer Solutions. *The Journal of Chemical Physics* **1942**, *10* (1), 51-61. DOI: 10.1063/1.1723621.
- [23] Huggins, M. L. Theory of Solutions of High Polymers<sup>1</sup>. *Journal of the American Chemical Society* **1942**, *64* (7), 1712-1719. DOI: 10.1021/ja01259a068.
- [24] Saeki, S.; Kuwahara, N.; Nakata, M.; Kaneko, M. Upper and lower critical solution temperatures in poly (ethylene glycol) solutions. *Polymer* **1976**, *17* (8), 685-689. DOI: 10.1016/0032-3861(76)90208-1.
- [25] Schild, H. G.; Tirrell, D. A. Microcalorimetric detection of lower critical solution

- temperatures in aqueous polymer solutions. *The Journal of Physical Chemistry* **1990**, 94 (10), 4352-4356. DOI: 10.1021/j100373a088.
- [26] Qiu, X.; Koga, T.; Tanaka, F.; Winnik, F. M. New insights into the effects of molecular weight and end group on the temperature-induced phase transition of poly(*N*-isopropylacrylamide) in water. *Science China Chemistry* **2013**, *56* (1), 56-64. DOI: 10.1007/s11426-012-4781-9.
- [27] Nakajima, N.; Harrell, E. R. Rheology of PVC Plastisol: Particle Size Distribution and Viscoelastic Properties. *Journal of Colloid and Interface Science* **2001**, *238* (1), 105-115. DOI: 10.1006/jcis.2001.7468.
- [28] Thormann, E. On understanding of the Hofmeister effect: how addition of salt alters the stability of temperature responsive polymers in aqueous solutions. *RSC Advances* **2012**, *2* (22), 8297-8305, 10.1039/C2RA20164J. DOI: 10.1039/C2RA20164J.
- [29] Zhang, Y.; Cremer, P. S. Interactions between macromolecules and ions: the Hofmeister series. *Current Opinion in Chemical Biology* **2006**, *10* (6), 658-663. DOI: 10.1016/j.cbpa.2006.09.020.

# **4.6 Supporting information**

**Table S1.** Synthetic parameters and molecular weights of poly(*N*-vinylamide)s

Entry	Monomer	Solvent	concentration of monomer	Initiator	[monomer]/[I]	Reaction	Yield	$DP^{(a)}$	M <sub>n</sub> /kDa	M <sub>w</sub> /kDa	M <sub>n</sub> /kDa	M <sub>w</sub> /kDa
			(mg/mL)		molar ratio	temperature	(%)		in H <sub>2</sub> O	in H <sub>2</sub> O	in DMF	in DMF
PNVA-70	NVA	isopropanol	50	AIBN	20	70	81	70	5.5	11.3	6.3	13.2
PNVA-176	NVA	ethanol	100	AIBN	33.3	60	95	176	14.5	37.4	16.6	36.9
PNVA-1057	NVA	water	100	VA-044	400	60	83	1057	90.4	333.2	98.9	379.4
PNVF-165	NVF	water	50	VA-044	4.5	60	49	165	11.7	21.9	insoluble	insoluble
PNVF-183	NVF	water	100	VA-044	9	60	56	183	12.8	27.5	insoluble	insoluble
PNVF-605	NVF	water	143	VA-044	160	60	86	605	43.1	124.3	insoluble	insoluble

<sup>(</sup>a) DP is calculated from  $M_n$  in water

**Table S2.** Synthetic parameters for alkylated poly(*N*-vinylacetamide)s

_	Molar ratio		Molar ratio	Reaction	Reaction	
Entry	[NaH]/[NVA]	Alkyl bromide	[Alkyl bromide]/[NVA]	temperature (°C)	time (hour)	
PNVA-C <sub>3</sub> -100%-70	10	1-bromopropane	12	25	72	
PNVA-C <sub>3</sub> -40%-176	2.4	1-bromopropane	2	25	72	
PNVA-C <sub>3</sub> -79%-176	5	1-bromopropane	6	25	72	
PNVA-C <sub>3</sub> -87%-176	7.5	1-bromopropane	9	25	72	
PNVA-C <sub>3</sub> -100%-176	10	1-bromopropane	12	25	72	
PNVA-C <sub>3</sub> -100%-1057	10	1-bromopropane	12	25	72	
PNVA-(iso-C <sub>3</sub> )-0%-176	10	2-bromopropane	12	25	72	
PNVA-C <sub>4</sub> -37%-70	1.8	1-bromobutane	1.5	25	72	
PNVA-C <sub>4</sub> -25%-176	1.2	1-bromobutane	1	25	72	
PNVA-C <sub>4</sub> -30%-176	1.5	1-bromobutane	1.25	25	72	
PNVA-C <sub>4</sub> -45%-176	1.8	1-bromobutane	1.5	25	72	
PNVA-C <sub>4</sub> -47%-176	2.1	1-bromobutane	1.75	25	72	
PNVA-C <sub>4</sub> -53%-176	2.4	1-bromobutane	2	25	72	
PNVA-C <sub>4</sub> -71%-176	3.6	1-bromobutane	3	25	72	
PNVA-C <sub>4</sub> -97%-176	6	1-bromobutane	5	25	72	
PNVA-(iso-C <sub>4</sub> )-7%-176	12	1-brom-2-methylpropane	10	25	72	
PNVA-allyl-97%-70	2.4	allyl bromide	2	0	19	
PNVA-allyl-4%-176	0.06	allyl bromide	0.05	0	19	
PNVA-allyl-70%-176	1.2	allyl bromide	1	25	72	
PNVA-allyl-87%-176	1.8	allyl bromide	1.5	25	72	
PNVA-allyl-97%-176	2.4	allyl bromide	2	25	72	

**Table S3.** Synthetic parameters for alkylated poly(*N*-vinylformamide)s

Entry	Volume of DMSO for PNVF solution (mL/g PNVF)	Volume of DMF for NaH suspension (mL/g PNVF)	Molar ratio [NaH]/[NVF]	Alkyl bromide	Molar ratio [Alkyl bromide]/[NVF]	Reaction temperature (°C)	Reaction time (hour)
PNVF-C <sub>3</sub> -93%-183	18	72	5	1-bromopropane	6	25	24
PNVF-C <sub>3</sub> -80%-605	18	72	2.1	1-bromopropane	1.75	25	24
PNVF-C <sub>3</sub> -100%-605	18	72	5	1-bromopropane	6	25	24
PNVF-(iso-C <sub>3</sub> )-12%-605	18	72	5	2-bromopropane	6	25	24
PNVF-C <sub>4</sub> -32%-183	72	36 (DMSO)	0.7	1-bromobutane	0.583	25	24
PNVF-C <sub>4</sub> -87%-183	18	72	2.1	1-bromobutane	1.75	25	24
PNVF-C <sub>4</sub> -100%-183	18	72	6	1-bromobutane	5	25	24
PNVF-C <sub>4</sub> -60%-605	18	72	2.1	1-bromobutane	1.75	25	24
PNVF-C <sub>4</sub> -90%-605	18	72	6	1-bromobutane	5	25	24
PNVF-(iso-C <sub>4</sub> )-15%-605	18	72	2.4	1-bromo-2- methylpropane	2	25	24
PNVF-allyl-59%-183	18	72	2.4	allyl bromide	2	0	24

**Table S4.** Synthetic parameters for poly(*N*-allyl-*N*-vinylacetamide-*stat-N*-alkyl-*N*-vinylacetamide)s

Entry	V_A <sup>(a)</sup>	V_B <sup>(b)</sup>	Molar ratio [NaH]/[NVA]	Alkyl bromide	Molar ratio [Alkyl bromide]/[NVA]	Reaction temperature (°C)	Reaction time (hour)
PNVA-(allyl-4%)-(C <sub>3</sub> -91%)-176	59	29.5	10	1-bromopropane	12	25	72
PNVA-(allyl-4%)-(C <sub>4</sub> -35%)-176	59	29.5	1.8	1-bromobutane	1.5	25	72

<sup>(</sup>a) V\_A: Volume of DMF for PNVA-allyl-4% solution (mL/g PNVA-allyl-4%-176); (b) V\_B: Volume of DMF for NaH suspension (mL/g PNVA-allyl-4%-176).

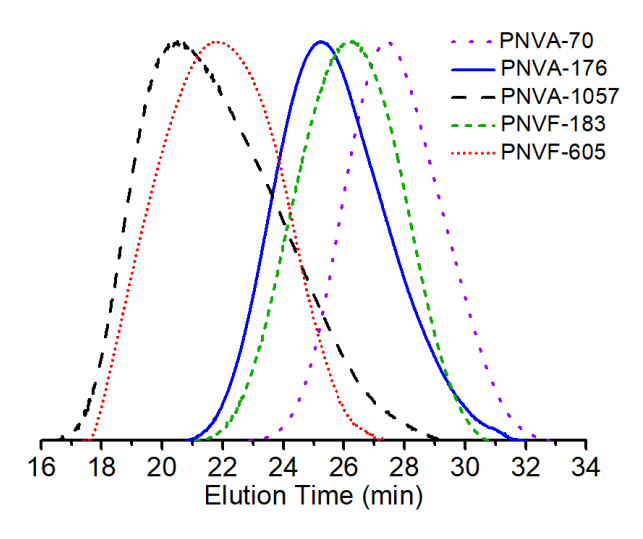


**Figure S1.** SEC traces of PNVAs and PNVFs measured in water. The suffix number represents the degree of polymerisation (DP) of the respective homopolymers.

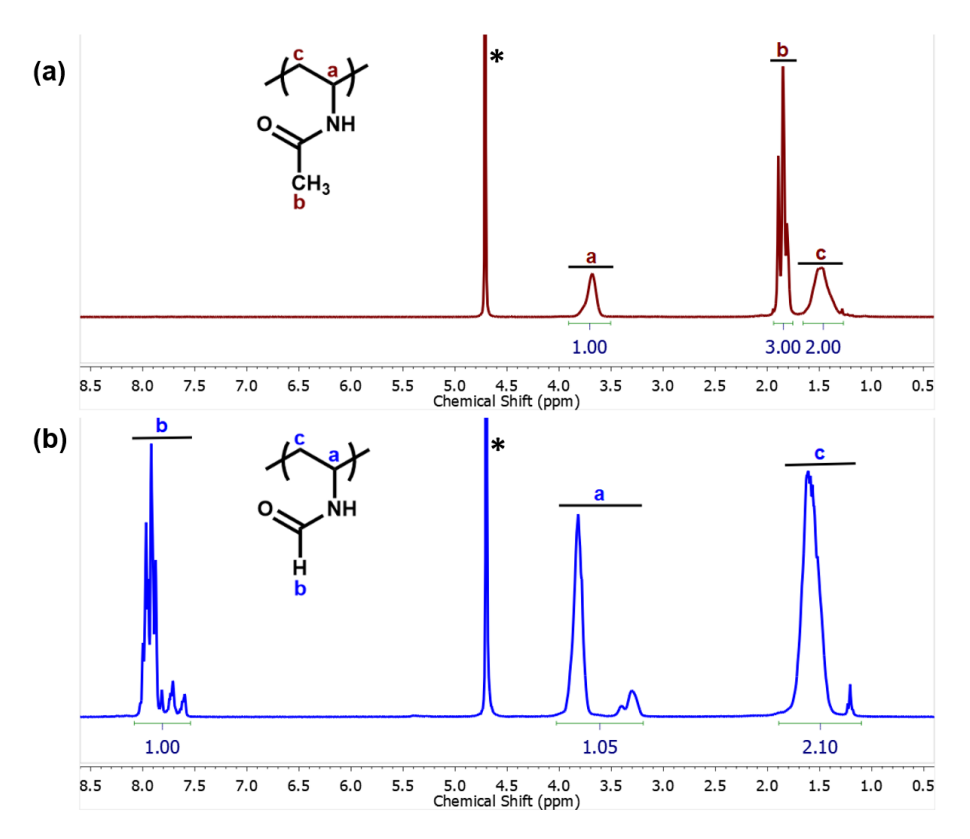


**Figure S2.** (a) <sup>1</sup>H-NMR spectrum of PNVA-176 measured in D<sub>2</sub>O:  $\delta = 3.91 - 3.50$  (<sup>1</sup>H, H<sub>a</sub>), 1.94 - 1.75 (3H, H<sub>b</sub>), 1.66 - 1.27 (2H, H<sub>c</sub>) ppm. (b) <sup>1</sup>H NMR spectrum of PNVF-183 measured in D<sub>2</sub>O:  $\delta = 8.10 - 7.53$  (1H, H<sub>b</sub>), 4.00 - 3.20 (1H, H<sub>a</sub>), 1.80 - 1.10 (2H, H<sub>c</sub>) ppm, and \* denotes residual water.

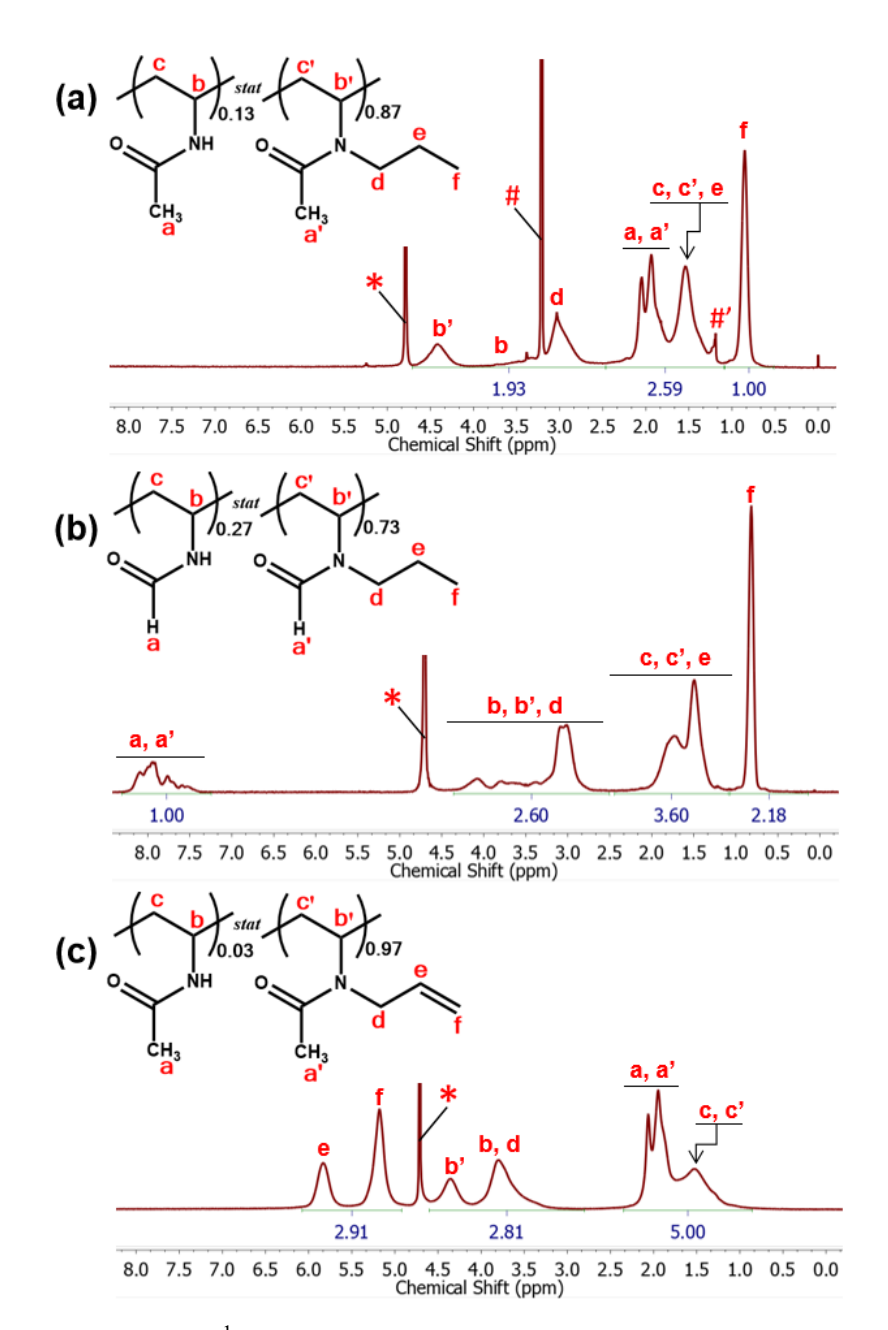


**Figure S3.** Examples of <sup>1</sup>H-NMR peak assignment for poly(N-alkyl-N-vinylamide)s: (a) PNVA-C<sub>3</sub>-87%-176 in CD<sub>3</sub>OD. DS = 5/(3K-2n+4); K is the ratio of peak at 1.2 - 2.2 ppm to peak at 0.8 ppm, n = 3 for n-propyl and n = 4 for n-butyl; (b) PNVF-C<sub>3</sub>-73%-605 in D<sub>2</sub>O. DS is calculated by peak f; (c) PNVA-allyl-97%-176 in D<sub>2</sub>O. DS is calculated by value of peaks e and f. The symbol \* denotes signal of residual water, # denotes solvent residual of CD<sub>3</sub>OD, and #' denotes impurity signal from CD<sub>3</sub>OD.

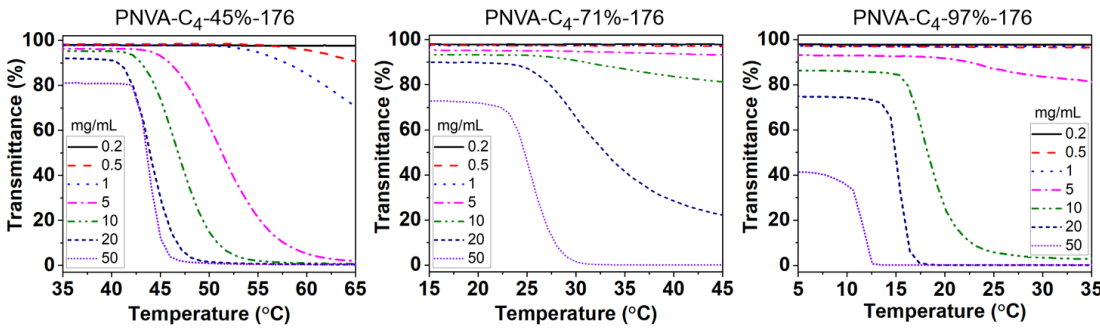


**Figure S4.** Transmittance-temperature curves of the aqueous solutions of PNVA- $C_4$ -DS-176 samples with DS of 45%, 71%, and 97%.

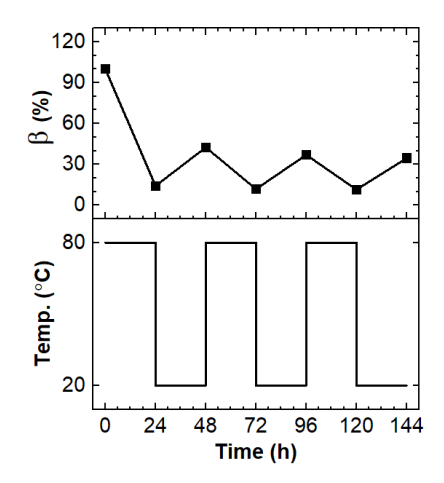


**Figure S5**. Reswelling coefficient ( $\beta$ ) of PNVA-(allyl-4%)-(C<sub>4</sub>-35%)-176 hydrogel at equilibrium at 20 ± 2°C in water treated by heating/cooling (80°C/20°C) cycles. Reswelling coefficient was calculated by the swelling ratio at the indicated time divided by the initial swelling ratio (time = 0).

# 5 Thermoresponsive double network hydrogels from *N*-alkylated poly(*N*-vinylacetamide)s

# 5.1 Introduction

Mechanically strong hydrogels have remained a privilege of natural tissue until recently. Only when researchers discovered the strong improvement in toughness of double network hydrogels, synthetic hydrogels could be prepared to approach the outstanding mechanical properties of natural water hydrous tissue. 1-3 Still the strength of the hydrogels in jelly fish or cartilage cannot be achieved.<sup>4, 5</sup> Structural drawbacks of synthetic hydrogels are their often rather high degree of swelling, i.e., firstly the high fraction of water molecules which they can take up, and secondly the lack of a mechanism which distributes strain through a large volume. Consequently, the stress upon deformation is carried by a very small fraction of the network chains at the same time, which then cannot resist the stress. Well-defined crack tips at the fracture front are formed, and irrespective of their softness the hydrogels appear brittle at larger strain.6 In contrast, hydrous tissues in plants as well as in animals, which mostly contain only about 70% of water, dissipate stress over large volumes and can be extremely tough. Most remarkable, however, is their ability to combine a low modulus at low strain with a high modulus at large strain as it is depicted schematically in Figure 1.

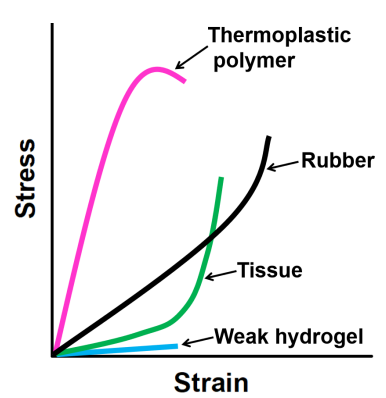


**Figure 1.** Representative stress-strain curves for conventional single network hydrogel, rubber and human tissue.<sup>6</sup>

Such at the first glance contradicting properties cannot be achieved by simply increasing the crosslinking density because this would yield a higher modulus already at small strain. Characteristic for natural hydrous tissue is their complex and often heterogeneous multicomponent composition. Different components like the stiff rod collagen fibrils and the flexible proteoglycans in cartilage are combined within anisotropic micro-structures.<sup>7,8</sup>

In view of this complexity, double networks appear just a first step to synthesize hydrogels with improved mechanical properties, irrespective of the fact that maximum stress values of 10 MPa and elongation values at break of 2000% have been reported. Typically such double networks are prepared by swelling a more densely crosslinked first network with the monomers of the second network. As a consequence, the first network is pre-strained within the matrix of the second network. Upon mechanical stretching or compression, the first network can dissipate energy, ultimately by breaking up into smaller patches. While such micro-networks within the macro-network may act like fillers (Filling a network with micro- or nano- particles is well known to enforce the mechanical strength significantly depending on the interaction between the colloidal particles and the network strands to the break-up mechanism can dissipate energy only once. When such a double network is exposed

to large strain, it is initially very strong, but it loses at least part of its strength upon repeated deformation.

Improvement of such double network hydrogels might be achieved when the first network is crosslinked by reversible bonds, which can recover after release of the stress while the strain was too little to break the second network. In Chapter 3 of this thesis, a series of reversibly crosslinked alkylated polyvinylamides have been described whereby their strength and uptake of water could be tailored over a wide range without losing hydrophilicity. When these networks are swollen with a crosslinking monomer mixture, double networks with a reversibly but tightly crosslinked first network could be prepared. However, the strength of the double network hydrogel is still expected to result as the sum of that from the constituent networks. In this chapter, we attempted to investigate whether we can observe a truly synergistic effect, where the strained double network is reinforced by the strain. Such reinforcement by strain is well known for natural rubber, which undergoes straininduced crystallization whereby the crystalline microdomains serve as additional crosslinks and filler at the same time. 11 For this purpose, we prepared double networks from the thermoresponsive alkylated polyvinylamides reported in Chapter 4 and the reversibly crosslinked hydrogels of Chapter 3. The questions to be answered are: (i) Can the combination of the well swollen thermoresponsive network below the LCST and the reversibly crosslinked network from Chapter 3 yield double networks with superior mechanical properties? (ii) Would the thermoresponsive component above the LCST form a filler within the reversibly crosslinked network which enhances the mechanical properties of the latter significantly? (iii) How does such a double network behave at the volume phase transition of the thermoreversible network component? In the last case, we hypothesize that the orientation by strain of the

thermoreversible network strands will cause a decrease of the LCST and might cause some strain induced increase of the modulus.

# 5.2 Experimental section

#### 5.2.1 Materials

N-vinylacetamide (NVA), sodium hydride (NaH) dispersed in paraffin liquid (60%), and 2,2'-azobis[2-(2-imidazolin-2-yl)propane]dihydrochloride (VA-044) were obtained from Tokyo Chemical Industry Co., Ltd. Anhydrous dimethylformamide (DMF), 1,2-ethanedithiol, and all alkyl bromides were received from Sigma-Aldrich. Anhydrous tetrahydrofuran (THF) was a product of Acros Organics. Ethanol was purchased from Fischer Chemical. Technical acetone was purchased from Höfer Chemie. 2,2-Dimethoxy-2-phenylacetophenone (DMPA) and technical n-hexane were purchased from VWR. Deuterated methanol and water were purchased from Deutero. 2,2'-azobis(2-methylpropionitrile) (AIBN, 98%, Sigma-Aldrich (Merck, Darmstadt, Germany)) was purified by recrystallization from methanol. All other reagents were used as received. Deionized water was used for all experiments. 1000 Da MWCO dialysis membrane was a product of Spectrum Laboratories, Inc.

#### **5.2.2 Sample denotation**

The following denotation was used for polymers: PNVA- $C_n$ -y-x represents poly(N-alkyl-N-vinylacetamide) with DP = x, n-alkyl side chains consisting of n methylene units,  $-(CH_2)_n$ -H, at a degree of substitution DS = y; PNVA-(allyl- $y_I$ )-( $C_n$ - $y_2$ )-x represents poly(N-allyl-N-vinylacetamide-stat-N-alkyl-N-vinylacetamide)s with DP = x and two types of side chains: allyl at DS of  $y_I$ , and  $C_n$  at DS of  $y_2$ .

# **5.2.3** Polymer synthesis

(a) Synthesis of PNVAs and PNVA- $C_n$  polymers

Same synthesis procedures of PNVAs and PNVA- $C_n$  polymers as described in Chapter 3 were adopted in this chapter. For the synthesis of PNVAs, NVA monomers were polymerized by free radical polymerization under oxygen free conditions. Ethanol was used as solvent with AIBN as the initiator for the synthesis of relatively low molecular weight PNVAs ( $M_n < 50$  kDa); while deionized water and VA-044 were used for the synthesis of relatively high molecular weight PNVAs ( $M_n > 50$  kDa).

As with the synthesis of PNVA- $C_n$  (n = 14 or 18) polymers, firstly, PNVA was dissolved in anhydrous DMF, while NaH was washed and suspended also in anhydrous DMF with successively cooling by an ice bath; Secondly, the PNVA@DMF solution was injected into NaH suspension; Lastly, the respective alkyl bromide was added and the reaction was carried out at room temperature (25°C) under  $N_2$  gas atmosphere.

PNVAs and PNVA-C<sub>n</sub> polymers were obtained via precipitation and successively dialysis against deionized water.

(b) Synthesis procedures of PNVA-allyl and PNVA-allyl- $C_n$  (n = 3 or 4) polymers Same synthesis procedures as documented in **Chapter 4** were applied in this chapter. For the synthesis of PNVA-allyl (DS < 5%) polymers, same procedures as that of PNVA- $C_n$  mentioned above (in 2.3a) was adopted, allyl bromide was used instead of alkyl bromides.

For the synthesis of PNVA-allyl- $C_n$  (n = 3 or 4), firstly, PNVA-allyl was dissolved in anhydrous DMF, while NaH was washed and suspended also in anhydrous DMF with successively cooling by ice bath; Secondly, the PNVA-allyl@DMF solution was

injected into the NaH suspension; Lastly, the respective alkyl bromide was added and the reaction was carried out at room temperature (25°C) under N<sub>2</sub> gas atmosphere.

PNVA-allyl- $C_n$  (n = 3 or 4) polymers were collected by precipitation and subsequent dialysis against deionized water.

#### **5.2.4** Characterization of polymers

As described in Chapter 3 and Chapter 4, the molecular structure of the polymers were determined using deuterated methanol as solvent measured by 400 MHz <sup>1</sup>H NMR; Molecular weight and polydispersity of the PNVAs were characterized by size exclusion chromatography (SEC) using water as solvent. Water (HiPerSolv CHROMANORM® HPLC grade, VWR) containing 0.1 mol/L sodium nitrate (NaNO<sub>3</sub>, p.a. level, Merck KGaA) and 0.01 wt% sodium azide (NaN<sub>3</sub>, extra pure, Merck KGaA) was used as eluent. The set-up consisted of a pre-column (8 × 50 mm) and three Novema Max gel columns (8 × 300 mm, 30, 100, and 1000 Å, Polymer Standards Service) with an Agilent 1200 HPLC pump, a refractive index detector (1200, Agilent), and an UV-detector (VWD, 1200, Agilent). The diameter of the gel particles measured 5 µm. Elution was done at a flow rate of 1.0 mL/min at 40 °C. Ethylene glycol (0.5 μL/mL, 99.5%, Fluka analytical) was added as internal standard. Calibration was performed using narrowly distributed poly(ethylene oxide) standards (Polymer Standards Service). All results were evaluated using the PSS WinGPC UniChrom software (Version 8.3.2). All results were evaluated using the PSS WinGPC UniChrom software (Version 8.3.2).

#### 5.2.5 Hydrogel preparation

(a) Preparation of single network physical gels from PNVA- $C_n$  (n=14 or 18) polymers

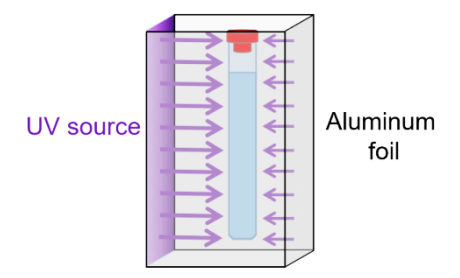
Physical gels of PNVA- $C_n$  (n = 14 or 18) were prepared by solution cast method. <sup>12</sup>

Firstly, the sample polymer was dissolved in ethanol in a flat-bottomed mould; then polymer film was obtained after solvent evaporation at room temperature; lastly, hydrogel was formed by swelling the polymer film in large amount of deionized water until equilibrium swelling. According to results reported in **Chapter 3**, it was assumed that the extraction of PNVA- $C_n$  (n = 14 or 18) polymers during swelling was negligible.

# (b) Preparation of single network hydrogels

- (1) PNVA-allyl or PNVA-allyl- $C_n$  (n = 3 or 4) was dissolved in ethanol, magnetic stirring and vortexing were used to obtain the homogenized solution;
- (2) Pre-determined amount of dithiol and DMPA were added to polymer solution, after the container was covered with aluminum foil, the mixture was homogenized by magnetically stirring and vortexing;
- (3) The mixture was transferred into a 5 mm diameter NMR tube by a syringe, and the tube was sealed by NMR tube cap.
- (4) The solution-loaded NMR tube was vertically placed and fixed onto the UV lamp with a gap of around 2 mm (as shown in **Scheme 2**), and the tube was covered with aluminum foil and rested for 30 minutes to get rid of fine bubbles inside of solution mixture;
- (5) UV irradiation (365 nm wavelength (UVP, UVL-56, 6 W)) was applied for 15 hours (the complete curing of most samples were observed within 2 hours UV irradiation, the extended radiation time was used to ensure maximum crosslinking of all samples especially those were a little whitish);
- (6) The NMR tube (after its cap was removed ) was transferred to a drying oven and dried at 65°C for over 3 days until constant mass was reached;

(7) The dried cylindrical gel body was immersed into large amount of water, and water was changed every 12 hours for over 3 days until equilibrium swelling ratio was reached.



**Scheme 2**. Schematic illustration of experimental setup for hydrogel preparation by UV crosslinking.

- (c) Preparation of double network hydrogels
  - (1) Polymers for both networks (network A: PNVA- $C_n$  (n = 14 or 18); network B: PNVA-allyl- $C_n$  (n = 3 or 4) or PNVA-allyl) were weighed separately and dissolved together in ethanol to form a mixed solution; magnetic stirring and vortexing were used to obtain the homogenized solution;
  - (2) Same procedure as steps (2) to (7) described in **5.2.5** (b) were adopted to obtain the double network hydrogel.

# 5.2.6 Characterization of hydrogels

(a) Polymer content in extraction

Mass of the polymer in the extraction liquid generated by **5.2.5 b** (7) was determined by lyophilization. It is proved that the extracted amount is negligible.

- (b) Swelling ratio measurement
  - (1) Swelling ratio (SR) of hydrogels at  $20 \pm 2$  °C and was calculated by **Equation**

$$SR = \frac{M_{gel} - M_{dry}}{M_{dry}} \tag{1}$$

where  $M_{gel}$  represents mass of swollen gel in water,  $M_{dry}$  represents mass of dry gel obtained by lyophilization of swollen gel.

#### (c) Temperature-dependent swelling behavior study

Hydrogel samples which were swollen to their equilibrium swelling at 20°C were heated at 50°C and afterwards cooled at 20°C. At predetermined time points, sample was removed from the water, surface attached water was blotted by precision wipe and the mass of the swollen hydrogels was determined by weighing, swelling ratio was calculated by the same method as **5.2.6 b(1)**.

#### (d) Dynamic mechanical analysis (DMA)

Before measurement, the sample hydrogels were submerged in water at a target temperature  $(T_l)$  for over 24 hours until equilibrium swelling ratio were reached. Shortly before the DMA measurement, after the surface water blotted by precision wipe, diameter of the hydrogel was measured immediately by a calliper and the degree of swelling was calculated as below:

Assuming that the density of polymers is approximately 1 g/cm<sup>3</sup> (equal to density of water), the swelling ratio for hydrogel samples at higher temperatures (> 20°C) used for DMA measurements was estimated by **Equation 2**.

$$SR(T) = \left(\frac{d(T)}{d(T_0)}\right)^3 \times (SR(T_0) + 1) - 1$$
 (2)

Where  $SR(T_0)$  and SR(T) represent the estimated swelling ratio at 20°C and T °C, respectively;  $d(T_0)$  and d(T) represent the diameter of cylindrical hydrogels at 20°C and T °C, respectively.

The mechanical properties of all hydrogels were investigated by TA Instruments Model Q800 DMA (V21.3 Build 96, TA Instruments, New Castle, DE) equipped with

submersion compression clamp. Before each measurement, the drive shaft position, clamp mass, clamp offset and clamp compliance were calibrated according to the standard protocol. Each sample was carefully transferred to the sample chamber and put in the centre of the platform, deionized water (temperature =  $T_1$ ) was added to make the sample fully submerged in water during testing to prevent dehydration, the furnace was kept closed during measurement to maintain constant temperature and avoid disturbance. After temperature  $T_1$  reached, the sample was kept at this temperature for another 10 minutes before measurement. Then, a pre-load force of 0.1 N was applied and thickness of the sample was measured using the initial displacement of clamp, afterwards, the static force was gradually ramped to 18 N at a rate of 0.5 N/min and the data were collected every 2 s while the sample was compressed. The data collected were analysed by Universal Analysis 2000 provided by TA instruments.

#### 5.3 Results and discussion

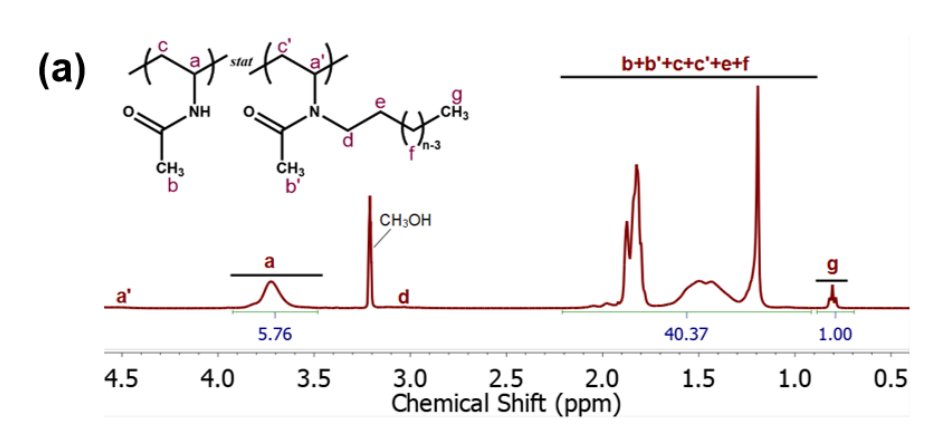
PNVA- $C_n$  and PNVA-allyl- $C_n$  were synthesized by *N*-substitution of PNVAs which were prepared by free radical polymerization. <sup>1</sup>H NMR was used to determine the degree of alkyl side chain substitution (*DS*) of the PNVA- $C_n$  polymers, signal assignments by the example of PNVA- $C_{18}$ -6%-176 are shown in **Figure 1a**. The *DS* was determined according to **Equation 3** as the ratio of alkylated NVA signals in the range from 0.8 ppm to 1.0 ppm to the total integrated peak area of NVA units in the range from 1.2 ppm to 2.2 ppm, denoted as *K*, whereby *n* is the number of carbon atoms in the  $C_n$  side chain.

$$DS = \frac{5}{3K - 2n + 4} \tag{3}$$

For polymers with allyl- and short alkyl substituents, integration from 1.2 ppm to 2.2 ppm to the integration from 0.8 ppm to 1.0 ppm is denoted as  $K_I$ , integration from 5.6 ppm to 6.1 ppm to the integration from 0.8 ppm to 1.0 ppm is denoted as  $K_2$ , n is the number of carbon atoms in the  $C_n$  side chain. **Figure 1b** depicts the  $^1$ H NMR spectrum of PNVA-(allyl-4%)-( $C_3$ -91%)-176 as an example. The  $DS_I$  and  $DS_2$  of PNVA-(allyl- $DS_I$ )-( $C_n$ - $DS_2$ ) were calculated by **Equations 4** and **5**:

$$DS_1 = \frac{15K_2}{3K_1 - 2n + 4} \tag{4}$$

$$DS_2 = \frac{5}{3K_1 - 2n + 4} \tag{5}$$



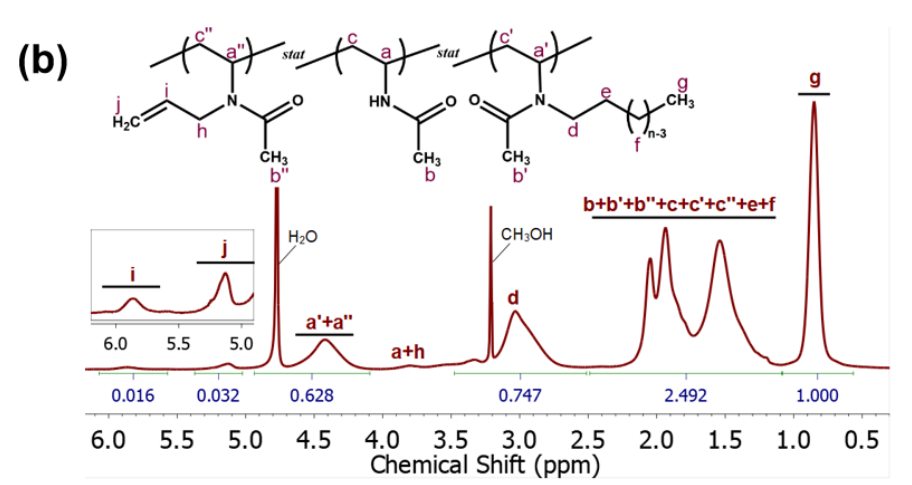


**Figure 1.**  $^{1}$ H NMR spectra of (a) PNVA- $C_{18}$ -6%-176 and (b) PNVA-(allyl-4%)-( $C_{3}$ -91%)-176 in deuterated methanol.

**Table 1** lists the characterization of the polymers which have been used further on.

**Table 1.** Polymers used for hydrogels preparation

Entry	Name	$M_n$ of PNVA backbone	DP	Substituent	DS	Approximate LCST <sup>a)</sup>
$A_1$	PNVA-C <sub>18</sub> -6%-176	15 kDa	176	n-octadecyl	6%	/
$A_2$	PNVA-C <sub>14</sub> -8%-1057	90 kDa	1057	n-tetradecyl	8%	/
$A_3$	PNVA-C <sub>18</sub> -6%-1057	90 kDa	1057	n-octadecyl	6%	/
$B_1$	PNVA-allyl-4%-176	15 kDa	176	allyl	4%	/
$B_2$	PNVA-(allyl-4%)-(C <sub>3</sub> -91%)-176	15 kDa	176	allyl; n-propyl	4%; 91%	60.0°C
$B_3$	PNVA-(allyl-4%)-(C <sub>4</sub> -35%)-176	15 kDa	176	allyl; n-butyl	4%; 35%	45.6°C
$B_4$	PNVA-(allyl-4%)-(C <sub>3</sub> -91%)-1057	90 kDa	1057	allyl; n-propyl	4%; 91%	64.0° C

a) Approximate LCST is the cloud point at inflection point of the transmittance-temperature curve of aqueous polymer solution at 100 mg/mL measured by UV-vis photometer at heating rate of 0.5°C/min.

Table 2. Composition, preparation parameter, swelling ratio (SR) and transparency of single network hydrogels (SN gel) and double network hydrogels (DN gel).

Sample	Polymer A	SR of A SN gel	Polymer B	SR of B SN gel	Concentration of B in ethanol (mg/mL) a)	Mass ratio A:B	SR of the DN gel	Transparency of the sample b)
SN_B <sub>1</sub> _208	/	/	$\mathbf{B}_1$	$20.0\pm0.8$	208	/	/	transparent (+++)
DN_A <sub>2</sub> _B <sub>1</sub> _(1:2.08)_208	$A_2$	$35\pm1.5$	$\mathbf{B}_1$	$20.0 \pm 0.8$	208	1:2.08	$17.2\pm0.5$	translucent (+)
SN_B <sub>2</sub> _300	/	/	$\mathrm{B}_2$	$36.3 \pm 0.2$	300	/	/	transparent (+++)
DN_A <sub>1</sub> _B <sub>2</sub> _(1:3)_300	$A_1$	$12.8 \pm 0.1$	$\mathrm{B}_2$	$36.3 \pm 0.2$	300	1:3	$57.9 \pm 0.6$	transparent (+++)
DN_A <sub>1</sub> _B <sub>2</sub> _(3:3)_300	$A_1$	$12.8 \pm 0.1$	$\mathrm{B}_2$	$36.3 \pm 0.2$	300	3:3	$22.1\pm1.4$	opaque (-)
DN_A <sub>1</sub> _B <sub>2</sub> _(5:3)_300	$A_1$	$12.8 \pm 0.1$	$\mathrm{B}_2$	$36.3 \pm 0.2$	300	5:3	Not gelled	/
DN_A <sub>2</sub> _B <sub>2</sub> _(1:3)_300	$A_2$	$35\pm1.5$	$\mathrm{B}_2$	$36.3 \pm 0.2$	300	1:3	$52.0\pm1.9$	a little whitish (++)
DN_A <sub>3</sub> _B <sub>2</sub> _(1:3)_300	$A_3$	$9.1 \pm 0.1$	$\mathrm{B}_2$	$36.3 \pm 0.2$	300	1:3	$41.8 \pm 0.4$	a little whitish (++)
SN_B <sub>3</sub> _300	/	/	$B_3$	$28.4 \pm 1.6$	300	/	/	transparent (+++)
DN_A <sub>2</sub> _B <sub>3</sub> _(1:3)_300	$A_2$	$35\pm1.5$	$B_3$	$28.4 \pm 1.6$	300	1:3	$29.8 \pm 0.4$	translucent (+)
DN_A <sub>2</sub> _B <sub>3</sub> _(3:3)_300	$A_2$	$35 \pm 1.5$	$B_3$	$28.4 \pm 1.6$	300	3:3	Not gelled	/
DN_A <sub>3</sub> _B <sub>3</sub> _(1:3)_300	$A_3$	$9.1 \pm 0.1$	$\mathrm{B}_3$	$28.4 \pm 1.6$	300	1:3	$17.6 \pm 0.02$	translucent (+)
DN_A <sub>3</sub> _B <sub>3</sub> _(3:3)_300	$A_3$	$9.1 \pm 0.1$	$\mathrm{B}_3$	$28.4 \pm 1.6$	300	3:3	Not gelled	/
SN_B <sub>4</sub> _150	/	/	$\mathrm{B}_4$	$82.8 \pm 6.3$	150	/	/	transparent (+++)
DN_A <sub>1</sub> _B <sub>4</sub> _(1:3)_150	$\mathbf{A}_1$	$12.8 \pm 0.1$	$\mathrm{B}_4$	$82.8 \pm 6.3$	150	1:3	$90.1\pm2.6$	transparent (+++)
DN_A <sub>1</sub> _B <sub>4</sub> _(2:3)_150	$A_1$	$12.8 \pm 0.1$	$\mathrm{B}_4$	$82.8 \pm 6.3$	150	2:3	$81.0 \pm 3.4$	transparent (+++)
DN_A <sub>2</sub> _B <sub>4</sub> _(1:3)_150	$A_2$	$35\pm1.5$	$\mathrm{B}_4$	$82.8 \pm 6.3$	150	1:3	$92.3 \pm 2.77$	transparent (+++)
DN_A <sub>3</sub> _B <sub>4</sub> _(1:3)_150	$A_3$	$9.1 \pm 0.1$	$\mathrm{B}_4$	$82.8 \pm 6.3$	150	1:3	$67.7 \pm 1.3$	transparent (+++)

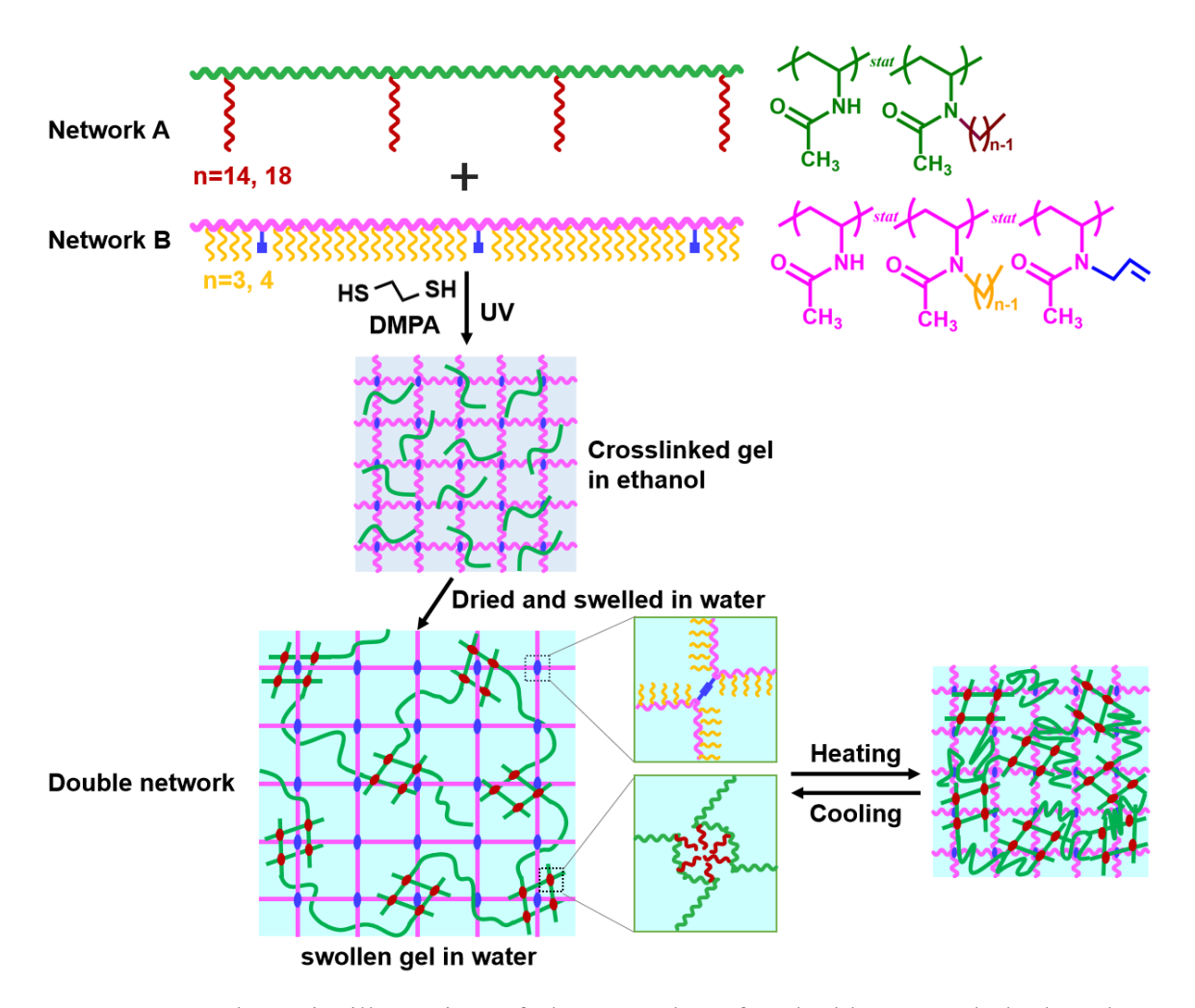
a) For all samples, concentration of the molar ratio of n(thiol): n(allyl) is 1:1, n(DMPA): n(allyl) is 1:5.
 b) All SN gels of A or B are completely transparent at 20°C after extracted and equilibrated in water; more plus sign '+' represent more transparent.

Double network hydrogels were prepared according to the procedure shown in **Scheme 3**. Herein, PNVA- $C_n$  (n = 14 or 18) polymers, which could further form physical gel networks by hydrophobic association of long alkyl side chains, were used to form network A; while thermoresponsive PNVA-allyl- $C_n$  (n = 3 or 4) polymers were employed for the network B.

Firstly, an alcoholic solution containing PNVA- $C_n$  polymer (entries  $A_1$ ,  $A_2$  and  $A_3$  in **Table 1**) and PNVA-allyl- $C_n$  (entries  $B_2$ ,  $B_3$ ,  $B_4$  in **Table 1**) were prepared and subsequently mixed with crosslinking reagents and transferred to a 5 mm NMR tube for UV crosslinking. After further drying, the solid DN gels were removed from the NMR tube and swollen in water.

This procedure is discriminated from the mostly used preparations of DN, where a first network is prepared and swollen by monomer and crosslinker, which is subsequently polymerized to form the second network. In our case two different polymers are dissolved and the second polymer is covalently crosslinked in the presence of a reversibly crosslinking polymer. The maximum concentration of the polymers is limited by their solubility.

From a large number of preparations, we chose only those which swelled in a homogeneous, affine way, i.e., kept their cylindrical shape rather perfectly. Whether gels were transparent or opaque is marked in **Table 2**, which lists the gels taken for further consideration. The molar ratio of initiator and crosslinker (with respect to the total molar of allyl groups in the solution for crosslinking) was kept the same.

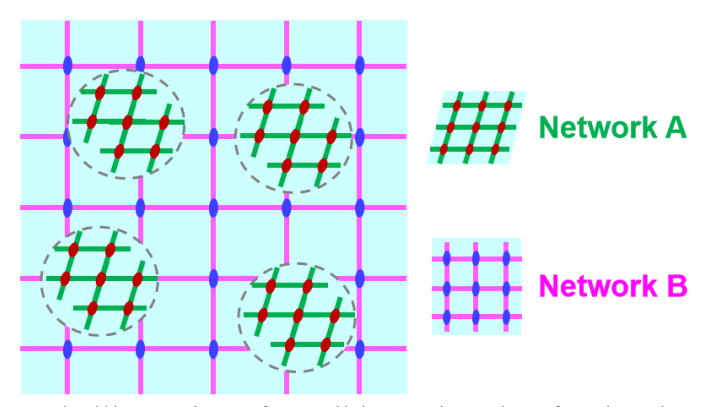


**Scheme 3.** Schematic illustration of the procedure for double network hydrogel preparation procedure and crosslink mechanism of each network.

According to **Chapter 3** and **Chapter 4**, it was confirmed that all PNVA- $C_n$  (n = 14 or 18) hydrogels, as well as all the UV-crosslinked PNVA-allyl- $C_n$  (n = 3 or 4) hydrogels could reach equilibrium swelling after 24 hours at room temperature and relatively high temperatures (e.g.,  $50^{\circ}$ C or above), thus it was expected that the double network hydrogels made from the combination of these two types of polymers could also reach equilibrium swelling state upon heating/cooling in short time.

It is noteworthy that the swelling ratio of the DN\_A<sub>n</sub>\_B<sub>2</sub>\_(1:3)\_300 (n = 1, 2, 3) double network hydrogels are all larger than both the swelling ratio of the constituent network-A (physical gel formed by  $A_n$ ) and the single network SN\_B<sub>2</sub>\_300. Furthermore, these DN gels are also a little whitish, while both  $A_n$ 

physical gels and SN\_B<sub>2</sub>\_300 are transparent at 20°C. These observations indicated that the DN gels are not ideally homogeneous, there exist larger domains formed by aggregation of either network A or B, and the size of some of these domains could be larger than 100 μm, the limit of scattering observed by a naked eye (see **Scheme 4**).



**Scheme 4.** Schematic illustration of possible explanation for the cloudiness of double network hydrogels.

Thermoresponsive deswelling/reswelling behavior of representative double network hydrogels were as shown in **Figure 2**. It is shown that both the deswelling and the first step in reswelling mostly finished in 24 hours, but a slow second step in reswelling can last years. We explain this tentatively by the formation of physical crosslinks formed by aggregation of short homotactic sequences in the polyvinylamide chains (as discussed in **Chapter 4**). In **Chapter 4**, it has been demonstrated that the swelling behavior of single network B<sub>2</sub> and B<sub>3</sub> gels are very similar, therefore, here we only use B<sub>2</sub> as a representative network B to investigate the similarity and differences in deswelling/reswelling behavior of the DN gels using A<sub>1</sub>, A<sub>2</sub> or A<sub>3</sub> for network A.

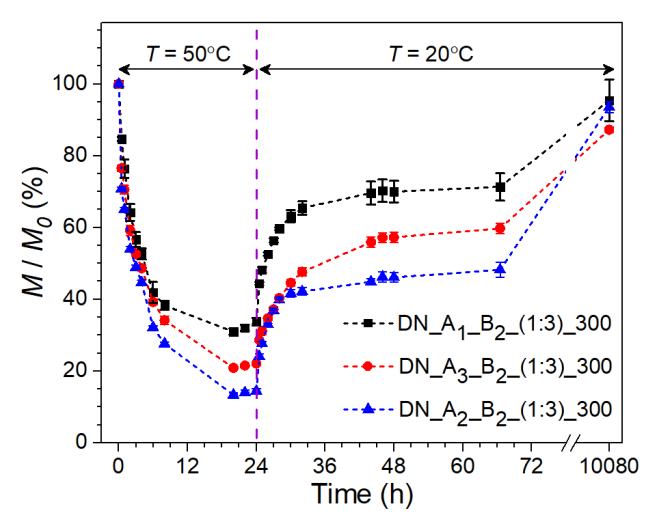


**Figure 2.** Thermoresponsive deswelling and reswelling kinetics of double network hydrogels.  $M_0$  represents the initial mass of each hydrogel sample with equilibrium swelling ratio at 20°C without pre-heating history; M represents the mass of hydrogel at indicated time after being treated by labelled temperature. The dashed lines serve as guides to the eye.

Three different UV-crosslinkable thermoresponsive polymers  $(B_2, B_3, \text{ and } B_4)$  were used as the polymer for network-B of the thermoresponsive double network hydrogels.

Firstly, we studied DN gels prepared by the combination of PNVA- $C_n$  (n = 14 or 18) and B<sub>2</sub> (PNVA-(allyl-4%)-(C<sub>3</sub>-91%)-176 with an approximate LCST of 60°C.

The representative stress-strain curves of single network-A, single network-B, thermoresponsive double network and non-thermoresponsive double network hydrogels under submersion uniaxial compression are depicted in **Figure 3**.

SN\_B<sub>2</sub>\_300 (crosslinked thermoresponsive single network hydrogel) broke at relatively small strain (around 50%) and low stress (< 0.1 MPa) at 30 to 50°C, and the toughness, strength and strain at break of the hydrogel are notably enhanced when the temperature was increased to 60°C (see **Figure 3a**). In comparison, the SN\_A<sub>2</sub> hydrogel (PNVA-C<sub>14</sub>-8%-1057) is tougher and stronger at 30°C, and the strain at break is close to 100% (see **Figure 3c**).

Compared with SN\_B<sub>2</sub>\_300, the thermoresponsive double network hydrogel DN\_A<sub>2</sub>\_B<sub>2</sub>\_(1:3)\_300 was stronger and broken at larger strain, the toughness started to increase notably from relatively lower temperature (50°C), and the ratio of modulus at large strain to initial modulus was much higher, which is similar to the mechanical property of human tissue.

When B<sub>2</sub> (PNVA-(allyl-4%)-(C<sub>3</sub>-91%)-176) in the aforementioned DN gel was replaced with B<sub>1</sub> (PNVA-allyl-4%-176), a non-thermoresponsive polymer with same number of allyl group along the chain, it was found that the stress-strain curves of the new double network hydrogel (DN\_A<sub>2</sub>\_B<sub>1</sub>\_(1:2.08)\_208) at different temperatures were roughly overlapped with each other, and the stress at break was very low. Improved hydrophobic aggregation and crosslinking of the PNVA-C<sub>n</sub> physical gels can certainly not explain the dramatic increase in stress at break, strain at break and toughness of the thermoresponsive double network hydrogels at higher temperatures. Yet the effect can undoubtedly be assigned to the collapse of the thermoresponsive polymer chains.

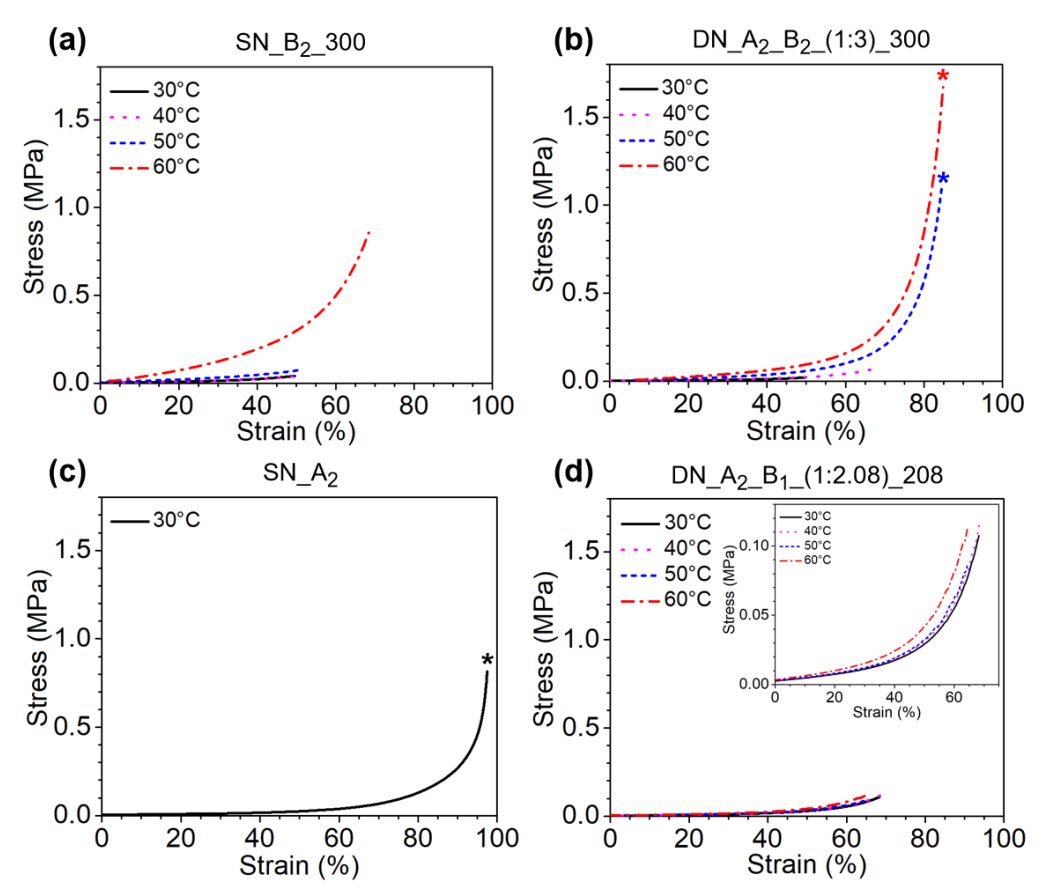


**Figure 3.** Stress-strain curves of representative hydrogels at different temperatures. (a) single network thermoresponsive hydrogel (SN\_B<sub>2</sub>\_300); (b) thermoresponsive double network hydrogel (DN\_A<sub>2</sub>\_B<sub>2</sub>\_(1:3)\_300); (c) physical gel from A<sub>2</sub> by solution casting method from ethanol solution; (d) non-thermoresponsive double network hydrogel (DN\_A<sub>2</sub>\_B<sub>1</sub>\_(1:2.08)\_208), inset is the curves shown in different scale range. Hydrogels shown in (b) and (d) have same molar concentration of allyl group in same volume of ethanol (used in the solution for crosslinking). The stars at the end of the curves in (b) and (c) indicate that the tested hydrogel sample was not broken until maximum static force (18 N) of the Q800 DMA was applied, thus the actual stress-strain curve of the indicated sample can be extended to higher strain/stress, so that the actual stress/strain/modulus at break and toughness of the sample can be much higher than the value measured at 18N.

Above all, we found it possible to prepare stronger and tougher hydrogels by the combination of PNVA-C<sub>n</sub> and thermoresponsive PNVA-allyl-C<sub>n</sub> polymers with suitable parameters (include, but not limited to: molecular weights, side chain length, degree of alkyl chain substitution, and concentration of both polymers).

To study the influence of molecular weight, side chain length, and mass fraction of PNVA-C<sub>n</sub> on the swelling and mechanical properties of thermoresponsive double network hydrogels (when B<sub>2</sub> was used for network-B), four thermoresponsive

DN gels using  $A_1$ ,  $A_2$  or  $A_3$  for network-A were prepared and their temperature-dependent swelling and mechanical properties were measured (See **Figure 4**).

The swelling ratio of all hydrogels with  $B_2$  started to decrease notably with increasing temperature from 20°C to 60°C, the shrinkage started at much lower temperature than the LCST of  $B_2$  (around 60°C); in contrast, the swelling ratio of hydrogel with  $B_1$  stayed almost the same over the explored temperature range (**Figure 4a**).

Comparing DN\_A<sub>n</sub>\_B<sub>2</sub>\_(1:3)\_300 (n = 1, 2, 3) thermoresponsive DN gels, they exhibited similar low initial modulus (in the range of 0.06 MPa to 1.0 MPa) but significant difference in modulus at break, and both modulus of all the three DN gels were increased notably with increasing temperature over 40°C (**Figure 4b** and **4c**), the significant effect of temperature on modulus started at higher temperature (40°C or above) than that on swelling ratio. The modulus at break for DN gels with A<sub>2</sub> (PNVA-C<sub>14</sub>-8%-1057), A<sub>3</sub> (PNVA-C<sub>18</sub>-6%-1057) and A<sub>1</sub> (PNVA-C<sub>18</sub>-6%-176) at 60°C were 21.3 MPa, 10.8 MPa and 1.3 MPa, respectively; and the corresponding swelling ratio of the DN gels were 3.8, 4.9 and 5.6. The vast difference in modulus at break between these three DN gels could be ascribed to the molecular weight of polymer used for network-A as well as the swelling ratio of the DN gels at the measurement temperature.

It was also found that the mass fraction of network-A polymer also played an important role in the swelling and mechanical properties of thermoresponsive DN gels. When the mass ratio of polymer  $A_1$  to  $B_2$  was increased from 1:3 to 3:3, the swelling ratio of DN\_A<sub>1</sub>\_B<sub>2</sub>\_(3:3)\_300 hydrogel was much lower than that of DN\_A<sub>1</sub>\_B<sub>2</sub>\_(1:3)\_300. Unlike the uniform and transparent gel body of DN\_A<sub>1</sub>\_B<sub>2</sub>\_(1:3)\_300, macroscopic heterogeneous structure was observed for the

DN\_A<sub>1</sub>\_B<sub>2</sub>\_(3:3)\_300 hydrogel. We explain this by a 3D web-like structure with aggregation of polymers at cross junctions of the web and void space around the junctions, which caused the super low initial modulus at all the measurement temperatures. Compression and heating above the collapse temperature made the web-like structure of DN\_A<sub>1</sub>\_B<sub>2</sub>\_(3:3)\_300 packed more densely, which led to much higher modulus at break than DN\_A<sub>1</sub>\_B<sub>2</sub>\_(3:3)\_300 hydrogel (**Figure 4a-4c**).

As shown in **Figure 4d**, although the DN\_A<sub>1</sub>\_B<sub>2</sub>\_(3:3)\_300 hydrogel was not the strongest DN gel among the samples, it was the most compressible sample with largest strain at break of 85% at 50°C or 60°C, which could also be explained by its special web-like structure: under compression, firstly the void space inside the DN gel became smaller without much force applied on the polymer structure. With the same A:B mass ratio, the DN gels with higher molecular weights network-A (DN\_A<sub>2</sub>\_B<sub>2</sub>\_(1:3)\_300 and DN\_A<sub>3</sub>\_B<sub>2</sub>\_(1:3)\_300) were more compressible than the one with lower molecular weight network-A (DN\_A<sub>1</sub>\_B<sub>2</sub>\_(1:3)\_300) because of the higher degree of entanglements of higher molecular weight polymers. Furthermore, the DN\_A<sub>2</sub>\_B<sub>2</sub>\_(1:3)\_300 fractured at larger strain at 40°C and 50°C compared to DN\_A<sub>3</sub>\_B<sub>2</sub>\_(1:3)\_300, because the crosslinks formed by C<sub>14</sub> side chains are more dynamic than that of C<sub>18</sub> side chains.

As shown in **Figure 4e**, for the strength of DN gels (i.e., stress at break), DN\_A<sub>2</sub>\_B<sub>2</sub>\_(1:3)\_300 exhibited the highest strength for the high molecular weight of A<sub>2</sub> and the flexibility of crosslinks formed by C<sub>14</sub> side chains. DN\_A<sub>1</sub>\_B<sub>2</sub>\_(3:3)\_300 also fractured at relatively high stress regardless of the low molecular weight network-A, which was caused by the super high mass content of network-A.

The toughness of all samples is as shown in **Figure 4f**. DN\_A<sub>2</sub>\_B<sub>2</sub>\_(1:3)\_300 and DN A<sub>1</sub> B<sub>2</sub> (3:3) 300 hydrogels showed highest toughness while

 $DN_A_1B_2(1:3)_300$  had the lowest toughness among the four thermoresponsive DN gels.

Due to the limitation of the Q800 DMA, the maximum static force that can be applied to the hydrogel samples under compression is 18 N. Therefore the stress-strain curves can only be recorded until 18N. The data of the following samples shown in **Figures 4c-f** were calculated by assuming that the hydrogels break at 18 N: DN\_A<sub>3</sub>\_B<sub>2</sub>\_(1:3)\_300 at 60°C, DN\_A<sub>2</sub>\_B<sub>2</sub>\_(1:3)\_300 at 50°C and 60°C, and DN\_A<sub>1</sub>\_B<sub>2</sub>\_(3:3)\_300 hydrogels at 50°C and 60°C, while the actual values at break would be no less than the data shown in **Figure 4**.

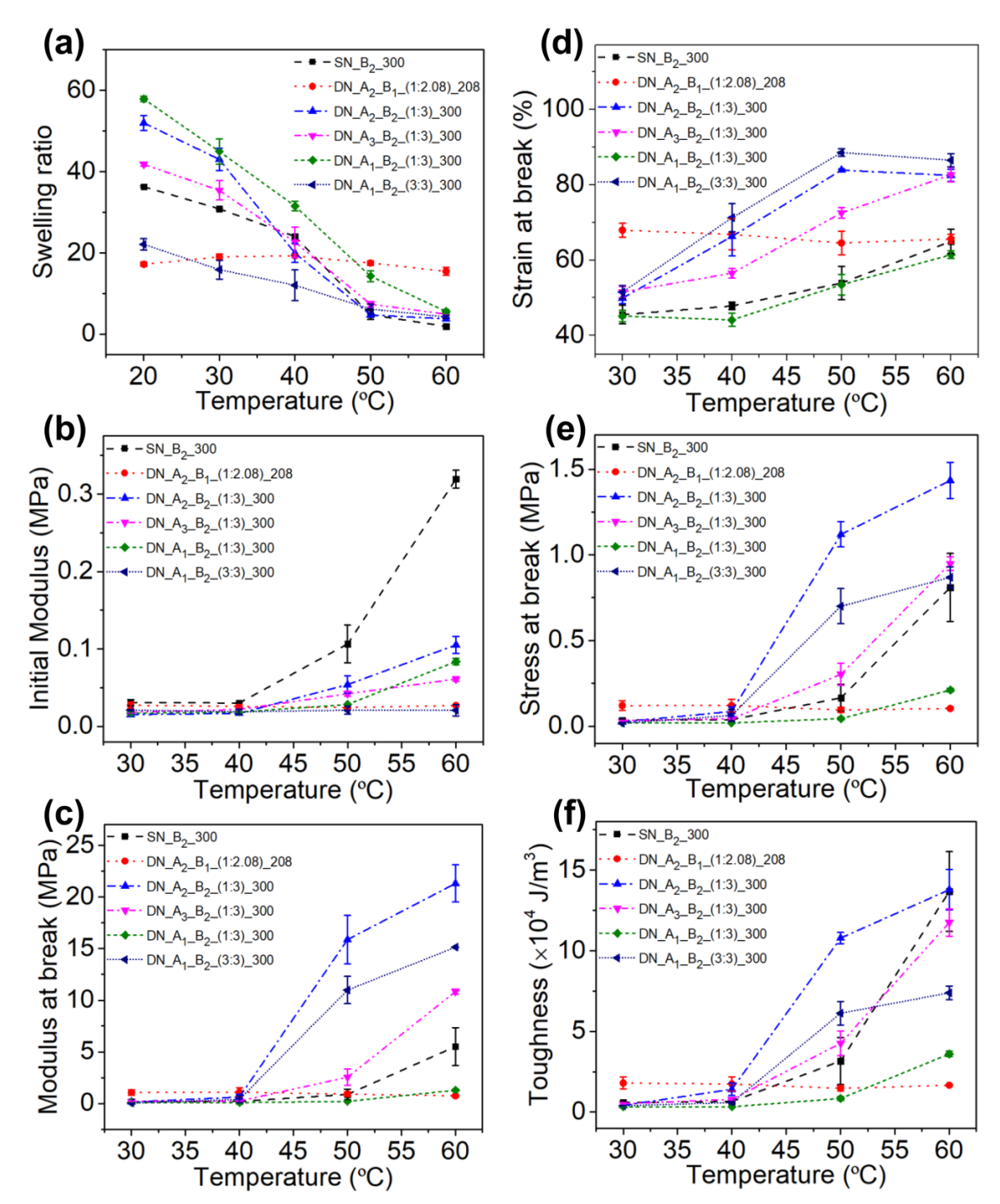


**Figure 4.** Temperature dependent swelling ratio and mechanical properties of hydrogels with B<sub>1</sub> or B<sub>2</sub> as polymers for the UV-crosslinkable network. (a) Swelling ratio; (b) initial modulus measured from slope over 0-10% strain; (c) modulus at break point; (d) Strain at break point; (e) stress at break point; (f) Toughness measured by the integral of the strain-stress curve taken from zero strain to strain at break. Note: DN\_A<sub>3</sub>\_B<sub>2</sub>\_(1:3)\_300 at 60°C, DN\_A<sub>2</sub>\_B<sub>2</sub>\_(1:3)\_300 at 50°C and 60°C, and DN\_A<sub>1</sub>\_B<sub>2</sub>\_(3:3)\_300 hydrogels at 50°C and 60°C were not broken until maximum static force (18 N) of the Q800 DMA was applied, all the data shown are measured from the stress-strain curves at the 18N (assume that sample broke at 18N).

The swelling and mechanical properties of thermoresponsive DN gels with PNVA-(allyl-4%)-(C<sub>4</sub>-35%)-176 (B<sub>3</sub>, approximate LCST: 45.6°C) as network-B are shown in **Figure 5**. Compared with the DN gels using B<sub>2</sub> as network-B polymer, notable enhancement of mechanical properties with temperature started at much lower temperature (from 20°C); the modulus at break for these B<sub>3</sub> DN gels are also stronger than their initial modulus, but the ratio of modulus at break to initial modulus is much lower; the modulus/strain/stress at break and toughness are much lower and not increased so many times with elevated temperature; the influence of side chain length of polymer for network-A in mechanical properties is not notable, the modulus/strain/stress at break as well as the toughness of DN gels with A<sub>2</sub> or A<sub>3</sub> are quite similar. In addition, the mechanical properties of DN gels with B<sub>3</sub> were a little better than the single network gel SN\_B<sub>3</sub>\_300 except the initial modulus, which indicated that the introduction of the A network can also probably enhance the mechanical performance of A-B<sub>3</sub> series of DN gels.

According to this comparison, it is shown that PNVA-(allyl-4%)-(C<sub>3</sub>-91%)-176 (B<sub>2</sub>), which has nearly full substitution, is a better choice for producing strong thermoresponsive DN gels compared with PNVA-(allyl-4%)-(C<sub>4</sub>-35%)-176 (B<sub>3</sub>), which is only partly substituted by alkyl side chains. The nearly full alkyl chain substitution of B<sub>2</sub> makes the DN gels relatively more homogeneous and less likely to get locally damaged when subjected to compression.

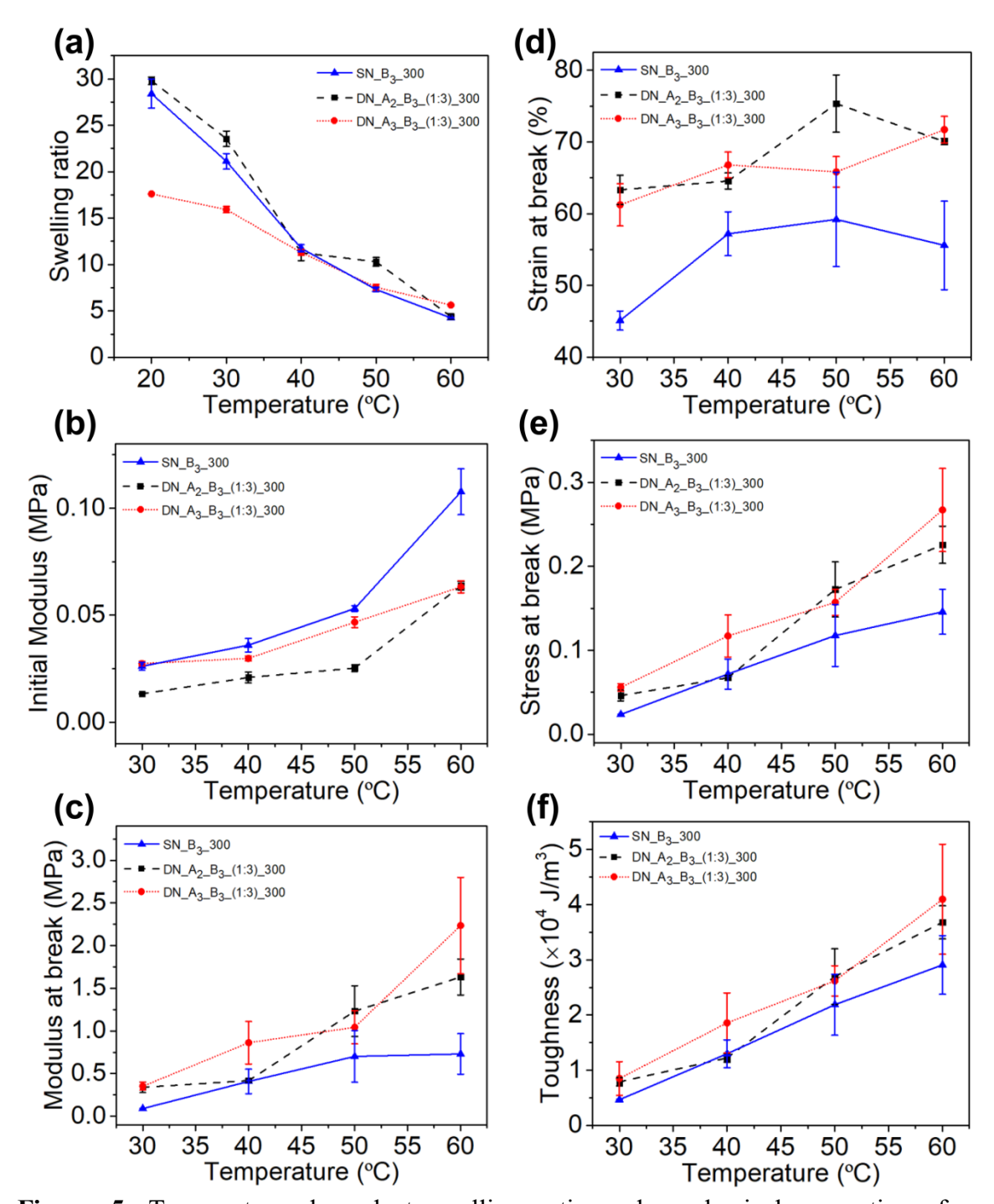


**Figure 5.** Temperature dependent swelling ratio and mechanical properties of hydrogels with B<sub>3</sub> as polymers for the UV-crosslinkable network. (a) Swelling ratio; (b) initial modulus measured from slope over 0-10% strain; (c) modulus at break point; (d) Strain at break point; (e) stress at break point; (f) Toughness measured by the integral of the strain-stress curve taken from zero strain to strain at break.

In order to investigate the influence of higher molecular network-B on the swelling and mechanical properties of thermoresponsive DN gels, we also prepared samples using PNVA-(allyl-4%)-(C<sub>3</sub>-91%)-1057 (B<sub>4</sub>, approximate LCST: 64°C).

Unfortunately, due to the very high viscosity, which can largely hinder the homogeneous mixing of the two polymers, we reduced the concentration of B<sub>4</sub> to 150 mg/mL but kept the polymer mass ratio of A:B also at 1:3.

The representative temperature-dependent stress-strain curves of the thermoresponsive single and double network hydrogels using B<sub>4</sub> are shown in **Figure** 6. At low temperatures (30°C to 50°C), both the SN and DN gels exhibited low strength (below 0.05 MPa) and low modulus, but the strain at break of the DN gel was extended to a little higher value; when the temperature was increased to 60°C, SN\_B<sub>4</sub>\_150 had lager modulus and strength, but a little lower strain at break compared to DN\_A<sub>3</sub>\_B<sub>4</sub>\_(1:3)\_150. The reason could be that polymer in network-A made the crosslinking of B<sub>4</sub> more sparsely, under the condition that the concentration of B<sub>4</sub> in solution is relatively low even without network-A.

Compared to the DN gels with  $B_2$  (same structure with lower molecular weight), notable enhancement of mechanical performance of hydrogels with  $B_4$  started at higher temperature (above 50°C), which is because the higher LCST of  $B_4$  polymer. The inversed molecular weight effect has been demonstrated in detail in Chapter 4.

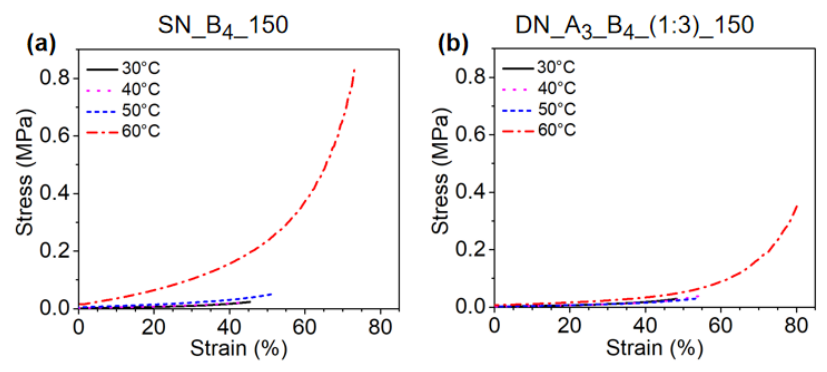


**Figure 6.** Stress-strain curves of representative hydrogels at different temperatures. (a) Single network thermoresponsive hydrogel (SN\_B<sub>4</sub>\_150); (b) thermoresponsive double network hydrogel (DN  $A_3$   $B_4$  (1:3) 150).

Temperature-dependent swelling and mechanical properties of DN gels using  $B_4$  are shown in **Figure 7**. The swelling ratios of  $A_n_B_4_(1:3)_150$  hydrogels are much higher than  $A_n_B_2_(1:3)_300$  samples, due to the largely reduced concentration of both networks. Although  $B_4$  has higher molecular weight than  $B_2$ , the reduced polymer concentration result in worse mechanical performance of the DN gels.

All the DN\_A<sub>n</sub>\_B<sub>4</sub>\_(1:3)\_150 (n = 1, 2, 3) hydrogels exhibited lower modulus, strength and toughness compared with the SN\_B<sub>4</sub>\_150 at temperatures over  $50^{\circ}$ C, while similar values below  $50^{\circ}$ C.

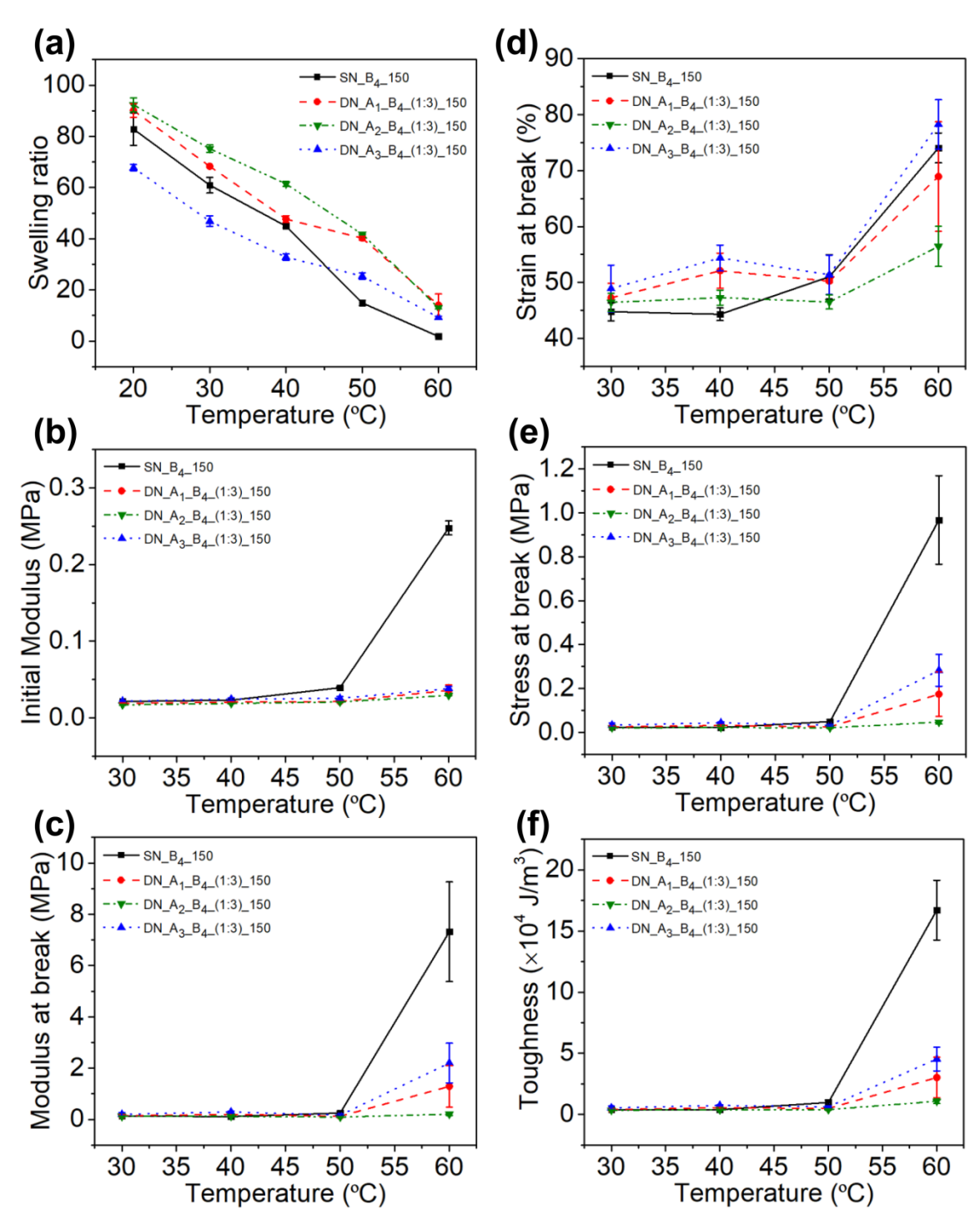


**Figure 7.** Temperature dependent swelling ratio and mechanical properties of hydrogels with B<sub>4</sub> as polymers for the UV-crosslinkable network. (a) Swelling ratio; (b) initial modulus measured from slope over 0-10% strain; (c) modulus at break point; (d) Strain at break point; (e) stress at break point; (f) Toughness measured by the integral of the strain-stress curve taken from zero strain to strain at break.

Above all, the swelling behavior and mechanical performance are dependent on the alkyl chain length, degree of substitution, molecular weight, total polymer concentration as well as the mass fraction of each polymer.

# 5.4 Conclusion

In this chapter, thermoresponsive double network hydrogels by the combination of PNVA- $C_n$  (n = 14 or 18) and PNVA-allyl- $C_n$  (n = 3 or 4) polymers were prepared and their temperature-dependent swelling behavior and mechanical properties under compression were studied. These thermoresponsive double network hydrogels exhibited tissue-like properties, they have very low modulus at small strain while very high modulus at large strain. Temperature can influence both the swelling ratio and mechanical properties, but the significant influence in mechanical properties always started at higher temperature than that in swelling.

It was also found that many factors including, but not limited to the alkyl chain length of polymer for network-A, the structure of network-B polymer, molecular weight and mass fraction of two networks, as well as the total polymer concentration can influence the swelling behavior and mechanical properties significantly. With the proper combinations and suitable preparation parameters, the mechanical performance can be ideally enhanced compared to the corresponding single network thermoresponsive hydrogels.

#### 5.5 References

[1] Gong, J. P.; Katsuyama, Y.; Kurokawa, T.; Osada, Y. Double-Network Hydrogels with Extremely High Mechanical Strength. *Advanced Materials* **2003**, *15* (14), 1155-1158. DOI: 10.1002/adma.200304907.

- [2] Gong, J. P. Why are double network hydrogels so tough? *Soft Matter* **2010**, *6* (12), 2583-2590. DOI: 10.1039/B924290B.
- [3] Nonoyama, T.; Gong, J. P. Double-network hydrogel and its potential biomedical application: A review. *Proceedings of the Institution of Mechanical Engineers, Part H: Journal of Engineering in Medicine* **2015**, *229* (12), 853-863. DOI: 10.1177/0954411915606935.
- [4] Kempson, G. E. 5 The Mechanical Properties of Articular Cartilage. In *The Joints and Synovial Fluid*, Sokoloff, L. Ed.; Academic Press, 1980; pp 177-238. DOI: 10.1016/B978-0-12-655102-0.50011-4.
- [5] Zhu, J.; Wang, X.; He, C.; Wang, H. Mechanical properties, anisotropic swelling behaviours and structures of jellyfish mesogloea. *Journal of the Mechanical Behavior of Biomedical Materials* **2012**, *6*, 63-73. DOI: 10.1016/j.jmbbm.2011.10.005.
- [6] Keith, A. N.; Clair, C.; Lallam, A.; Bersenev, E. A.; Ivanov, D. A.; Tian, Y.; Dobrynin, A. V.; Sheiko, S. S. Independently Tuning Elastomer Softness and Firmness by Incorporating Side Chain Mixtures into Bottlebrush Network Strands. *Macromolecules* **2020**, *53* (21), 9306-9312. DOI: 10.1021/acs.macromol.0c01725.
- [7] Sophia Fox, A. J.; Bedi, A.; Rodeo, S. A. The Basic Science of Articular Cartilage: Structure, Composition, and Function. *Sports Health* **2009**, *1* (6), 461-468. DOI: 10.1177/1941738109350438.
- [8] Mansour, J. M. Biomechanics of cartilage. *Kinesiology: the mechanics and pathomechanics of human movement* **2003**, *2*, 66-79.
- [9] Haque, M. A.; Kurokawa, T.; Gong, J. P. Super tough double network hydrogels and their application as biomaterials. *Polymer* **2012**, *53* (9), 1805-1822. DOI: 10.1016/j.polymer.2012.03.013.
- [10] Utech, S.; Boccaccini, A. R. A review of hydrogel-based composites for biomedical applications: enhancement of hydrogel properties by addition of rigid inorganic fillers. *Journal of Materials Science* **2016**, *51* (1), 271-310. DOI: 10.1007/s10853-015-9382-5.
- [11] Gent, A. N.; Zhang, L.-Q. Strain-Induced Crystallization and Strength of Rubber. *Rubber Chemistry and Technology* **2002**, *75* (5), 923-934. DOI: 10.5254/1.3547692.
- [12] Zhang, C.; Demco, D. E.; Rimal, R.; Köhler, J.; Vinokur, R.; Singh, S.; Tenbusch, J.; Möller, M. Hydrophobic Interaction within Sparsely *N*-Alkylated Poly(*N*-vinylacetamide)s Enables Versatile Formation of Reversible Hydrogels. *Macromolecules* **2023**, *56* (23), 9616-9625. DOI: 10.1021/acs.macromol.3c01706.